CHARACTERIZATION OF REACTANTS, REACTION MECHANISMS AND REACTION PRODUCTS LEADING TO EXTREME ACID RAIN AND ACID AEROSOL CONDITIONS IN SOUTHERN CALIFORNIA

Final Report
ARB Contract No. A0-141-32

by

Michael R. Hoffmann, J. J. Morgan, D. J. Jacob,
J. W. Munger and J. M. Waldman

Environmental Engineering Science
W. M. Keck Laboratories
California Institute of Technology
Pasadena, California 91125

31 March 1983

ABSTRACT

Analyses of fogwater collected by inertial impaction in the Los Angeles basin and the San Joaquin Valley indicated unusually high concentrations of major and minor ions. The dominant ions measured were NO_3^-, SO_4^{2-}, NH_4^+ and H^+. Nitrate exceeded sulfate on an equivalent basis by a factor of 2.5 in the central and coastal regions of the Los Angeles basin, but was approximately equal in the eastern Los Angeles basin and the San Joaquin Valley. Maximum observed values for NH_4^+, NO_3^- and SO_4^{2-} were 10., 12., and 5. meq L^{-1}, while the lowest pH observed was 2.2. Iron and lead concentrations over 0.1 mM and 0.01 mM, respectively, were observed. High concentrations of chemical components in fog appeared to correlate well with the occurrence of smog events. Concentrations in fogwater were also affected by the physical processes of condensation and evaporation. Light, dissipating fogs routinely showed the highest concentrations.

The chemistry of urban fog has been modelled using a hybrid kinetic and equilibrium computer code. Extreme acidity found in Southern California fog may be due either to condensation and growth on acidic condensation nuclei or *in situ* S(IV) oxidation. Important oxidants of S(IV) were found to be O_2 as catalyzed by Fe(III) and Mn(II), H_2O_2 and O_3. Formation of hydroxymethanesulfonate ion (HMSA) via the nucleophilic addition of HSO_3^- to $CH_2O(\ell)$ significantly increased the droplet capacity for S(IV) but did not slow down the net S(IV) oxidation rate leading to fog acidification. Gas phase nitric acid, ammonia and hydrogen peroxide were scavenged efficiently, although aqueous phase hydrogen peroxide was depleted rapidly by reduction with S(IV). Nitrate production in the aqueous phase was found to be dominated by HNO_3 gas phase scavenging. Major aqueous-phase species concentrations were controlled primarily by condensation, evaporation, and pH.

TABLE OF CONTENTS

LIST OF FIGURES

LIST OF FIGURES (Continued)

LIST OF FIGURES (Continued)

LIST OF TABLES

LIST OF TABLES (Continued)

LIST OF TABLES (Continued)

I. OVERVIEW

Sulfur dioxide can be oxidized to sulfate aerosols either homogeneously in the gas phase or heterogeneously in atmospheric microdroplets (Hoffmann and Jacobs, 1983). Field studies indicate that the relative importance of homogeneous and heterogeneous processes depends on a variety of climatological factors such as relative humidity and the intensity of incident solar radiation (Wilson and McMurry, 1981).

Cass (1975) has shown that the worst sulfate pollution episodes in Los Angeles occur during periods of high relative humidity and when the day begins with low clouds or fog in coastal areas, while Cass and Shair (1980) have reported that nighttime conversion rates (5.8%/hr) for SO_2 in the Los Angeles sea breeze/land breeze circulation system are statistically indistinguishable from typical daytime conversion rates (5.7%/hr) for the month of July. Morgan and Liljestrand (1980) in their study of rainfall in the Los Angeles basin, have reported that light, misting precipitation events resulted in low pH values (e.g. pH = 2.9) and correspondingly high SO_4^{2-} and NO_3^- concentrations.

Results of these investigations along with the results of Gartrell et al. (1963), Smith and Jeffery (1975), Cox (1974), Diffenhoeffer and dePena (1978), Enger and Högström (1979), Wilson and McMurry (1981), and McMurry et al. (1981) indicate that aqueous-phase oxidation of SO_2 is a significant pathway for the total transformation of SO_2.

Recently, Waldman et al. (1982) have characterized the chemistry of winter fogs in the Los Angeles basin and they have reported that nighttime fog water has extremely low pH values (e.g. pH = 2.2) and extremely high concentrations of sulfate, nitrate, ammonium ion and trace metals. Observed

Table 1A. Fog Water Composition in Southern California†: Observed Concentration Ranges

Location	pH	NO_3^- (μeq/L)	SO_4^{2-} (μeq/L)	NH_4^+ (μeq/L)
Pasadena (11-23-81)	2.92-4.85	1220-3520	481-944	1290-2380
Lennox (12-18-81)	2.52-2.81	2070-3690	610-1970	950-1570
Bakersfield (1-14-82)	2.90-3.07	3140-5140	2250-5000	5370-10520
extremes	2.20	12000	5060	10,520
LA Clouds* (11-23-81)	2.95-3.80	100-1393	113-544	34-477
LA Rain (81-82)	3.67-5.21	1.4-471	3.1-125	1-115

†From Waldman et al. (1982)

*Cloud water samples were collected by Meteorology Research Incorporated (MRI) and analyzed by Caltech.

Table 1B. Fog Water Composition in Southern California†: Observed Concentration Ranges

Location	Fe(μg/L)	Mn(μg/L)	Pb(μg/L)	Cu(μg/L)	Ni(μg/L)	CH_2O(mg/L)	SO_3^{2-}(μeq/L)
Pasadena (11-23-81)	920-1770	34.56	1310-2540	88-105	7.6-13.6	3.1-3.4	151-235
Lennox (12-18-81)	1020-2080	25-81	828-2400	9-150	2.3-51.5	3.9-7.6	30-250
Bakersfield (1-14-82)	240-6600	--	241-366	40-400	125-590	6.1-14	--
extremes	23700	812	2540	144	51.5	12.8	250
LA Clouds* (11-23-82)	14-1260	1.5-59	10-197	23-1510	10-200	0.13-1.6	54-258
LA Rain (81-82)	1.6-13.2	1-2.8	2-88	2.2-16.9	--	--	--

†From Waldman et al. (1982)

*Cloud water samples were collected by MRI and analyzed by Caltech.

ranges reported by Waldman et al. (1982) are summarized in Tables1A and B. Of special interest are the high values observed for SO_4^{2-}, NO_3^-, S(IV), CH_2O, Fe, Mn, Pb and Cu in the fog water droplets. These values and their time-dependent changes indicate that nighttime fogs provide a very reactive and complex environment for the incorporation and transformation of SO_2 and NO_x to their acidic products, H_2SO_4 and HNO_3. Concomitant incorporation of NH_3 gas and calcareous dust into the droplet phase results in the partial neutralization of the generated acidity. In Chapter V of this report, the detailed thermodynamic speciation and possible reaction kinetics that lead to sulfate and nitrate production in nighttime urban fog will be discussed.

Because of their similarity to clouds with respect to physical characteristics fogs are likely to reflect the same chemical processes occurring in clouds and to some degree in aqueous microdroplets. Cloud and fog water droplets are in the size range of 2 to 100 μm whereas aqueous microdroplets will be in the range of 0.01 to 1 μm. On the other hand, raindrops are approximately 100 times larger than cloud and fog water droplets (e.g. 0.1 to 3 mm). In the Los Angeles study, Waldman et al. (1982) found that fog water was more concentrated in the primary constituents than the overlying cloud water which was in turn more concentrated than rain water during overlapping periods of time. These results suggest that fog and low lying clouds may play an important role in the diurnal production of sulfate and nitrate in the Los Angeles basin during certain times of the year when the meteorological conditions are propitious for fog and cloud formation. Furthermore, Hegg and Hobbs (1981) have observed sulfate production rates in cloud water over Western Washington that

ranged from 4.0 to 300%/hr and pH values from 4.3 to 5.9. The sulfate production rate appeared to increase with an increase in pH. Similar pH values and sulfate levels were observed in stratus clouds over the Los Angeles basin (Hegg and Hobbs, 1981).

Historically, fog events have been correlated with severe pollution episodes in which elevated concentrations of SO_2 and particulate aerosol have been observed (U.S. EPA, 1971). During many of these extended fog periods excess deaths were recorded (Wilkins, 1954ab; Holland, 1972; Friedlander and Ravimohan, 1968; Larsen, 1970). The London fog of 1952 was particularly bad in this regard. For example during the London fog of 1952 the daily mass emission rate of SO_2 has been estimated to be 1.82×10^9 g, the affected area to be 1.3×10^9 m^2, the height of the inversion layer to be 150 m and the liquid water content at 1.23×10^{12} g (Meetham, 1964). Given the daily observed increase in the gas-phase SO_2 concentration of 0.18 ppm and an established droplet residence time of 0.25 days (Wilkins, 1954b), the sulfate concentration of the fog water can be estimated to be approximately 11.0 meq/L with an apparent conversion rate of 12.5%/hr. This estimated value can be compared to the sulfate ranges observed in the Los Angeles fog water which were 0.8 to 3 meq/L. However, the London fog lasted for 5 days while the Los Angeles fogs of 1981-1982 persisted for no more than 8-10 successive hours.

As pointed out by Calvert (1983), gas-phase reactions involving O_3, $HO\cdot$, HO_2 oxidation of SO_2 are too slow to account for the above transformation rates. Alternatively, the catalytic autoxidation of SO_2 in aqueous microdroplets has been suggested as a viable non-photolytic pathway for the rapid production of sulfuric acid in humid atmospheres (Hoffmann and

Jacob, 1983). In addition, H_2O_2 and O_3 have been given serious consideration as the major oxidants of dissolved SO_2 as discussed by Martin (1983) and Schwartz (1983). Oxidation by H_2O_2 seems to be most favorable because of its extremely high rate of reaction (Hoffmann and Edwards, 1975; Penkett et al., 1979; Martin and Damschen, 1981) and its pH dependency which favors the reaction at low pH. In comparison the metal catalyzed autoxidations tend to exhibit decreasing reaction rates with a decrease in pH (Hegg and Hobbs, 1978). Similarly, the reaction rate of O_3 with S(IV) decreases with a decrease in pH.

Limiting factors in the metal catalyzed pathways will be the total concentration of the active metal catalyst and its speciation as a function of pH. As shown in Table 1B,Los Angeles fog water has high concentrations of Fe, Mn, Cu, Ni, and Pb. Of these metals, Fe, Mn and Cu are expected to be the most effective catalysts for the autoxidation of S(IV) (Hoffmann and Jacob, 1983). On a micromolar basis the highest observed concentration for Fe and Mn were 424 to 14.8, respectively, while the average Fe and Mn concentrations in Los Angeles fog water were observed to be 51.6 μM and 1.7 μM, respectively. For comparison, Thornton (1981) has reported that the world wide mean concentrations for Fe in urban, rural and remote rainfall are 4.5, 3.1 and 0.13 μM, respectively. In many calculations of the droplet phase SO_2 oxidation rate (Middleton et al., 1980), the assumed Fe concentrations range from 1 to 360 μM and the assumed Mn concentrations range from 1 to 37 μM. At the upper range of the concentration scales the metal catalyzed reactions may play an important role in the overall SO_2 oxidation rate in light of the rate laws discussed by Martin (1983). The role of metal ion speciation and kinetic models for fog water chemistry will be discussed in Chapter V.

In order to translate laboratory results on the kinetics of various pathways for SO_2 oxidation in aqueous systems to atmospheric droplet systems, detailed rate laws, mechanisms, activation energies and ionic strength dependencies should be determined. In very few cases, this complete information has been assembled. However, in the case of metal catalyzed systems, there are numerous discrepancies among investigators concerning the detailed kinetic information (Hoffmann and Boyce, 1982). Metal catalyzed autoxidations can proceed via four distinctly different mechanistic pathways (Hoffmann and Boyce, 1982). These include a thermally-initiated free-radical chain reaction involving a series of one-electron transfer steps, an inner-sphere metal-sulfite complexation pathway involving metal oxides and oxyhydroxides in suspension, and photo-assisted pathways in which the oxidation is initiated by the absorption of light by S(IV), by metal ions, by metal oxide surfaces, or by a specific metal-sulfite complex. The details of these different reaction pathways will be discussed in the next chapter.

The mechanism of the oxidation of S(IV) by hydrogen peroxide is fairly well understood (Hoffmann and Edwards, 1975; McArdle and Hoffmann, 1983). This reaction proceeds via a nucleophilic displacement of H_2O_2 on bisulfite (HSO_3^-) ion and is catalyzed by specific and general acid catalysis. The significance of this latter feature for open atmospheric systems has been discussed by Martin (1983) and Schwartz (1983). On the other hand, the mechanism of the oxidation of sulfite by ozone (Penkett et al., 1979) and its various catalytic influences are less well understood. Most likely, the reaction with ozone proceeds via a free radical mechanism involving the sulfite radical and peroxymonosulfite radical species.

References - Chapter I

Cass, G. R. (1975) "Dimensions of the Los Angeles SO_2/SO_4^{2-} Problem," Environmental Quality Laboratory No. 15, California Institute of Technology, Pasadena, CA.

Cass, G. R. and F. H. Shair (1980) "Transport of Sulfur Oxides Within the Los Angeles Sea Breeze/Land Breeze Circulation System," in Proceedings of the 2nd Joint Conference on Applications of Air Pollution Meteorology, American Meteorological Society, pp. 320-327.

Calvert, J. G. (1983) The Mechanisms of the Gas Phase Oxidations of SO_2, NO and NO_2 in the Atmosphere, in Acid Precipitation, J. G. Calvert, ed., Ann Arbor Science Publ., Ann Arbor, MI (in press).

Cox, R. A. (1974) "Particle Formation from Homogeneous Reactions of Sulfur Dioxide and Nitrogen Dioxide," Tellus 26, 235-240.

Diffenhoeffer, A. C. and R. G. dePena (1978) "A Study of Production and Growth of Sulfate Particles in Plumes from a Coal-Fired Power Plant," Atmos. Environ. 12, 297-306.

Enger, L. and U. Hogstrom (1979) "Dispersion and Wet Deposition of Sulfur from a Power Plant Plume," Atmos. Environ. 13, 797-810.

Friedlander, S. K. and A. L. Ravimohan (1968) "A Theoretical Model for the Effect of an Acute Air Pollution Episode on a Human Population," Environ. Sci. Tech. 2, 1101-1108.

Gartrell, J. E., J. W. Thomas and S. B. Carpenter (1963) "Atmospheric Oxidation of SO_2 in Coal-Burning Power Plant Plumes," Amer. Ind. Hyg. Assoc. Quart. 24, 113-120.

Hegg, D. A. and P. V. Hobbs (1978) "Oxidation of Sulfur Dioxide in Aqueous Systems with Particular Reference to the Atmosphere," Atmos. Environ. 12, 241-253.

Hegg, D. A. and P. V. Hobbs (1981) "Cloud Water Chemistry and the Production of Sulfates in Clouds," Atmos. Environ. 15, 1597-1604.

Hoffmann, M. R. and S. D. Boyce (1982) "Catalytic Autoxidation of Aqueous Sulfur Dioxide in Relationship to Atmospheric Systems," Adv. Environ. Sci. Tech. 12, Wiley-Interscience, New York, pp. 147-189.

Hoffmann, M. R. and D. J. Jacob (1983) Kinetics and Mechanisms of the Catalytic Oxidation of Dissolved Sulfur Dioxide in Aqueous Solution: An Application to Nighttime Fogwater Chemistry, in Acid Precipitation, J. G. Calvert, ed., Ann Arbor Science Publ., Ann Arbor, MI (in press).

Hoffmann, M. R. and J. O. Edwards (1975) "Kinetics and Mechanism of the Oxidation of Sulfur Dioxide by Hydrogen Peroxide in Acidic Solution," J. Phys. Chem. 79, 2096-2098.

Holland, W. W. (1972) "Air Pollution and Respiratory Disease," Technomic Publ. Co., Inc., Westport, CT.

Larsen, R. I. (1970) "Relating Air Pollutant Effects to Concentration and Control," J. Air Poll. Control Assoc. 20, 214-225.

McArdle, J. V. and M. R. Hoffmann (1983) "Kinetics and Mechanism of the Oxidation of Aquated Sulfur Dioxide by Hydrogen Peroxide at Low pH," J. Phys. Chem. (in press).

McMurry, P. H., D. J. Rader and J. L. Smith (1981) "Studies of Aerosol Formation in Power Plant Plumes. I. Parameterization of Conversion Rate for Dry, Moderately Polluted Ambient Conditions," Atmos. Environ. 15, 2315-2329.

Martin, L. R. (1983) Kinetic Studies of Sulfite Oxidation in Aqueous Solution, in Acid Precipitation, J. G. Calvert, ed., Ann Arbor Science Publ., Ann Arbor, MI (in press).

Martin, L. R. and D. E. Damschen (1981) "Aqueous Oxidation of Sulfur Dioxide by Hydrogen Peroxide at Low pH," Atmos. Environ. 15, 1615-1622.

Meetham, A. R. (1964) "Atmospheric Pollution: Its Origin and Prevention," 3rd ed., D. W. Bottom and S. Cayton, eds., Pergamon Press, Oxford, England.

Middleton, P., C. S. Kiang and V. A. Mohnen (1980) "Theoretical Estimates of the Relative Importance of Various Urban Sulfate Aerosol Production Mechanisms," Atmos. Environ. 14, 463-472.

Morgan, J. J. and H. M. Liljestrand (1980) "Measurement and Interpretation of Acid Rainfall in the Los Angeles Basin," W. M. Keck Laboratory of Hydraulics & Water Resources, California Institute of Technology, Pasadena, California, Report No. AC-2-80.

Penkett, S. A., B. M. R. Jones, K. A. Brice and A. E. J. Eggleton (1979) "The Importance of Atmospheric Ozone and Hydrogen Peroxide in Oxidizing Sulfur Dioxide in Cloud and Rainwater," Atmos. Environ. 13, 123-137.

Schwartz, S. E. and J. E. Freiberg (1981) "Mass-Transport Limitation to the Rate of Reaction of Gases in Liquid Droplets: Application to Oxidation of SO_2 in Aqueous Solutions," Atmos. Environ. 15, 1129-1144.

Smith, F. B. and G. H. Jeffrey (1975) "Airborne Transport of Sulphur Dioxide from the U.K.," Atmos. Environ. 9, 643-659.

Thornton, J. D. (1981) "The Metal and Strong Acid Composition of Rain and Snow in Minnesota: Land Use Effects," M.S. Thesis, University of Minnesota, Minneapolis, MN.

U.S. EPA (1971) "Guide for Air Pollution Avoidance. Appendix B. History of Episodes," PH-22-68-32, 123-135.

Waldman, J. M., J. W. Munger, D. J. Jacob, R. C. Flagan, J. J. Morgan and M. R. Hoffmann (1982) "Chemical Composition of Acid Fog," Science 218, 677-680,

Wilkins, E. T. (1954a) "Air Pollution Aspects of the London Fog of December, 1952," J. Roy. Meteorol. Soc. 80, 267-278.

Wilkins, E. T. (1954b) "Air Pollution and the London Fog of December, 1952," J. Roy. Sanit. Instit. 74, 1-21.

Wilson, J. C. and P. H. McMurry (1981) "Studies of Aerosol Formation in Power Plant Plumes - I. Secondary Aerosol Formation in the Navajo Generating Station Plume," Atmos. Environ. 15, 2329-2339.

II. BACKGROUND ANALYSIS

A. *Physics of Fogs and Clouds*

1. Microphysical characteristics

Atmospheric aerosols have characteristic sizes which range from 10^{-2} μm for Aitken condensation nuclei to 10^{4} μm for rain droplets. For very small particles, only diffusional transport processes are important; for very large ones, inertial and gravitational processes are most significant. Fog and cloud droplets have sizes which fall near the middle of the above range, with mass mean diameters of approximately 10 μm. Inertia and, to a lesser extent, gravitation dominate the transport forces which affect fog and cloud droplets.

Drop size distributions measured in fogs and clouds generally exhibit a characteristic shape, even for spectra formed under a variety of meteorological conditions. Usually, the concentration rises sharply to a maximum and decreases gently toward larger sizes, giving a positively skewed distribution (Figure 1a).

Either log-normal or gamma distribution functions can be used to fit the spectrum as well as the empirical, two-parameter, Best distribution:

$$1-F = \exp[-(d/C)^{k}] \qquad (1)$$

where F is the fraction of liquid water volume composed of drops with diameters less than d, while C and k are fitting parameters. Bimodality, such as seen in Figure 1a, also is observed. Warner (1969) proposed that mixing processes which lead to the entrainment of drier air into the saturated air mass are responsible.

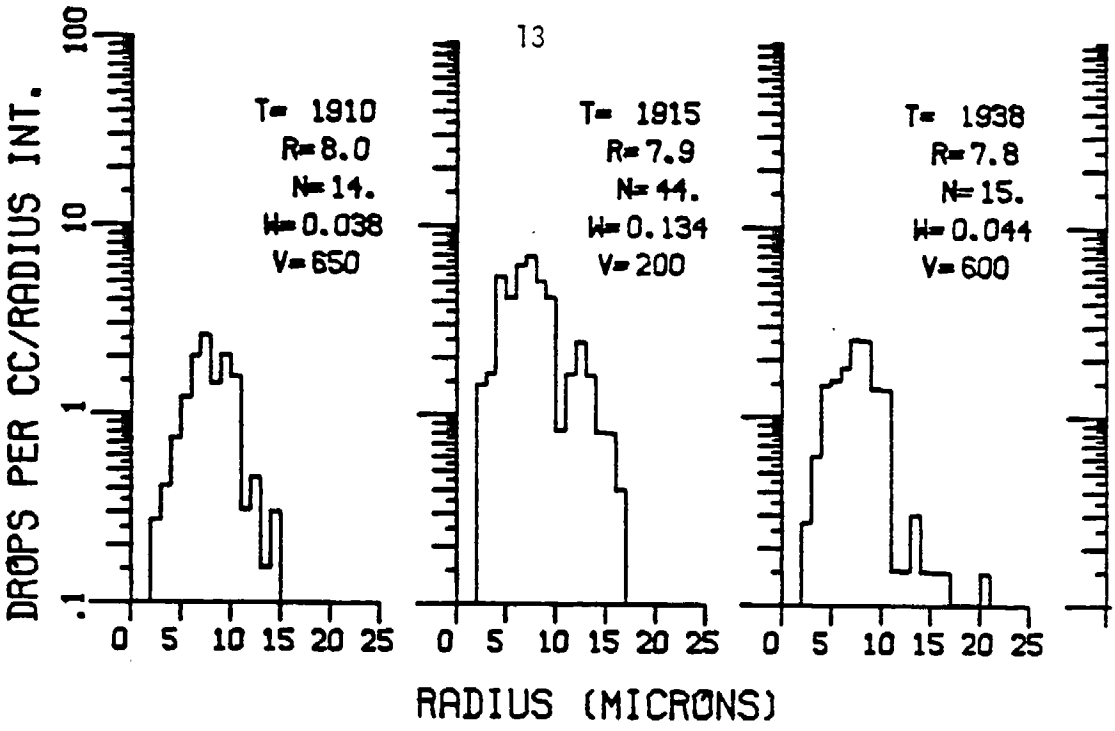

(a) Droplet Spectra for Marine Fog off the Coast of Southern California. T=time (PST); R=mass mean radius (um); N=number concentration (#/cm^3); W=LWC (g/m^3); V=visibility (m). (Mack et al, 1977)

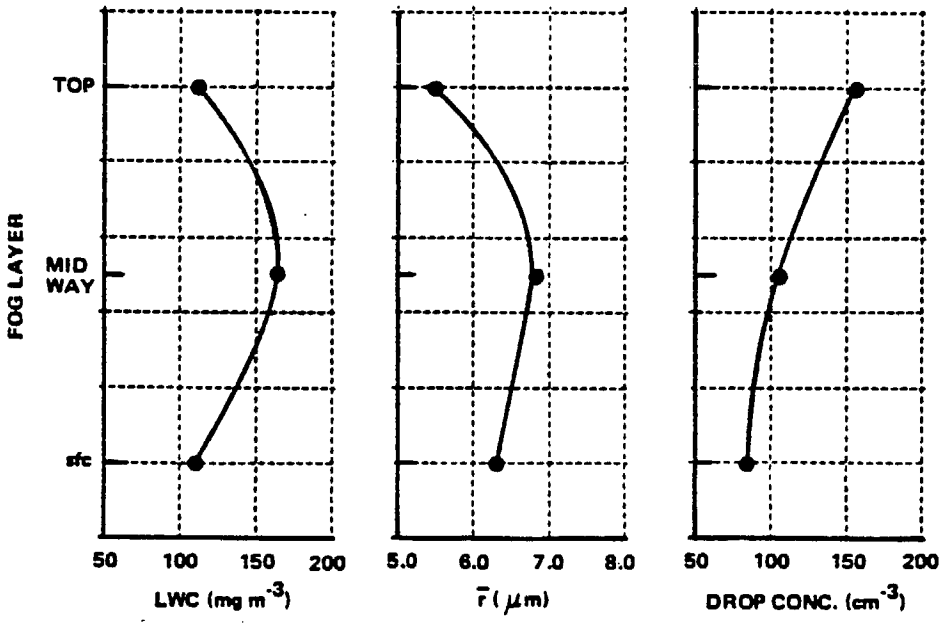

(b). Average Fog Microphysics at Three Levels in Radiation Fog Located Inland. (Mack and Pilie, 1973)

Figure 1

Three important parameters which describe fog and cloud microphysics are the mass mean diameter (or radius), the number concentration, and the liquid water content (LWC), shown for an inland fog as a function of height in Figure 1b. Pruppacher and Klett (1978) highlight several characteristic features of cloud water content: (a) LWC increases with depth above the cloud base and decreases toward the cloud top; (b) LWC parallels drop size rather than drop concentration; and (c) the observed LWC is less than that which would be computed based on a saturated adiabatic ascent of moist air. Goodman (1977) and Mack and Pilie (1973) routinely observed (a) and (b) for fogs.

Atmospheric droplets are formed by condensation of water vapor at or near saturation. For clouds, relative humidity is found virtually always in the range of 98-102%. Neiberger and Wurtele (1949) report frequent observations of fog formed in ambient relative humidity below 100%, as low as 81%. The activation of condensation nuclei which leads to droplet formation is a balance between the offsetting effects of surface curvature and dissolved hygroscopic nuclei, which raises and lowers the saturation vapor pressure, respectively, at the droplet surface. The size at which a nucleus is activated decreases with relative humidity. Radiative cooling of the liquid droplets has also been deemed as consequential to further condensation in fogs and clouds (Roach, 1976).

Warm fog (i.e. at temperatures above freezing point for water) reportedly accounts for 95% of fog occurrences worldwide (Sax et al., 1975). Water clouds are frequently found at supercooled temperatures, especially above -10°C (Pruppacher and Klett, 1978). Below 0°C occurrence of liquid

fog and cloud water is due to the tendency of water, particularly in small quantities, to supercool. Further supercooling eventually leads to ice crystal formation, an important step in many precipitation phenomena.

Fog microphysics are observed to exhibit characteristic differences based on air mass trajectory. Air masses with maritime, versus continental, trajectories are found to lead to clouds (Pruppacher and Klett, 1978) and fogs (Goodman, 1979) with lower number concentrations, larger droplets, and broader size distributions. Bimodality is more common for maritime distributions. The differences in spectra are largely accounted for by the correspondingly different condensation nucleus characteristics. Cloud modification by urban pollution has been observed, and markedly different drop size spectra are found to be due to pollutant effluent aerosols (Barrett et al., 1979).

2. Factors Important to Formation and Occurrence

Although microphysical processes have significant impact on condensation nuclei activation and precipitation chemistry, synoptic-scale features such as baroclinic instabilities and geostrophic winds provide the framework of environmental conditions which profoundly influence the formation and occurrence of fogs and clouds. Mason (1971) underscores the complexity of cloud physics as a problem of scale with "interactions between processes ranging from nucleation phenomena on the molecular scale to dynamics of extensive cloud systems on the scale of hundreds or thousands of kilometers."

Integral to the formation of atmospheric water droplets is the presence of condensation nuclei. Homogeneous nucleation of water vapor in the absence of ions or aerosol particles will only occur at very high levels of

supersaturation. The size range of importance for condensation nuclei is between 0.01 μm and 10 μm; very small nuclei are not generally active at ambient vapor saturation, while very large ones tend to be removed by gravitational settling.

The adiabatic cooling due to vertical motion is most important for the formation of clouds. This is not the case for fogs, because their extensive ground contact suppresses vertical motions. The two primary classifications of fogs are advection and radiation. The former are usually brought on by the large-scale horizontal motion which brings a warm, moist air mass in contact with a cooler surface layer or the reverse (Pilie et al., 1979). Radiation fog initiated by radiative cooling and inhibited by turbulent diffusion (Roach et al., 1976). Rodhe (1962) notes the importance of turbulent eddy exchange on formation of both classes of fog.

Taylor (1917) is credited with conducting the first serious study of fog occurrence. He observed that radiation fog formed consistently under the same conditions: clear skies, light or no wind, and high relative humidity. However, under these conditions, fog was observed only a half of the times. He recognized the importance of ground radiation and that dew suppressed supersaturation of the ground layer. His conclusion that radiative cooling of the air was not significant to fog formation has been reviewed, and its importance is now recognized (Roach et al., 1976). Roach (1976) postulates that supersaturation of an air mass may not be important, which is consistent with the observation of fogs at relative humidities below 100% (Neiburger and Wurtele, 1949).

While low winds are usually prerequisite for radiation fog, advection fogs have been observed to move onshore during periods of maximum onshore winds (Goodman, 1977). California coastal fog formation has been described in terms of prevailing northwesterly surface winds and their reversal (i.e. Santa Anas) plus radiative cooling occurring at night (Pilié et al.,1979).

The liquid water content of fogs is generally much lower than for clouds. Brown and Roach (1976) highlight the importance of gravitational settling of water droplets to successfully model radiation fog. From field observations, Roach et al. (1976) state that the LWC of fog is a small fraction of the total water calculated to have condensed out by cooling. The balance of water is believed to have been deposited on the ground.

B. *Scavenging by Fogs and Clouds*

Fog and cloud droplets form by condensation of water vapor on the active CCN of the atmospheric aerosol and grow by accretion of water vapor. As they grow they are in contact with atmospheric gases and particles which they may absorb; as these scavenged particles and gases dissolve liquid-phase reactions occur, which may in turn affect the absorption properties of the droplet. In this section the various scavenging processes and their efficiencies will be discussed.

1. Scavenging of aerosol particles

Droplets scavenge aerosol particles through nucleation and diffusion processes; scavenging by inertial impaction, which may be important in the case of raindrops, is insignificant in the case of fog and clouds because of the small size and low sedimentation velocities of fog and cloud droplets.

Phoretic forces, to be discussed, may significantly affect scavenging properties during the growth and evaporation stages of the droplets. Electrical charging of the droplets and/or the particles will also affect the scavenging efficiencies through the associated Coulomb force (Zebel, 1968; Williams, 1974). However it is generally considered that except in the most severe thunderstorms with the associated high electric field the influence of electrical effects on scavenging is minor (Slinn, 1974); it will be neglected in further discussion.

a) Scavenging by diffusion

Particles can be absorbed by diffusing to a droplet, either through Brownian motion or through turbulence created by microscale eddies in the atmosphere.

Consider a monodisperse cloud of N droplets cm^{-3} falling through a monodisperse aerosol of n particles cm^{-3}; the sizes of the droplets and of the particles are respectively D and dp, their terminal fall velocities are $V_T(D)$ and $V_T(dp)$, and the diffusion coefficient for the particles is D. Assume that $N \ll n$ so that we can reduce the problem to that of a single droplet falling through the aerosol and assume further that $dp \ll D$. Let r be a radial coordinate representing the distance to the center of the droplet; the diffusion equation for the system can be written:

$$(V_T(D)-V_T(dp))\cdot\nabla n = \nabla\cdot(D\nabla n) \qquad (2)$$

with the boundary conditions:

$$n(r) = 0 \text{ for } r = \frac{D}{2}$$

$$n(r) = n_o \text{ for } r \longrightarrow \infty$$

Approximate mathematical solutions to this equation are given by Levich (1962) and Friedlander (1977) among others. The solutions can be expressed in terms of the scavenging rate λ ($\frac{dn}{dt} = -\lambda n$) of the system:

$$\lambda = N(V_T(D)-V_T(dp))\pi D^2\left(\frac{2\ Pe'^{1/3}}{Pe'}\right) \tag{3}$$

where Pe' is the dimensionless Peclet number:

$$Pe' = \frac{D(V_T(D)-V_T(dp))}{\mathcal{D}} \tag{4}$$

The Peclet number expresses the relative importances of convection (plus eventual boundary-layer diffusion) to diffusion in the diffusion scavenging process.

The diffusion coefficient $\mathcal{D}$ of the particles is the sum of the Brownian diffusion coefficient $\mathcal{D}_B$ and the turbulent diffusion coefficient $\mathcal{D}_T$. $\mathcal{D}_B$ is given by Einstein (1905) as

$$\mathcal{D}_B = \frac{kT}{f} \tag{5}$$

where

k is the Boltzmann constant

T is the temperature

f is the friction coefficient

An interpolation formula for f is

$$f = \frac{3\pi\mu dp}{C} \tag{6}$$

where μ is the viscosity of air and C is a slip correction factor which has been empirically evaluated (Davies, 1945):

$$C = 1 + \frac{2\ell}{dp}(1.257 + 0.400 \exp\ (\frac{-0.55dp}{\ell})) \tag{7}$$

where ℓ is the mean free path of the air molecules.

$\mathcal{D}_T$ is given by Fuchs (1964):

$$\mathcal{D}_T = \frac{1}{16}(\frac{\varepsilon}{\nu})^{1/2} D^2 \tag{8}$$

where ε is the atmospheric energy dissipation rate per unit mass and ν is the kinematic viscosity of air.

Brownian motion dominates the diffusion process for the scavenging of the smaller particles of the aerosol. $\mathcal{D}_B$ decreases strongly with increasing dp, and for the scavenging of the larger particles turbulence plays the major role in diffusion processes. Figure 2 gives $\lambda/N = f(d_p)$ for D = 20 μm, ε = 0.1 erg $g^{-1}s^{-1}$. Scavenging by diffusion is found to be slow; only the very small particles of the aerosol are scavenged with any efficiency during the lifetime of a fog or a cloud (which is generally a few hours).

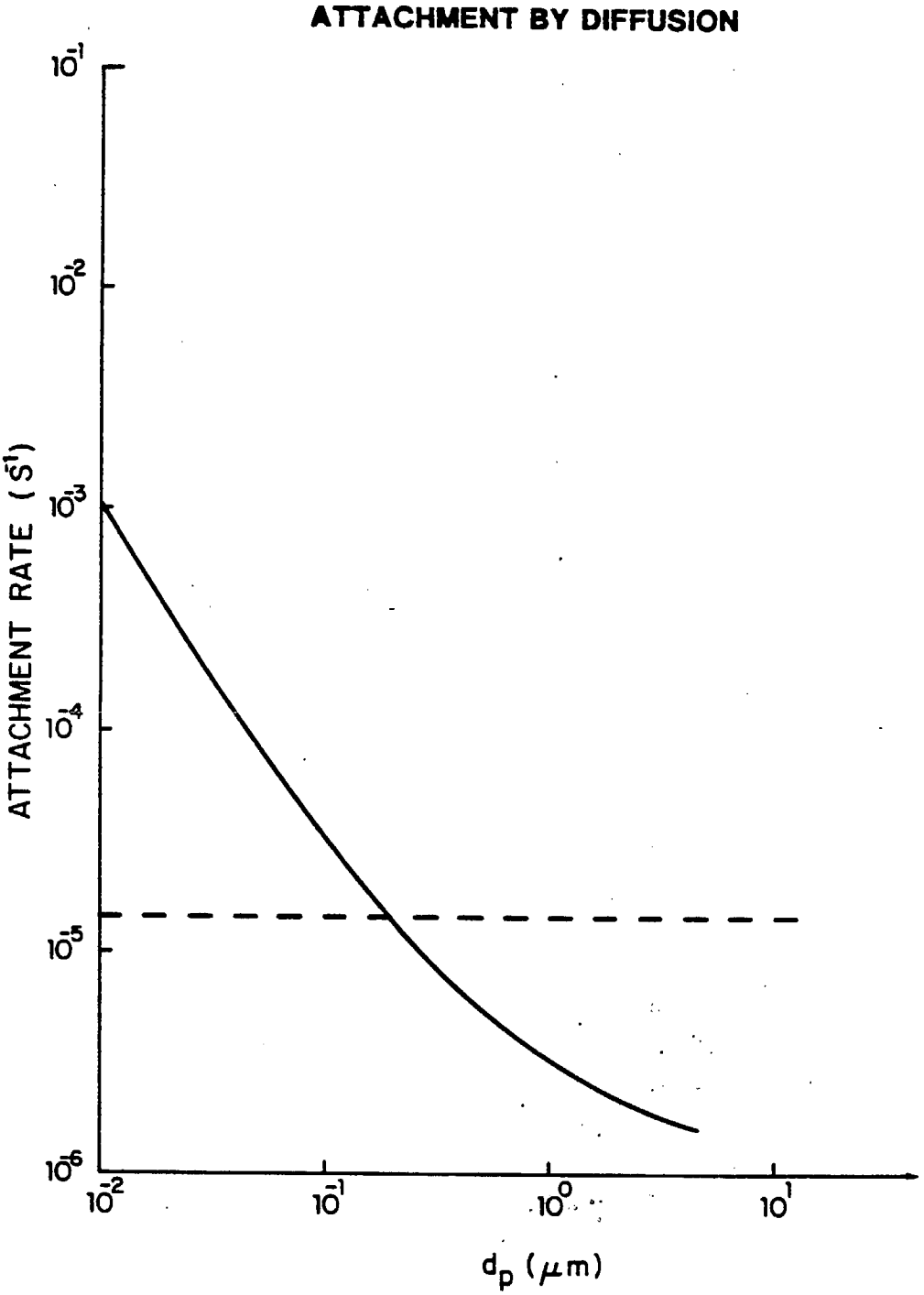
ATTACHMENT BY DIFFUSION
ATTACHMENT RATE (S^{-1})
10^{-1}
10^{-2}
10^{-3}
10^{-4}
10^{-5}
10^{-6}
10^{-2}
10^{-1}
10^{0}
10^{1}
d_p (μm)

Figure 2

b) Scavenging by nucleation

The larger, wettable particles of the atmospheric aerosol (active CCN) are sites for the condensation of water vapor; the activation size of a CCN is a function of its chemical composition and of the ambient supersaturation as discussed in subsection A. The incorporation of the activated CCN into the droplet is an important pathway for the scavenging of aerosol by fog and cloud.

The volume size distribution of the aerosol, as given in Figure 3 for typical urban aerosols, gives an idea of the fraction of the total aerosol mass scavenged by this mechanism. The trimodal distribution characteristic of an urban auto influenced aerosol is generally the one observed in the Los Angeles Basin (Appel et al., 1980); each mode corresponds to particles different both in their formation patterns and their chemical composition (Whitby, 1978; Dzubay and Stevens, 1975). The coarse-particle mode consists essentially of hygroscopic sea salt and soil dust particles which are very easily activated in any fog. The 0.1-1 μm particle size mode is composed mainly of particles generated during combustion processes; these particles have variable hygroscopicity and since their size ranks them as the smaller CCN they may or may not be activated, depending upon their chemical composition. The small-particle mode is made up of particles generated by gas-to-particle conversion; these particles are too small to be effective CCN.

Following this discussion it can be seen from Figure 3 that active CCN will constitute at least 30-40% and up to 90-95% of the total mass of the aerosol. Nucleation is thus found to be a very important pathway for the in-cloud scavenging of the atmospheric aerosol.

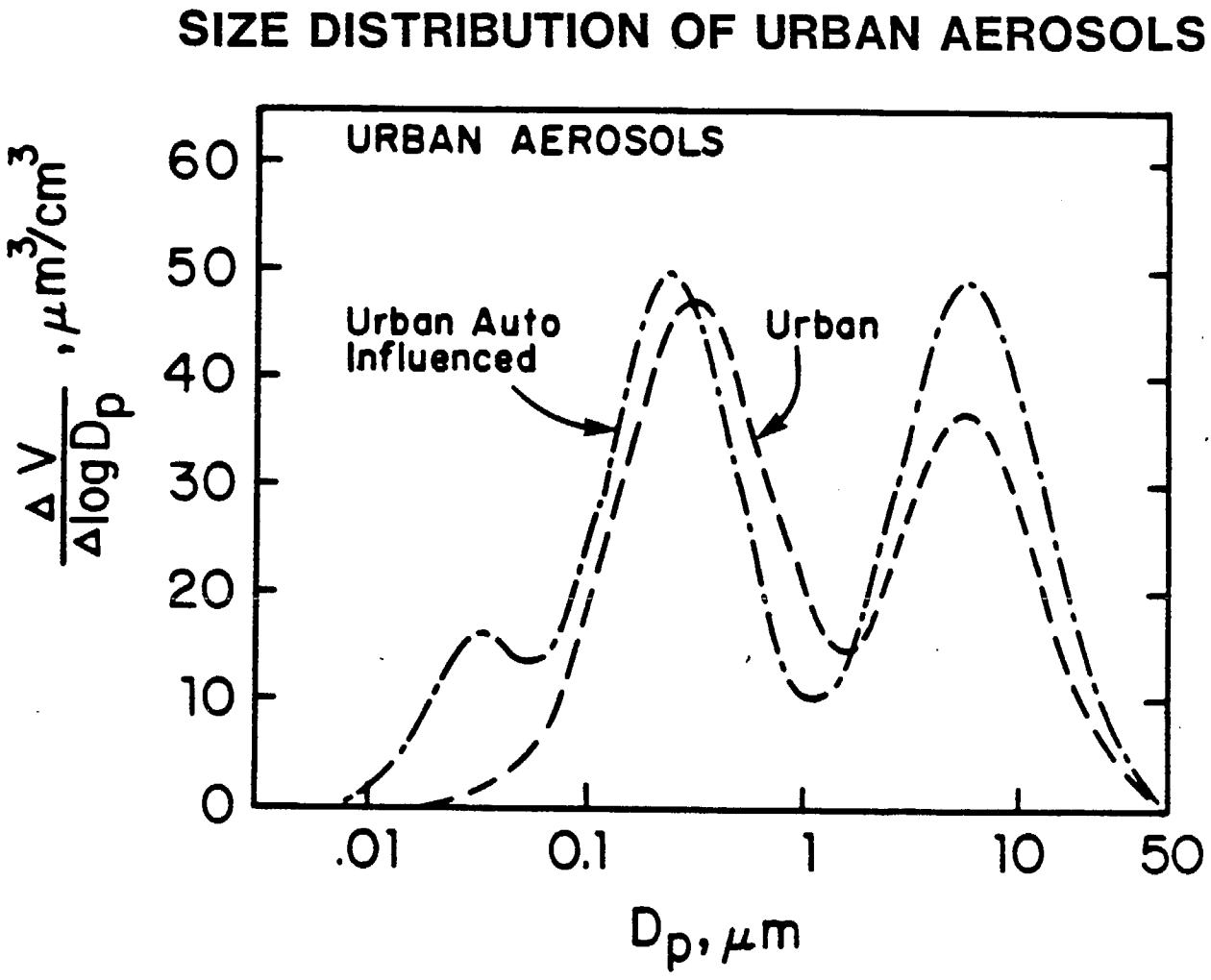
SIZE DISTRIBUTION OF URBAN AEROSOLS
URBAN AEROSOLS
Urban Auto Influenced
Urban
60
50
40
30
20
10
0
.01
0.1
1
10
50
$\frac{\Delta V}{\Delta \log D_p}$, $\mu m^3/cm^3$
$D_p, \mu m$

Figure 3

c) Phoretic forces

Phoretic forces - thermophoresis and diffusiophoresis - may strongly affect the capacity of a cloud to scavenge particles by diffusion (Slinn and Hales, 1974).

Thermophoresis describes the drifting of particles in the direction of the heat flux as a result of temperature nonuniformities in the atmosphere; diffusiophoresis describes the flux of particles in the direction of the flux of water vapor as the result of a water vapor concentration gradient. As fog forms and the droplets condense and grow there is a thermophoretic particle flux away from the droplet and a diffusiophoretic particle flux toward the droplet, whereas when fog dissipates and the droplets evaporate the thermophoretic particle flux is towards the droplet and the diffusiophoretic particle flux is away from the droplet.

Slinn and Hales (1974) show that except for very large particles - with which we are not concerned anyway since they are activated CCN - thermophoresis is the dominant phoretic effect. So the overall result of phoretic forces is to slow down scavenging by diffusion during the formation of the cloud and to enhance it during the dissipation of the cloud.

d) Conclusion

We have seen that roughly 30% to 95% of the total aerosol mass is scavenged by nucleation as the fog or the cloud forms. Compared to this, diffusion processes result only in a slow scavenging of the very small particles of the aerosol; this scavenging rate may be affected by phoretic forces but remains probably slow throughout the lifetime of the fog. Because of this, and because the very small particles scavenged by diffusion do not account for a significant fraction of the total mass of the atmospheric

aerosol (Figure 3), scavenging by diffusion may be neglected with respect to scavenging by nucleation. Scavenging by nucleation is thus the only chemically significant aerosol scavenging process in fogs or clouds.

2. Scavenging of gases

Atmospheric gases are absorbed by the droplets according to Henry's Law and dissociate in the liquid phase through a set of well-documented equilibria given in subsection C. All these equilibria are established very quickly with respect to the time scales involved for atmospheric changes or other chemical reactions in the system (Seinfeld, 1980).

The SO_2 absorbed by the droplets is oxidized to S(VI) following several mechanisms described in subsection C. In raindrops these reactions may be limited by mass transfer inside the drop or from the gas to the surface of the drop instead of by chemical kinetics because of the large size of the drops. However, in cloud and fog droplets $\leq$ 50 μm Freiberg and Schwartz (1981) and Schwartz and Freiberg (1981) show that mass transfer is not a rate-limiting factor. Baboolal et al. (1981) show that this is also true (but for different reasons) for the few fogwater "boulders" (50 μm < dp < 100 μm). All droplets can then be considered well-mixed at all times.

C. *Chemistry of fogs and clouds*

The soluble components of the active CCN, on which the aqueous droplet forms, provide it with an initial chemical loading. As the droplet grows it absorbs gases from the atmosphere, and liquid-phase reactions occur within. In this section and the next the chemistry of the active CCN and the liquid-phase reactions and equilibria resulting from the absorption of atmospheric gases will be discussed.

1. The chemistry of the active CCN

From Figure the chemistry of the aerosol particles likely to be activated in a fog can be estimated as it has been shown that activated CCN comprised the whole coarse-particle mode and a fraction of the 0.1 to 1 μm mode.

The coarse particles are essentially sea salt and wind-blown dusts, and account for the major part of the Na, Mg, K, Cl, Si, Ca, Al, Ti and Fe found in the aerosol (Friedlander, 1973; Dzubay and Stevens, 1975). The 0.1 - 1 μm particles include flyash and most of the nitrate and sulfate aerosols chiefly present (at least in this size range) as their ammonium salts. In the ACHEX study for the Los Angeles Basin, Appel et al. (1980) reports a mass median diameter of 0.1 to 0.6 μm for sulfate particles and 0.6 to 1.2 μm for nitrate particles. A fraction of these 0.1 - 1 μm particles will be activated; since nitrates are larger than sulfates they are also more likely to be activated. The water-soluble components of the active 0.1 - 1 μm CCN will include NH_4^+, SO_4^{2-}, NO_3^- and metals such as Fe, V, Mn, Cu, NO, etc. from fly ash.

In conclusion, the active CCN will account for the following components:

- most of the Na^+, Mg^{2+}, K^+, Cl^-, Si^{4+}, Ca^{2+}, Al^{3+}, Ti^{4+} and Fe^{3+}
- a fraction of the NH_4^+, SO_4^{2-}, NO_3^-, V^{5+}, Mn^{2+} . . .

By dissolving in the newly formed fog droplets these components will provide it with its "initial" chemical loading.

2. Absorption of gases and liquid-phase reactions

As droplets form they absorb gases from the atmosphere; subsequently dissociation of the absorbed gases in the liquid-phase may occur. Some of

relevant equilibria and the corresponding thermochemical data are given in Table III. At the pH encountered in fogs and clouds (pH 2-7) just about all of the ammonia and gaseous nitric acid are instantaneously absorbed by the droplets because of their high Henry's Law coefficients; for other gases absorption is much more limited.

The scavenging of NO_x and SO_2 from the atmosphere leads to the formation of NO_3^- and SO_4^{2-} by liquid-phase oxidation. These reactions are discussed in depth by Hoffmann and Jacob (1983) and Schwartz (1983).

D. *Reactions within droplets*

The relative importances of the various $SO_2 \cdot H_2O$ and $NO_2(aq)$ transformation pathways is now well-documented (Martin et al., 1980; Schwartz, 1983) even though the detailed kinetics are still poorly understood.

The reactions for aqueous-phase disproportionation of NO_x to form nitric and/or nitrous acid are:

$$2NO_2(g) + H_2O(\ell) \longrightarrow 2H^+ + NO_3^- + NO_2^- \qquad (9)$$

$$NO(g) + NO_2(g) + H_2O(\ell) \longrightarrow 2H^+ + 2NO_2^- \qquad (10)$$

$$3NO_2(g) + H_2O(\ell) \longrightarrow 2H^+ + 2NO_3^- + NO_{(g)} \qquad (11)$$

These reactions would be major contributors to the droplet chemistry if allowed to reach equilibrium (Schwartz and White, 1981). However at the low partial pressures of NO_x found in the atmosphere they are very slow and consequently unimportant on the time scales of concern for a fog or a cloud. The work in this area has been reviewed by Schwartz (1983). Additional reactions are listed in Table IV.

Table III. Equilibria and thermodynamic data*

Reaction	$\Delta G^{o}_{298.15}$ (kcal moles^{-1})	$\Delta H^{o}_{298.15}$ (kcal moles^{-1})	$K_{(aq.)}$ (M atm^{-1} or M)
$H_2O(\ell) \rightleftharpoons H^+ + OH^-$	19,093	13,345	$1,008 \times 10^{-14}$
$CO_2(g)+H_2O(\ell) \rightleftharpoons H_2CO_3^*(\ell)$	2,005	-4.846	3.390×10^{-2}
$H_2CO_3^*(\ell) \rightleftharpoons H^+ + HCO_3^-$	8.687	1.825	4.283×10^{-7}
$HCO_3^- \rightleftharpoons H^+ + CO_3^{2-}$	14.09	3.55	4.687×10^{-11}
$NH_3(g) \rightleftharpoons NH_3(\ell)$	-2.41	-8.17	5.844×10^{1}
$NH_3(\ell) \rightleftharpoons NH_4^+ + OH^-$	6.503	8.65	1.709×10^{-5}
$SO_2(g) \rightleftharpoons SO_2(\ell)$	-0.130	-6.247	1.245
$SO_2(\ell) \rightleftharpoons HSO_3^- + H^+$	2.578	-4.161	1.290×10^{-2}
$HSO_3^- \rightleftharpoons SO_3^{2-} + H^+$	9.850	-2.23	6.014×10^{-8}
$HNO_3(g) \rightleftharpoons H^+ + NO_3^-$	-8.92	-17.46	3.460×10^{6}
$H_2O_2(g) \rightleftharpoons H_2O_2(\ell)$		-1.500	3.33×10^{3}
$O_3(g) \rightleftharpoons O_3(\ell)$		-13.24	2.62×10^{-4}

*data from Liljestrand and Morgan (1981), Schumb et al. (1955), and Beutier and Renon (1978)

Kinetic data and rate laws for the aqueous-phase oxidation of S(IV) to S(VI) are reviewed by Martin (1983) and Hoffman and Jacob (1983). The important oxidants for this reaction are H_2O_2 and O_3; oxidation by dissolved O_2 may also be important if catalyzed by Fe^{3+} and Mn^{2+}, for which a catalytic synergism is reported. Oxidation by NO_x and by O_2 catalyzed by trace metals other than Fe^{3+} and Mn^{2+} are now believed to be insignificant. Reaction stoichiometries and kinetic expressions are listed in Table V and VI, respectively.

Aldehydes are ubiquitous contaminants in the atmosphere. They have especially high concentrations in urban atmospheres, where vehicle emissions are a significant or even dominant source (NRC 1981). Aldehydes are also produced via a number of reaction pathways from a variety of precursors in both clean and polluted atmospheres. These include the reaction of OH• radical on methane to form CH_2O and the reaction of OH radical or ozone on alkanes and alkenes. HO_2• radical is a byproduct of these reactions. Aldehydes are reactive and will decompose photolytically or by reaction with free radicals. More radicals and $HONO_2$ are possible byproducts of aldehyde decomposition. The half-life of gaseous CH_2O is fairly short (2-3 hr), but dissolution in water and formation of the hydrated form ($OHCH_2OH$) protects it from photodecomposition. Besides their importance in free-radical chain reactions aldehydes may be important in S(IV) chemistry by forming stable S(IV) adducts. Measurements of aldehyde concentrations in fog, cloud and rainwater are important to a complete understanding of the chemistry involved.

Table IV. Reaction stoichiometries relevant to the aqueous phase production of nitrate.

1. $2NO_2(g) + H_2O(\ell) \longrightarrow 2H^+ + NO_3^- + NO_2^-$

2. $NO(g) + NO_2(g) + H_2O(\ell) \longrightarrow 2H^+ + 2NO_2^-$

3. $3NO_2(g) + H_2O(\ell) \longrightarrow 2H^+ + 2NO_3^- + NO(g)$

4. $2NO_2(aq) + H_2O(\ell) \longrightarrow 2H^+ + NO_2^- + NO_3^-$

5. $NO(aq) + NO_2(aq) + H_2O(\ell) \longrightarrow 2H^+ + 2NO_2^-$

6. $N_2O_4(aq) \longrightarrow 2H^+ + NO_2^- + NO_3^-$

7. $2NO_2(aq) \rightleftharpoons N_2O_4(aq)$

8. $NO_2(aq) + Fe^{2+} \longrightarrow NO_2^-(aq) + Fe^{3+}$

9. $H_2O(\ell) + NO_2(aq) + Fe^{3+} \longrightarrow NO_3^- + 2H^+ + Fe^{2+}$

Table V. Reaction stoichiometries relevant to the aqueous production of sulfate

1. $H_2O_2 + SO_2 \cdot H_2O \longrightarrow 2H^+ + SO_4^{2-} + H_2O_2$

2. $O_3 + SO_2 \cdot H_2O \longrightarrow 2H^+ + SO_4^{2-} + O_2$

3. $O_2 + 2SO_2 \cdot H_2O \xrightarrow[Mn^{2+}]{Fe^{3+}} 4H^+ + 2SO_4^{2-}$

4. $H_2O + N_2O_{4(\ell)} + H_2O \cdot SO_2 \longrightarrow 2HNO_2 + H^+ + HSO_4^-$

5. $4HNO_2(\ell) + 2H_2O \cdot SO_2 \longrightarrow 4NO(aq) + 2H^+ + 2HSO_4^- + 2H_2O$

Table VI. Kinetic expressions for the aqueous-phase osidation of S(IV) to S(VI) at 25°C*

	Reaction	Rate
1.	$SO_2 + H_2O_2$	$\frac{d[S(VI)]}{dt} = \frac{(8\pm2)\times10^4[H_2O_2][SO_{2(aq)}]}{0.1 + [H^+]}$
2.	$SO_2 + O_3$	$\frac{d[S(VI)]}{dt} = \frac{1.9\times10^4([SO_{2(aq)}]+[HSO_3^-])[O_3]}{[H^+]^{1/2}}$
3.	$SO_2 + O_2$ (in presence of Fe and Mn)	$\frac{d[S(VI)]}{dt} = 1970[Mn^{2+}]^2+82[Fe^{3+}]\left(1 + \frac{2.67\times10^3[Mn^{2+}]^{1.5}}{6.31\times10^{-5}+[Fe^{3+}]}\right)[S(IV)]$

*Martin et al. (1980)

E. *Fog as a Precursor to Smog*

1. Introduction

The links between fog, its occurrence and air pollution problems have been noted since the ninteenth century. The "London fog" was one of the earliest and most notorious links observed. The mix of marine moisture and smoke from coal burning was devastating to the health of the populace and to the buildings of the city.

As the chemical mechanisms leading to air pollutant transformations became better understood, the significance of atmospheric water became increasingly apparent. Aqueous-phase processes have been recognized for their importance in the oxidation of atmospheric sulfur dioxide to sulfuric acid. These processes are believed to be important steps in the development of acid rain as well as sulfate aerosol. Another area of impact for atmospheric moisture is the role it plays in visibility degradation. Particulate concentration and relative humidity together contribute to the severity of haze and the occurrence of fog.

2. Fog and Sulfate Aerosol Concentration in Los Angeles

The correlation between days of high sulfate aerosol concentration in Los Angeles and the occurrences of fog or high relative humidity is a striking implication of the significance of aqueous-phase oxidation (Cass, 1975). In a compilation of all days of record between 1965-74 for which 24-hour average sulfate levels exceeded 30 $\mu g\ m^{-3}$ at downtown Los Angeles, coastal fog was observed on half of the days. Furthermore, for virtually each of the 62 days of record, the forecast and/or observation of fog, drizzle or high relative humidity were the case. Cass concludes that the observed high sulfate

concentrations are driven largely by meteorological factors that influence the oxidation rate and the effective mixing volume of the air basin.

The dissolution of gaseous SO_2, leading to aqueous-phase oxidation, has been studied in the laboratory (Möller, 1980; Holt et al., 1981), in clouds (Hegg and Hobbs, 1981; Scott, 1978), and in cloud chambers (Steele et al., 1981; Penkett and Garland, 1974). This process along with the photochemical pathway are generally incorporated onto models of acid rain formation (Adamowicz, 1979; Barrie, 1981). The SO_2 oxidation rates in Los Angeles have been calculated (Roberts, 1975) and found to vary from 1 to 15% hr^{-1}. Sander and Seinfeld (1976) estimate the SO_2 oxidation rate in a photochemical model to have a maximum of 4.5% hr^{-1} due to purely gas-phase processes. The mean rates of oxidation to form sulfate for summer months in 1972-74 as calculated by Roberts (Cass, 1981) are approximately 6% hr^{-1}, that is in excess of the maximum photochemical rate. In addition, the rate calculated for foggy winter months exceeds that for non-foggy winter months (e.g. April -3% hr^{-1} versus November - 1% hr^{-1}).

Another factor which has significant consequence on the transport and transformation of sulfur oxides within the Los Angeles Basin is the sea breeze/land breeze circulation system (Cass and Shair, 1980). This characteristic wind reversal pattern results in the nightly transport of pollutants seaward and the return of aged material inland on the following day. The mesoscale "sloshing" motion serves to increase the retention time available for the oxidation of SO_2 emissions and exacerbates the daily and annual average sulfate concentrations within the basin. Basinwide, the land breeze draws the daytime photochemical products to the coastal region, where a large proportion of the SO_2 emissions are situated. Fog and high relative

humidity are common as the marine layer thickens, leading to the frequent Los Angeles area forecast, "late evening and early morning low clouds and fog along the coast."

3. Fog, Haze and Visibility

The degradation of visibility caused by anthropogenic pollutants and their subsequent conversion products is one of the most obvious and perhaps annoying air pollution problems. A plethora of field investigations has highlighted the dominance of water-soluble submicronous aerosol for the atmospheric light extinction. Sulfates have been estimated as the most important single contributor in reviews of historic data bases and long term trends in the northeast and southwest United States (Trijonis and Yuen, 1978a,b).

White and Roberts (1977), utilizing simultaneous measurements of light-scattering coefficient and ambient aerosol composition in the Los Angeles Basin (Hidy et al., 1974), determined that sulfates and, to a lesser extent, nitrates, are much more effective light scatterers on a per-mass basis than other particulate components. They conclude that sulfates may be responsible for approximately half the light extinction in Los Angeles, while nitrate contributes one quarter. This is in spite of the approximately reverse ratio of sulfur-to-nitrogen oxide emissions in the Los Angeles area (Cass, 1978).

From the data in Los Angeles from 1965-74, Cass (1979) found an increase in light scattering per unit sulfate or nitrate mass on days of high relative humidity. This would be expected due to the hygroscopic nature of these aerosol components. From an investigation of light extinction in radiation fog, Garland, Branson and Cox (1973) reported that about a half of the

extinction coefficient was accounted for by the deliquesced hygroscopic aerosol components, notably sulfate, chloride, nitrate and ammonium, even though pollutant levels were moderate. In an early analysis of Los Angeles haze, clouds and fogs, Neiburger and Wurtele (1949) developed a qualitatively successful formulation of the relationship between visibility and relative humidity between 60% and 100%. They conclude that increases of relative humidity due to radiative cooling of a stable air mass result in the activation of more nuclei rather than the further growth of existing drops.

Thus, as a large number of aerosol grow into the most efficient light-scattering size range, the overall light extinction for a given suspended aerosol mass increases. Cass (1975) notes that for sulfate, the atmospheric moisture has a positive feedback on the degradation of visibility due to the accelerated sulfite oxidation.

A conceptual description for the significance of atmospheric moisture as it relates to aerosol is presented in Fig.6 (Chp. IV). The hygroscopic character of aerosol sulfates and nitrates implies that aqueous processes would be important even below atmospheric saturation of water vapor. In the California Stratus Investigation of 1944 (Neiburger and Wurtele, 1949), maximum relative humidities recorded in Los Angeles vicinity fogs and clouds were frequently less than 100%. Barrett et al. (1979) describe the differences they found between unpolluted marine aerosol, urban smog, and oil-refinery effluent aerosols. Condensation on these different aerosols lead to three types of cloud droplet spectra. Clouds nucleated by marine aerosol had spectra heavily skewed toward larger drop size, while clouds nucleated by

urban smog were dominated by small droplets. The oil-refinery effluent lead to an intermediate droplet spectra. Parungo and Pueschul (1980) observe strong sources of NO in oil-refinery emissions, which are significantly oxidized and converted to large nitrate particles and serve as nuclei to form large cloud droplets. From cloud chamber studies (Steele et al., 1981) atmospheric oxidants such as ozone were found to enhance the dark gas-phase oxidation of NO followed by dissolution of the resultant nitric acid vapor. Further studies (Gertler et al., 1982) document the alteration of the aerosol size distribution following the condensation/evaporation cycle in the cloud chamber. Changes of the aerosol composition have been reported over the course and after fog episodes (Roach et al., 1976).

F. *Relationship of Cloud/Fog Chemistry to Acid Rain*

As noted in Section II-C, atmospheric water droplets are active in the oxidation of SO_2 and NO_x to sulfate and nitrate. During precipitation events the SO_4^{2-} and NO_3^- accumulated in the clouds will be washed out. Additional NO_3 and SO_4^{2-} is produced by reactions on NO_x and SO_2 scavenged as the rain falls through the atmosphere. Previous studies in the Los Angeles area indicate that rain is acidic (Liljestrand and Morgan, 1981; Morgan and Liljestrand, 1980). Our sampling program during the winter of 1981-82 has continued this data base of precipitation chemistry in Los Angeles. Sulfate and nitrate concentrations of 120 and 160 μeq/L, respectively, with a pH of 3.7 (200 μeq ℓ^{-1} as H^+) were recorded. This pH is comparable to some of our fog and cloud data but the sulfate and nitrate are less concentrated in the rain.

G. *Depositional Flux, Fog and Dew Processes.*

In terms of source-receptor relationships, depositional flux of pollutant emissions are nominally divided between wet and dry processes. Lerman (1979) estimates that, for the same ambient concentrations, the flux of chemical species due to precipitation is 10^2 to 10^4 times the dry flux. Scavenging of gas and aerosol by raindrops is a significantly more efficient and rapid transport process. However, in Southern California, rainfall is an intermittent occurrence, while dry flux has the cumulative effect of removing the pollutant species to the surface. Liljestrand (1980) calculated that greater than 90% of the estimated depositional flux of acidity in the Los Angeles Basin was due to dry versus wet flux. His calculations showed that more than 70% of basin emissions were not deposited locally; the difference was assumed to have been removed by either advective transport or chemical neutralization.

Dry deposition of nitrogen-containing species in the Los Angeles Basin are being calculated by an urban-scale photochemical airbed model (McRae, 1982). The model draws attention to the fate of nitric acid and to its neutralization by ammonia. Neutralization to form NH_4NO_3 aerosol has been calculated to increase with relative humidity and decrease with temperature (Stelson and Seinfeld, 1981). The fate of these species is in need of further clarification to determine to what extent they contribute to pollutant fluxes in the basin.

The potential for pollutant deposition caused by fog and by dew have received surprisingly little attention. Brimblecombe (1978) suggests that transfer of SO_2 into leaf wetness (from dew) is an equilibrium process rather

than transport limited. He calculates that a maximum deposition into dew over the United Kingdom could be only 2.3% of the SO_2 emissions where dew deposit is less than 0.5 cm per year. However, significant surface wetness could be caused by fog as well; Roach et al., (1976) calculate from field study that 90% of the condensed water in radiation fog is deposited on the ground. Recent findings (Waldman et al., 1982) suggest that fog is a very efficient scavenger of ambient aerosols and vapor-phase nitric acid. Whether the solutes deposited during for are volatilized after the fog lifts or are neutralized at the surface is an area in need of further research.

Most depositional models consider processes in at least two regions in the bulk atmosphere and near the surface (Slinn, 1974). For gaseous and small particle fluxes, surface processes such as filtration, sorption and resuspension are important. For larger particles (dp > 10 microns), Davidson (1977) found that deposit to the surface was limited by the processes above it such as turbulent eddy diffusion, inertial deposition and sedimentation. The study of pollen deposition (Rayner, 1974) showed interesting results: the flux of particles ($20 \leq dp \leq 100$ micron) to grasslands was in excess of that due to sedimentation alone. The effect of turbulent diffusion was considered primarily responsible.

Deposition flux is usually presented in the following form: $J = -(D + \varepsilon_p)dc/dz - v_s c$ where D and ε_p and J is the molecular and eddy diffusivities and total flux, respectively, and v_s is the sedimentation velocity. Eddy diffusivity has been recognized as a strong function of atmospheric stability (Sehmel and Hodgson, 1974), which serves to squelch

turbulent transport. Raynor (1974) found that pollen deposition in forested areas was very close to the sedimentation limit.

For radiation fog, temperature profiles are usually isothermal or inversional and wind speeds are low, giving rise to high atmosphere stability. Sedimentation of fog droplets is likely to be the most important process leading to deposition. In advection fog, moderate winds can be attained, causing ground layer turbulence (Rodhe, 1962). Advection fog have a greater fraction of large droplets relative to radiation fog (Pinnick et al., 1979), indicating that transport mechanisms, most likely turbulence, are active in addition to sedimentation.

In both classes of fog, Davidson's conclusion that surface layer processes are not rate limiting indicates that measurement of flat plate deposition would be a good approximation of the total flux. A caveat must be acknowledged here: radiation flux (upwards) which promotes fog formation is dependent on the surface layer. Thus, inhibition or promotion of fog on a local scale will impact the flux.

An analogous meteorological phenomenon to fog is the formation of dew. Riley (1961) outlines the conditions which promote dew, and they are strikingly similar to those leading to radiation fog. His list of conditions include that the radiating vegetation surface on which vapor may condense be well insulated from the heat supply of the soil. Similarly, Taylor (1917) noted that on many nights which fit his criteria for fog formation (clear skies, light or no winds, and high relative humidity), dew was deposited instead. Some successful correlations have been made to relate dew duration to commonly measured weather parameters (Crowe et al., 1973). The significance

of dew to the moisture budget is clear in many locations where there is a greater amount of free moisture from frequently occurring dews than from highly seasonal rainfall. Los Angeles and much of the agricultural sections of California fit that description. This source of moisture is important also in terms of plant pathology, e.g. growth of fungi, and, perhaps, pollutant uptake.

References - Chapter 2

Adamowicz, R. (1979) "A Model for the Reversible Washout and Production of Sulfate in Raindrops," Atmos. Environ. 13, 105-121.

Appel, B. R., S. M. Wall, Y. Tokiwa and M. Haik (1980) "Simultaneous Nitric Acid, Particulate Nitrate, and Acidity Measurements in Ambient Air," Atmos. Environ. 14, 549-554.

Appel, B. R., E. L. Kothny, E. M. Hoffer and J. J. Wesolowski (1980) "Sulfate and Nitrate Data from the California Aerosol Characterization Experiment (ACHEX)," Adv. Environ. Sci. Tech. 9, 315-336.

Baboolal, B., H. R. Pruppacher and J. H. Topalian (1981) "A Sensitivity Study of a Theoretical Model of SO_2 Scavenging by Water Drops in Air," J. Atmos. Sci. 38, 856-870.

Barrett, E., F. P. Parungo and R. F. Pueschel (1979) "Cloud Modification by Urban Pollution: A Physical Demonstration," Meteorol. Resch. 32, 136-149.

Barrie, L. A. (1981) "The Prediction of Rain Acidity and SO_2 Scavenging in Eastern North America," Atmos. Environ. 15, 31-41.

Beutier, D. and H. Renon (1978) "Representation of NH_3-H_2S-H_2O, NH_2-CO_2-H_2O, NH_3-SO_2-H_2O Vapor-Liquid Equilibria," Ind. Eng. Chem. Process Des. Dev. 17, 220.

Brimblecombe, P. (1978) "Dew as a sink for SO_2," Tellus 30, 151-157.

Brown, R. and W. T. Roach (1976) "The Physics of Radiation Fog: II - A Numerical Study," Quart. J. R. Met. Soc. 102, 335-354.

Cass, G. R. (1975) "Dimensions of the Los Angeles SO_2/SO_4^{2-} Problem," Environmental Quality Laboratory No. 15, California Institute of Technology, Pasadena, CA.

Cass, G. R. (1978) "Methods for Sulfate Air Quality Management with Applications to Los Angeles," Ph.D. Thesis, California Institute of Technology, Pasadena, CA.

Cass, G. R. (1979) "On the Relationship between Sulfate Air Quality and Visibility with Examples in Los Angeles," Atmos. Environ. 13, 1069-1084.

Cass, G. R. and F. H. Shair (1980) "Transport of Sulfur Oxides Within the Los Angeles Sea Breeze/Land Breeze Circulation System," in Proceedings of the 2nd Joint Conference on Applications of Air Pollution Meteorology, American Meterological Society, pp. 320-327.

Cass, G. R. (1981) "Sulfate Air Quality Control Strategy Design," Atmos. Environ. 15, 1227-1249.

Crowe, M. J., et al. (1978) "Forecasting Dew Duration at Pendleton, Oregon, Using Simple Weather Observations," J. Appl. Met. 17, 1482-1487.

Davidson, C. I. (1977) "Deposition of Trace Metals Containing Aerosols on Smooth, Flat Surfaces and on Wild Oat Grass (Avena fatua)," Ph.D. Thesis, California Institute of Technology, Pasadena, CA.

Davies, C. N. (1945) "Definitive Equations for the Fluid Resistance of Spheres," Proc. Phys. Soc. 57, 259-270.

Dzubay, T. G. and R. K. Stevens (1975) "Ambient Air Analysis with Dichotomous Sampler and X-Ray Fluorescence Spectrometer," Environ. Sci. Tech. 9, 663-668.

Einstein, A. (1905) "Über Die Von Der Molekular Kinetischen Theorie Der Wärme Gerforderte Bewegung Von In Ruhenden Flüssigkeiten Suspendierten Teilchen," Annal. Physik 17, 549-560.

Freiberg, J. E. and S. E. Schwartz (1981) "Oxidation of SO_2 in Aqueous Droplets: Mass-Transport Limitation in Laboratory Studies and the Ambient Atmosphere," Atmos. Environ. 15, 1145-1154.

Friedlander, S. K. (1973) "Chemical Element Balances and Identification of Air Pollutant Sources," Environ. Sci. Tech. 7, 235-240.

Friedlander, S. K. (1977) Smoke, Dust and Haze, John Wiley and Sons, New York.

Fuchs, N. A. (1964) The Mechanics of Aerosols, Pergamon Press, Oxford, England.

Garland, J. A., J. R. Bronson and L. C. Cox (1973) "A Study of the Contribution of Air Pollution to Visibility in a Radiation Fog," Atmos. Environ. 7, 1079-1092.

Gertler, A. W., D. F. Miller, D. Lamb and U. Katz (1982) SO_2 and NO_2 Reactions in Cloud Droplets, Ann Arbor Science, Inc., Ann Arbor, MI.

Goodman, J. (1977) "The Microstructure of California Coastal Fog and Stratus," J. Appl. Meteor. 16, 1056-1067.

Hegg, D. A. and P. V. Hobbs (1981) "Cloudwater Chemistry and the Production of Sulfates and Clouds," Atmos. Environ. 15, 1597-1604.

Hidy, G. M., et al. (1974) "Characterization of Aerosols in California (ACHEX)," Science Center, Rockwell International, California Air Resources Board Contract No. 358.

Hoffmann, M. R. and D. J. Jacob (1983) "Kinetics and Mechanisms of the Catalytic Oxidation of Dissolved Sulfur Dioxide in Aqueous Solution: An Application to Nighttime Fogwater Chemistry," in Acid Precipitation, J. G. Calvert, ed., Ann Arbor Science Publ., Ann Arbor, MI (in press).

Holt, B., R. Kumer and P. Cunningham (1981) "Oxygen-18 Study of the Aqueous-Phase Oxidation of SO_2," Atmos. Environ. 15, 557-566.

Lerman, A. (1971) Geophysical Processes, Wiley-Interscience, New York.

Levich, V. G. (1962) Physiochemical Hydrodynamics, Prentice-Hall, Engelwood Cliffs, NJ.

Liljestrand, H. M. (1980) "Atmospheric Transport of Acidity in Southern California by Wet and Dry Mechanisms," Ph.D. Thesis, California Institute of Technology, Pasadena, CA.

Liljestrand, H. M. and J. J. Morgan (1981) "Spatial Variations of Acid Precipitation in Southern California," Environ. Sci. Tech. 15, 333-338.

Mack, E. J. and R. J. Pilie (1973) "The Microstructure of Radiation Fog at Travis Air Force Base," Calspan Corp., Buffalo, New York, Report No. CJ-5076-M-2.

Mack, E. J., U. Katz, C. W. Rogers, D. W. Gaucher, K. H. Piech, C. K. Aker and R. J. Pilie (1977) "An Investigation of the Meteorology, Physics, and Chemistry of Marine Boundary Layer Processes," Calspan Corp., Buffalo, New York, Report No. CJ-6017-M-1.

Martin, L. R. (1983) "Kinetic Studies of Sulfite Oxidation in Aqueous Solution," in Acid Precipitation, J. G. Calvert, ed., Ann Arbor Science Publ., Ann Arbor, MI (in press).

Martin, L. R., D. E. Damschen and H. S. Judeikis (1980) "Sulfur Dioxide Oxidation Reactions in Aqueous Solutions," Aerospace Report ATR-81(7700)-1.

Mason, B. J. (1971) The Physics of Clouds, 2nd ed., Oxford University Press, London.

McRae, G. (1982) "Dry Deposition of Nitrogen-Containing Species," in Acid Precipitation, Ann Arbor Science Publ., Ann Arbor, MI (in press).

Möller, D. (1980) "Kinetic Model of Atmospheric SO_2 Oxidation Based on Unpublished Data," Atmos. Environ. 14, 1067-1076.

National Research Council (1981) Formaldehyde and Other Aldehydes, National Academy Press, Washington, D.C.

Neiburger, M. and M. G. Wurtele (1949) "On the Nature and Size of Particles in Haze, Fog, and Stratus of the Los Angeles Region," Chem. Rev. 44, 321-335.

Parungo, F. P. and R. F. Pueschel (1980) "Conversion of Nitrogen Oxide Gases to Nitrate Particles in Oil Refinery Plumes," J. Geophys. Res. 85, 4507-4511.

Penkett, S. A. and J. A. Garland (1974) "Oxidation of SO_2 in Artificial Fogs by O_3," Tellus 26, 284-289.

Pilié, R. J., E. J. Mack, C. W. Rogers, U. Katz and W. C. Kocmond (1979) "The Formation of Marine Fog and the Development of Fog-Stratus Systems Along the California Coast," J. Appl. Met. 18, 1275-1286.

Pinnick, R. G., S. G. Jennings, P. Chylek and H. J. Avermann (1979) "Verification of a Linear Relationship Between IR Extinction, Absorption and LWC of Fogs," J. Atmos. Sci. 36, 1577-1586.

Pruppacher, H. R. and J. D. Klett (1978) Microphysics of Clouds and Precipitation, D. Reidel, Holland.

Rayner, G. S. (1976) "Experimental Studies of Pollen Deposition to Vegetated Surfaces," in Atmosphere-Surface Exchange of Particulate and Gaseous Pollutants (1974), NTIS No. CONF-740921.

Riley, J. (1961) "Moisture and Cotton at Harvest Time in the Mississippi Delta," Mon. Wea. Rev. 89, 341-353.

Roach, W. T. (1976) "On the Effect of Radiative Exchange on the Growth by Condensation of a Cloud or Fog Droplet," Quart. J. R. Met. Soc. 102, 361-372.

Roach, W. T., R. Brown, S. J. Coughey, J. A. Garland and C. J. Readings (1976) "The Physics of Radiation Fog: I - A Field Study," Quart. J. R. Met. Soc. 102, 313-333.

Roberts, P. T. (1975) "Gas-to-Particle Conversion: Sulfur Dioxide in a Photochemically Reactive System," Ph.D. Thesis, California Institute of Technology, Pasadena, CA.

Rodhe, B. (1962) "The Effect of Turbulence on Fog Formation," Tellus 14, 49-86.

Sander, S. P. and J. H. Seinfeld (1976) "Chemical Kinetics of Homogeneous Oxidation of Sulfur Dioxide," Environ. Sci. Tech. 10, 1114-1123.

Sax, R. I., et al. (1975) "Weather Modification . . . An Editorial Overview," J. Appl. Meteor. 14, 652-672.

Schumb, W. C., C. N. Satterfield and R. C. Wentworth (1955) Hydrogen Peroxide, ACS Monograph Series, Reinhold, New York.

Schwartz, S. E. and J. E. Freiberg (1981) "Mass Transport Limitation to the Rate of Reaction of Gases in Liquid Droplets: Application to Oxidation of SO_2 in Aqueous Solutions," Atmos. Environ. 15, 1129-1144.

Schwartz, S. E. and W. H. White (1981) "Solubility Equilibria of the Nitrogen Oxides and Oxyacids in Dilute Aqueous Solution," Adv. Env. Sci. Eng. 4.

Schwartz, S. E. (1983) "Gas-Aqueous Reactions of Sulfur and Nitrogen Oxides in Liquid-Water Clouds," in Acid Precipitation, J. G. Calvert, ed., Ann Arbor Science Publ., Ann Arbor, MI (in press).

Sehmel, G. A. and W. H. Hodgson (1976) "Predicted Dry Deposition Velocities," in Atmosphere-Surface Exchange of Particulate and Gaseous Pollutants (1974), NTIS No. CONF-740921.

Scott, W. D. (1978) "The pH of Cloud Water and the Production of Sulfate," Atmos. Environ. 12, 917-921.

Seinfeld, J. H. (1980) Lectures in Atmospheric Chemistry, AIChE Monograph Series 76.

Slinn, W. G. N. and J. Hales (1970) "Phoretic Processes in Scavenging," in Precipitation Scavenging, AEC Symposium Series 22.

Slinn, W. G. N. (1974) "Precipitation Scavenging: Some Problems, Approximate Solutions, and Suggestions for Future Research," in Precipitation Scavenging, ERDA Symposium Series 41.

Steele, R. L., A. W. Gertler, U. Katz, A. Lamb and D. F. Miller (1981) "Cloud Chamber Studies of Dark Transformations of SO_2 in Cloud Droplets," Atmos. Environ. 15, 2341-2352.

Stelson, A. W. and J. H. Seinfeld (1982) "Relative Humidity and Temperature Dependence of the Ammonium Nitrate Dissociation Constant," Atmos. Environ. 16, 983-992.

Taylor, G. I. (1917) "The Formation of Fog and Mist," Quart. J. R. Met. Soc. 183, 241-268.

Thornton, J. D. (1981) "The Metal and Strong Acid Composition of Rain and Snow in Minnesota: Land Use Effects," M.S. Thesis, University of Minnesota, Minneapolis, MN.

Trijonis, J. and K. Yuan (1978a) "Visibility in the Northeast: Long-Term Visibility Trends and Visibility/Pollutant Relationships," Research Triangle Park, NC, EPA-600/3-78-075.

Trijonis, J. and K. Yuan (1978b) "Visibility in the Southwest: Exploration of the Historical Data Base," Research Triangle Park, NC, EPA-600/3-78-039.

U.S. EPA (1971) "Guide for Air Pollution Avoidance. Appendix B. History of Episodes," PH-22-68-32, 123-135.

Waldman, J. M., J. W. Munger, D. J. Jacob, R. C. Flagan, J. J. Morgan and M. R. Hoffmann (1982) "Chemical Composition of Acid Fog," Science 218, 677-680.

Warner, J. (1969) "The Microstructure of Cumulus Cloud. Part I - General Features of the Droplet Spectrum," J. Atmos. Sci. 26, 1049-1059.

Whitby, K. T. (1978) "The Physical Characteristics of Sulfur Aerosols," Atmos. Environ. 12, 135-159.

White, W. H. and P. T. Roberts (1977) "On the Nature and Origins of Visibility-Reducing Aerosols in the Los Angeles Air Basin," Atmos. Environ. 11, 803-812.

Wilkins, E. T. (1954a) "Air Pollution Aspects of the London Fog of December, 1952," J. Roy. Meteorol. Soc. 80, 267-278.

Wilkins, E. T. (1954b) "Air Pollution and the London Fog of December, 1952," J. Roy. Sanit. Instit. 74, 1-21.

Williams, H. (1974) "Analysis of In-Cloud Scavenging Efficiencies," Precipitation Scavenging, ERDA Symposium Series 41.

Wilson, J. C. and P. H. McMurry (1981) "Studies of Aerosol Formation in Power Plant Plumes - I. Secondary Aerosol Formation in the Navajo Generating Station Plume," Atmos. Environ. 15, 2329-2339.

Zebel, G. (1968) "Capture of Small Particles by Drops Falling in Electric Fields," J. Colloid Interf. Sci. 27, 394-404.

CHAPTER III

CHEMICAL COMPOSITION OF ACID FOG

by

Jed M. Waldman, J. William Munger, Daniel J. Jacob
Richard C. Flagan, James J. Morgan, and Michael R. Hoffmann*

ABSTRACT

Fog water collected in Los Angeles and Bakersfield, California was found to have higher concentrations of major chemical components than previously observed in atmospheric water droplets. The pH of fog water was found to be in the range of 2.2 to 4.0. Dominant processes controlling the fog-water chemistry appear to be condensation and evaporation of water vapor on pre-existing aerosol and scavenging of gas phase nitric acid.

Submitted to Science: March 15, 1982

Revised: May 1, 1982

Accepted: May 16, 1982

*To Whom Correspondence Should be Addressed

CHEMICAL COMPOSITION OF ACID FOG

ABSTRACT

Fog water collected in Los Angeles and Bakersfield, California was found to have higher concentrations of major chemical components than previously observed in atmospheric water droplets. The pH of fog water was found to be in the range of 2.2 to 4.0. Dominant processes controlling the fog-water chemistry appear to be condensation and evaporation of water vapor on pre-existing aerosol and scavenging of gas phase nitric acid.

In the fall of 1981, a field study was initiated to determine the chemical composition of fog water in the Los Angeles basin. Results show that the fog water is significantly more acidic and concentrated with respect to chemical composition than cloud and rain water collected in Southern California. Earlier, Liljestrand and Morgan (1) determined the chemical composition of rain in Los Angeles and reported that light, misting rainfalls had the highest acidity (2). Previous fog water studies (3) in non-urban environments have reported concentration levels of major ions comparable to those reported for cloud (4) and rain (5) water. However, urban fogs tend to form under more polluted conditions than clouds. The present research program expands upon these previous studies in an attempt to focus on the chemical and physical processes that occur in the atmospheric aqueous phase before a precipitation event. In the Los Angeles basin fog and cloud water processes may represent a significant pathway for SO_2 and NO_x oxidation and for the concomitant production of acidity. Furthermore, morning fog and low clouds along the coast have been strongly correlated with high sulfate aerosol concentrations during the afternoon in the Los Angeles basin (6).

In this study, fog water was collected with a rotating arm collector (7). Droplets impact in slots along the ends of the arm and are driven outward by centrifugal force into sample collection bottles which serve effectively to isolate the collected liquid. In cloud chamber tests, the lower particle size cutoff for this collector was estimated to be 8 μm. Two of the collection sites were located in the Los Angeles basin (Pasadena and Lennox) and the third was located in the San Joaquin Valley near Bakersfield. The Pasadena site was located in a residential neighborhood 25 km from downtown Los Angeles;

the Lennox site was located 2 km from the Los Angeles International Airport adjacent to a freeway and near two power plants and one oil refinery; and the site in the San Joaquin Valley was located in Oildale, which is surrounded by secondary oil recovery operations.

Concentration ranges of major chemical components observed during five separate fog events are listed in Table 1. These ranges represent the low and high values measured in time-sequenced samples over the duration of the particular fog events (8).

The first fog event in Pasadena followed a day with good air quality; the second fog event was preceded by a hazy day. Concentrations of most ions in the latter fog water were much higher than in the first fog event. The third fog event was sampled in Lennox on the second night of dense coastal fog. Smog and dense haze had persisted throughout the preceding day, accompanied by high ambient NO_x concentrations along the coast. These samples had even higher concentrations than the Pasadena fog samples. In addition, the fog water contained a significant amount of solid material, especially in the final sample taken as the fog dissipated. Most of the particles remained suspended in the samples after standing several days, which suggests that they were too small to have been collected unless incorporated in larger droplets.

A single fog event in the San Joaquin Valley at Bakersfield was monitored during a period of extended fog throughout the entire valley. The southern portion of the San Joaquin Valley has a number of oil fields in which steam injection, oil recovery methods are used. Consequently, the sulfur emissions are high for a non-urban, agricultural area. The fog-water analyses, which were characterized by low pH values (pH 2.9) and high SO_4^{2-} (5.0 meq/L), NO_3^- (5.1 meq/L) and NH_4^+ (9.8 meq/L), reflect the dichotomous land use in the San Joaquin Valley.

Finally, a single fog-water sample was collected on the night of 17 January 1982 in Pasadena. The pH of this sample (pH 2.25) was unusually low with correspondingly high levels of NO_3^- (12 meq/L), SO_4^{2-} (5 meq/L) and NH_4^+ (8 meq/L); however, the duration of this final fog event in Pasadena was relatively short ($\sim$ 1 hr.).

Concentrations of major components in the California fog samples were significantly higher than in previously reported samples of fog, cloud and rainwater as shown for comparison in Table 1. In the case of SO_4^{2-}, NO_3^-, NH_4^+ and H^+, the observed concentrations were 10-100 times higher than the previously reported values. Concentrations of Na^+, K^+, Ca^{2+}, Mg^{2+} and Cl^- were high but more in line with values reported for fog and cloud water in other areas. High concentrations of formaldehyde, iron, manganese and sulfite (30-260 μeq/L) were also found. Observed concentrations of S(IV) appear to be in excess of those predicted by Henry's Law considerations although formation of sulfonic acid derivatives and iron sulfito complexes can account for this apparent discrepancy (9).

Figure 1 illustrates changes in total ionic concentration with respect to time for three fog events. A concave trend in the concentration vs. time profile (decreasing at the beginning and rising toward the end) was observed. Changes in absolute concentration of individual ions that are proportional to the changes in total concentration indicate that water vapor condensation or evaporation of the fog droplets are dominant processes. Sharp decreases in concentration during the first few hours of the fogs in Lennox were due primarily to initial droplet deliquescence on pre-existing aerosol. Similarly, most of the increase in concentration that was observed as the fogs dissipated was due to evaporation and regeneration of fine aerosol. These physical effects apparently play a dominant role in determining fog chemistry in the Los Angeles basin.

The dominant ions in the fog water were NH_4^+, H^+, NO_3^- and SO_4^{2-}, and their highest concentrations were observed after days of dense haze. During the early phases of the Lennox fogs, these ions comprise $\geq$ 90% of the total ionic concentration. This suggests that pre-existing aerosol is a major determinant of the chemical composition of fog-water, since these four species are the major components of the daytime aerosol haze (10).

In Los Angeles, the NO_3^- to SO_4^{2-} equivalent ratio in fog water was about 2.5, which is comparable to the reported emission ratio (3). The corresponding ratio in Los Angeles precipitation was close to 1.0 (1). In the Bakersfield fog, the nitrate to sulfate equivalent ratio was approximately one.

The observed changes in fog-water composition may have resulted either from chemical changes in the droplets or advection of different air masses over the sites. In Pasadena, $[H^+]$ and $[NO_3^-]$ simultaneously increased as a function of time suggesting the transport of HNO_3 or N_2O_5 into the droplets (11). On 7 December in Lennox, $[NH_4^+]$ doubled from the third to the fourth sampling period while there was a corresponding decrease in $[H^+]$. Transfer of gaseous NH_3 into the droplets could account for this neutralization. However, the delay in the $[NH_4^+]$ increase after the onset of fog suggests that advection of fog formed on condensation nuclei with different characteristics was responsible. During the last few hours of that event, an increase in $[Ca^{2+}]$, $[Mg^{2+}]$ and [Fe] was observed. This increase coincides with the morning rush hour traffic on the adjacent freeway and can be attributed to the incorporation of road and soil dust into the fog. Finally, the fogs in Lennox started out with a high acidity that was progressively neutralized, while the fogs in Pasadena became more acidic during a fog event. This result suggests differences in the composition of the aerosol preceding the fog at each site and differences in gas or solid to liquid transfer characteristics.

In conclusion, results of this study have shown that concentrations of major chemical species in fog water collected in Los Angeles and Bakersfield are significantly higher than previously reported in atmospheric water droplets. The chemistry of fog water in Los Angeles appears to be dominated by the composition of the haze-forming aerosol that precedes it. Subsequent effects of condensation and evaporation control the observed concentration levels. Secondary aerosol, which has high NH_4^+, H^+, NO_3^-, and SO_4^{2-} levels, deliquesces initially to give a concentrated fog water. Further condensation of water results in dilution. After initial formation, the fog water appears to incorporate additional NH_3, HNO_3 and calcareous dust. As the fog dissipates due to evaporation higher concentrations are again observed.

In light of the inordinately high concentrations of acidic components found in Los Angeles fog, further research is needed to determine the role of aqueous atmospheric droplets in SO_2 and NO_x conversion and acidity transport processes. High levels of H^+, NO_3^- and SO_4^{2-} found in fog water may have a significant effect on health and on materials and plants in urban areas such as Los Angeles and non-urban areas such as Bakersfield.

Jed M. Waldman
J. William Munger
Daniel J. Jacob
Richard C. Flagan
James J. Morgan
Michael R. Hoffmann *

Environmental Engineering Science
W. M. Keck Laboratories
California Institute of Technology
Pasadena, CA 91125

REFERENCES AND NOTES

1. H. M. Liljestrand and J. J. Morgan, Environ. Sci. Tech., 12, 1271 (1978); H. M. Liljestrand, Atmospheric Transport of Acidity in Southern California by Wet and Dry Mechanisms, Ph.D. Thesis, California Institute of Technology, Pasadena, CA (1980); H. M. Liljestrand and J. J. Morgan, Environ. Sci. Tech., 15, 333 (1981).
2. J. J. Morgan and H. M. Liljestrand, California Air Resources Board Report, W. M. Keck Laboratory, California Institute of Technology, Pasadena, CA, Report No. AC-2-80 (1980).
3. H. Houghton, J. Meteor., 12, 355 (1955); O. M. Petrenchuk and V. M. Drozdova, Tellus, 18, 280 (1966); E. Mack and U. Katz, Calspan Corp. Report, Buffalo, NY, Report No. CJ-6017-M-1 (1977).
4. H. Mrose, Tellus, 18, 266 (1966); T. Okita, J. Meteor. Soc. Japan, 46, 120 (1968); C. S. Martens and R. C. Harriss, J. Geophys. Res., 78, 949 (1973); R. Castillo, personal communication (1980); R. E. Falconer and P. D. Falconer, J. Geophys. Res., 85, 7465 (1980), P. D. Falconer, Ed., Atmospheric Sciences Research Center, SUNY, Albany, Publication 806 (1981).
5. V. M. Drozdova and E. P. Makhon'ko, J. Geophys. Res., 75, 3610 (1970); L. Granat, Tellus, 24, 550 (1972); C. V. Cogbill and G. E. Likens, Water Res. Research, 10, 1133 (1974).
6. G. R. Cass, Methods for Sulfate Air Quality Management with Applications to Los Angeles, Ph.D. Thesis, California Institute of Technology, Pasadena, CA (1977); G. R. Cass, EQL Memorandum, California Institute of Technology, Pasadena, CA, Memo No. 5 (1975).

7. The Caltech RAC was modified from an original design by E. J. Mack and R. Pilie, U.S. Patent No. 3885532 (1975). The impaction surfaces move at a velocity of approximately 50 m/s. A sampling velocity that is much greater than the ambient wind speed serves to minimize the bias due to anisokinetic sampling/ K. R. May in Airborne Microbes, P. H. Gregory and J. L. Monteith, Eds. (1967). Thermodynamic and mass transfer calculations suggest that evaporation of the fog water is insignificant during the time of collection.

8. Immediately after collection, the pH of the sample was measured and aliquots were separated to be preserved for later analyses. Major metal cations were determined by atomic absorption spectrophotometry (AAS) and major anions by ion chromatography (IC). Ammonium ion and formaldehyde were determined by standard colorimetric methods. Addition of nitric acid (Ultrex grade) was used to preserve the trace metals; sulfite was stabilized by reaction with formaldehyde at pH 4.

9. L. D. Hanse, L. Whiting, D. J. Eatough, T. E. Jensen, R. M. Izatt, Anal. Chem., 48, 634 (1976).

10. B. R. Appel, E. L. Kothny, E. M. Hoffer, and J. J. Wesolowski, in The Character and Origins of Smog Aerosols, G. M. Hidy, ed., Adv. Environ. Sci. Tech., 9, 315-336 (1980).

11. J. H. Seinfeld, Air Pollution, McGraw-Hill, New York (1975).

12. Financial support for this research was provided by the California Air Resources Board (AO-141-32) and logistical support was provided by the South Coast Air Quality Management District. Special acknowledgement is extended to Drs. G. Cass, D. Lawson and J. H. Seinfeld for assistance.
All correspondence should be addressed to M. R. Hoffmann.

TABLE I

Location	# Samples	Date	pH	$\mu eq\ \ell^{-1}$ H^+	Na^+	K^+	NH_4^+	Ca^{2+}	Mg^{2+}	F^-	Cl^-	NO_3^-	SO_4^{2-}	$mg\ \ell^{-1}$ Fe	CH_2O	Reference
Pasadena	4	11/15/81	5.25-4.74	5.6-55	12-496	4-39	370	19-360	7-153	120	56-280	130-930	62-380	0.894-2.1	-	This study
Pasadena	4	11/23/81	4.85-2.92	14-1200	320-500	33-53	1290-2380	140-530	99-360	180-410	480-730	1220-3520	481-944	0.92-1.77	3.1-3.5	"
Lennox	8	12/7/81	5.78-2.55	2-2820	28-480	6-160	1120-4060	44-4350	17-1380	115-395	111-1110	820-4560	540-2090	0.34-24	4.6-12.8	"
Lennox	3	12/17/81	2.81-2.52	1550-3020	80-166	19-40	950-1570	73-190	43-99	180-500	90-197	2070-3690	610-1970	1.02-2.08	-	"
Bakersfield*	3	1/14/82	3.07-2.90	850-1260	151-1220	39-224	5370-10520	165-1326	20-151	126-242	203-592	3140-5140	2250-5000	-	6.1-14.4	"
Pasadena*	1	1/17/62	2.25	5625	2180	500	7870	2050	1190	637	676	12000	5060	-	-	"
Los Angeles Rain (vol wt means at 9 sites)		1978-79	5.4-4.4	4-39	4-37	0.24-4.9	1-36	3.9-17	1.7-11	-	5-52	11-44	7-56	.004-.17	-	Liljestrand & Morgan (1)
Coastal Calif. Fogs		9-10/76	-	-	78-944	8-26	1-578	9-102	17-175	-	96-1230	23-234	52-490	-	-	Meck and Katz (3)
Whiteface Mtn.		7-8/00	4.2-3.2	63-530	1-55	1-6	4-310	-	-	11-54	1-15	7-190	40-600	-	-	Falconer (4)
Fog & Clouds USSR		1961-64	5.3-4.7	5-20	30-104	15-44	33-100	20-50	17-83	-	59-177	2-13	13-185	-	-	Petrenchuk & Drozdova (3)

*$[Na^+]$, $[K^+]$, $[Ca^{2+}]$, $[Mg^{2+}]$, and $[NH_4^+]$ for filtered aliquots

TABLE AND FIGURE CAPTIONS

Table 1. Ranges in ionic concentration observed during six fog events (8). Representative concentrations for other fog, cloud and rain samples are presented for comparison. The ranges shown in values for this study are from sequential samples during individual events with the exception of the sixth event. For comparison data, the ranges represent many events.

Figure 1. Ionic composition in serial samples collected during three Los Angeles fog events. The width of each bar represents the sampling interval. Fog formation and dissipation (i.e. beginning and end of individual fog events) are indicated by arrows. Fog had formed at least one hour prior to the first sample on 7 December 1981; sampling on 17 December 1981 was ended before the fog dissipated. The effect of dilution and concentration can be seen by the proportional changes in ionic concentration.

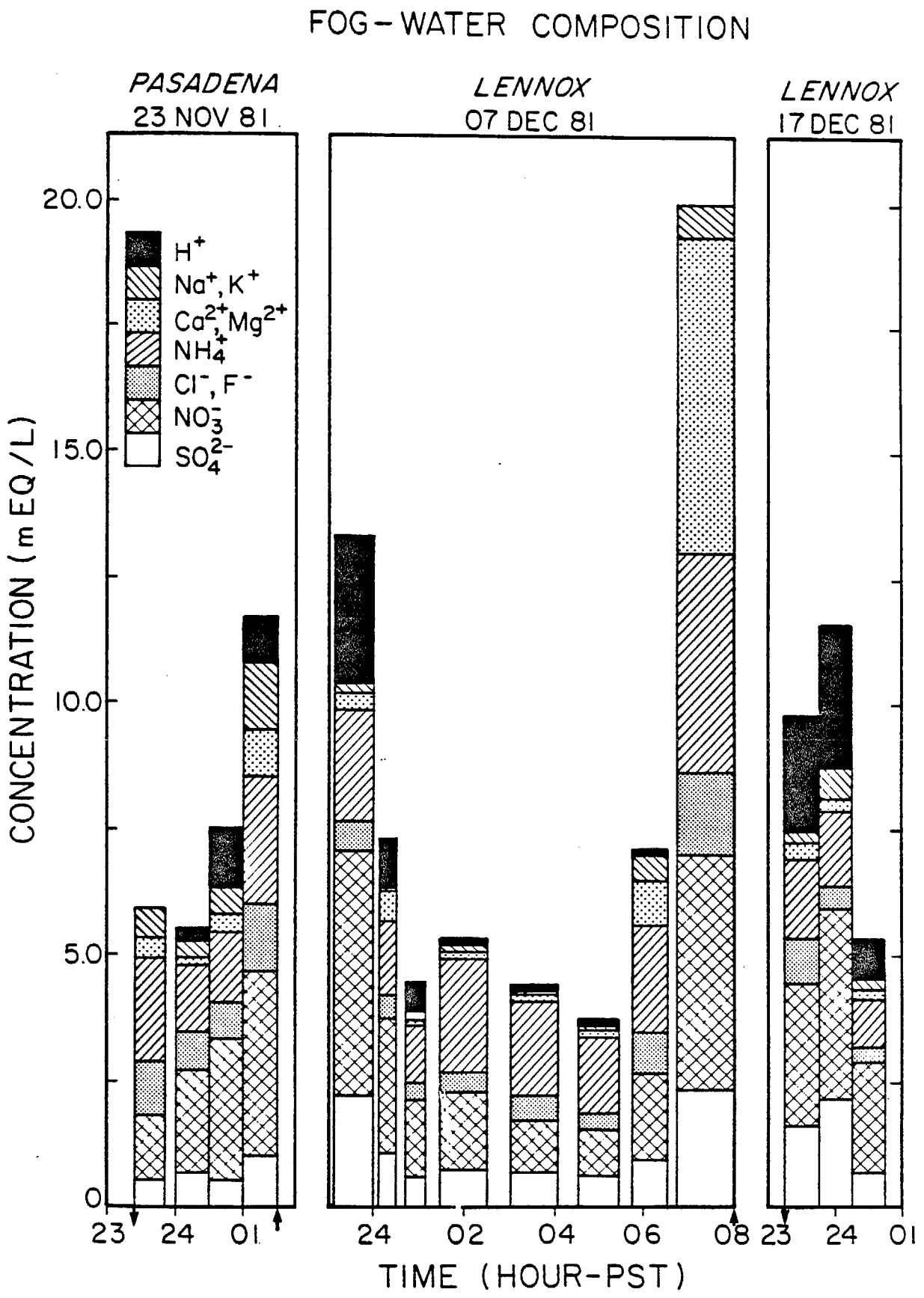
FOG-WATER COMPOSITION
PASADENA
23 NOV 81
LENNOX
07 DEC 81
LENNOX
17 DEC 81
20.0
15.0
10.0
5.0
0
CONCENTRATION (m EQ/L)
H+
Na+, K+
Ca2+, Mg2+
NH4+
Cl-, F-
NO3-
SO4 2-
23
24
01
24
02
04
06
08
23
24
01
TIME (HOUR-PST)

FIGURE 1

Addendum

Waldman et al. (1982) Chemical Composition of Acid Fog

Calculation of Evaporative Loss From Caltech Fog Collector

Introduction

Two approaches have been taken to calculate the range of evaporation rate of fog water from the impactor surfaces of the rotating arm collector (RAC) during operation. For both cases, the concentration gradient which serves as the forcing function of evaporation is due to the stagnation pressure and temperature increases of air at the impactor surfaces. The surfaces are taken to be wetted with a uniform film of fog water. Solute effects on vapor pressure are neglected. The circulation of air within the impactor slots has not been determined. For one approach, diffusion through a stagnant gas is modeled. For a second approach, the evaporation rate is calculated for the tangential flow or air across a flat liquid surface. These approximations give a range of the evaporation rate in the worst case.

(a) Mole fraction gradient due to compressible flow.

Because of its compressibility, the air that impinges the RAC slots experiences a rise above ambient temperature and pressure.

Compressibility effects:

$$\frac{T_o}{T_a} = 1 + \frac{k-1}{2} M^2 \qquad (1a)$$

$$\frac{P_o}{P_a} = \left(\frac{T_o}{T_a}\right)^{\frac{k}{k-1}} \qquad (1b)$$

T_a, T_o = ambient, stagnation temperature (°K)

P_a, P_o = ambient, stagnation pressure (abs.)

k = ratio of specific heats = 1.4 for air

M = Mach number - ratio of fluid to sonic speed

Ambient air:

T_a = 10°C = 283 K

P_a = 1 amt = 101.3 kPa

Sonic speed:

$$c = \sqrt{kRT_a} \tag{2}$$

= 337 m/s

R = gas constant

= 287 m^2/s^2-°K

Stagnation point:

V = relative speed of RAC slots

≅ 60 m/s

so

M = 0.178

giving

T_o = 284.79 K

P_o = 103.57 kPa

Vapor pressure:

P_v @ T_a = 1.227 kPa (3a)

P_v @ T_o = 1.386 kPa (3b)

Assuming ideal gas behavior, the molar fraction

$$x_i = \frac{P_{vi}}{P_a}$$

Therefore

$$x_a = 0.01211$$

$$x_o = 0.01338$$

(b) Diffusion from RAC slots through stagnant gas film.

$$\text{Flux} = \frac{CD}{H}(x_o - x_a) \quad \text{in g-mole/cm}^2\text{/s} \tag{4}$$

C = concentration of air

= air density/molecular weight

= 4.2×10^{-5} g-mole/cm^3 @ 10°C

D = diffusion coefficient for air-water

= 0.24 cm^2/s @ 10°C (5)

H = depth of RAC slot

≅ 0.5 cm

giving

$$\text{Flux} = 2.6 \times 10^{-8} \text{ g/mole/cm}^2\text{-s}$$

Therefore

E = mass evaporation rate

= Flux x A x (18 g/g-mole) x $(\frac{60s}{min})$

A = Area of slots

= 20 cm^2

$$E = 5.5 \times 10^{-4} \text{ g/min}$$

(c) Forced evaporation.

The mass transfer rate for tangential flow across a flat, smooth liquid surface is given:

$$W = \bar{k}_m \left(\frac{x_o - x_a}{1 - x_o}\right) \times \text{Area in g-mole/s} \qquad (6a)$$

=

$\bar{k}_m$ = mass transfer coefficient integrated over the length of the plate

$$= j_D Re_L S_c^{1/3} cD/L \qquad (6b)$$

j_D = Chilton-Colburn j-factor for mass transfer

Re_L = plate Reynolds number

S_c = Schmidt number

$= \nu/D$

u = tangential fluid velocity

L = plate length

For the worst case, the relative RAC slot speed, v, is used for u, although velocities within the slots are caused by eddies and are likely to be less than v.

$$j_D = f\left(Re_L = \frac{6000 \text{ cm/s} \times 10 \text{ cm}}{0.141 \text{ cm}^2/\text{s}} = 4.3 \times 10^5\right) \qquad (6c)$$

$$= 0.001$$

Since j_D is given (Z) for both sides of a flat surfaces, the above value

will give the mass transfer for both sides.

$$S_c = 0.141/0.24$$
$$= 0.588$$

Giving

$$W = j_p Re_L S_c^{1/3} cD\left(\frac{x_o - x_a}{1-x_o}\right) \times \text{width}$$
$$= 10^{-3} \times 4.3\times10^{-5} \times (0.588)^{1/3} \times 4.2\times10^{-5} \text{g-mole/cm}^3 \times 0.24 \text{ cm}^2/\text{s}$$
$$\times \frac{0.01338-0.01211}{1-0.01338} \times 1 \text{ cm}$$
$$= 4.6\times10^{-6} \text{ g-mole/s}$$

$$E = W \times \left(\frac{18 \text{ g}}{\text{g-mole}}\right) \times \left(\frac{60\text{s}}{\text{mn}}\right)$$
$$= 5.0\times10^{-3} \text{ g/min}$$

Summary

The evaporation rate of fog water in the RAC slots is calculated to be in the range 0.55 - 5.0×10^{-3} g/min. The collection rate for the RAC operation is 0.1-1.0 g/min. In the worst case, the evaporation loss is calculated to be 5%. For the lower collection rates observed in light fogs, the assumption of a uniform fog-water film in the slots is less likely to be valid, reducing the evaporative surface area and, hence the loss. Note, for part (c), if the eddy velocity in the slot is assumed to be only 10 m/s, then the maximum evaporation rate is calculated to be 2.0×10^{-3} g/min or a worst case evaporative loss of 2%.

Equation References

1. R. M. Olson (1977), Essentials of Engineering Fluid Mechanics, 3rd edition, p. 301-2 (Eqn. 9.8b & 9.9a).

2. Ibid., p. 299 (Eqn. 9.4)

3. Perry and Chilton (1973), Chemical Engineer's Handbook, 5th edition, p. 3-206 (Table 3-276).

4. Bird, Stewart, and Lightfoot (1960), Transport Phenomena, p. 525 (Eqn. 17.2-15).

5. R. E. Trebal (1980), Mass Transfer Operations, 3rd edition, p. 31 (Table 2.1).

6. Bird, Stewart, and Lightfoot, op. cit., p. 646 (Table 21.2-1) p. 410 (Figure 13.3-3).

CHAPTER IV

FOGWATER CHEMISTRY IN AN URBAN ATMOSPHERE

by

J. William Munger, Daniel J. Jacob,
Jed M. Waldman and Michael R. Hoffmann*

Environmental Engineering Science
W. M. Keck Laboratories
California Institute of Technology
Pasadena, California 91125

for

Journal of Geophysical Research
Oceans and Atmospheres

August 1982
Revised:
January 1983
Accepted: February 1983

*To whom correspondence should be addressed.

Abstract

Analyses of fogwater collected by inertial impaction in the Los Angeles basin and the San Joaquin Valley indicated unusually high concentrations of major and minor ions. The dominant ions measured were NO_3^-, SO_4^{2-}, NH_4^+ and H^+. Nitrate exceeded sulfate on an equivalent basis by a factor of 2.5 in the central and coastal regions of the Los Angeles basin, but was approximately equal in the eastern Los Angeles basin and the San Joaquin Valley. Maximum observed values for NH_4^+, NO_3^- and SO_4^{2-} were 10., 12., and 5. meq L^{-1}, while the lowest pH observed was 2.2. Iron and lead concentrations over 0.1 mM and 0.01 mM, respectively, were observed. High concentrations of chemical components in fog appeared to correlate well with the occurrence of smog events. Concentrations in fogwater were also affected by the physical processes of condensation and evaporation. Light, dissipating fogs routinely showed the highest concentrations.

Introduction

Laboratory [Schwartz, 1982; Martin, 1982; Hoffmann and Jacob, 1982] and field [Cass and Shair, 1980; Cox, 1974; McMurry et al., 1981; Smith and Jeffery, 1975; Wilson and McMurry, 1981] studies have indicated that droplet-phase chemistry is important in SO_2 oxidation. Droplet-phase oxidation of SO_2 occurs, in part, via the following reactions

$$SO_2(g) \overset{K_H}{\rightleftharpoons} SO_2(aq) \tag{1}$$

$$SO_2(aq) \overset{K_{a1}}{\rightleftharpoons} H^+ + HSO_3^- \tag{2}$$

$$2HSO_3^- + O_2 \xrightarrow[Mn(II)]{Fe(III)} 2HSO_4^- \tag{3}$$

$$HSO_4^- \overset{K_{a2}}{\rightleftharpoons} H^+ + SO_4^{2-} \tag{4}$$

In Los Angeles, Cass [1975] observed a correlation between the occurrence of high sulfate aerosol levels during the afternoon and the presence of coastal fog and low clouds in the morning. The mean SO_2 to SO_4^{2-} conversion rate during July in Los Angeles is 6% hr^{-1} [Cass, 1981], whereas gas-phase reactions at most can account for conversion rates of 4.5% hr^{-1} [Sander and Seinfeld, 1976]. Morgan and Liljestrand [1980] reported that light misting rainfalls emanating from low stratus clouds in Los Angeles resulted in pH values as low as 2.9 with correspondingly high SO_4^{2-} and NO_3^- concentrations. Waldman et al. [1982] have previously reported pH values near 2.2 in urban fog. Furthermore, Hegg and Hobbs [1981] have reported S(IV) to S(VI) conversion rates of 4.0 to 300% hr^{-1} in wave clouds over western Washington.

In addition to its importance as a chemical reaction site, fog may exert a significant influence on scavenging and deposition, on human health, and on vegetation. Fog forms in the ground layer where gases and aerosols are most concentrated. Because fog droplets are approximately 100 times smaller than rain drops, they should be more concentrated than rain and mass transfer should not limit the kinetics of fog droplet reactions [Schwartz, 1982; Baboolal et al., 1981].

In light of these results and the expectation that fog droplets (or the fine aerosol remaining after fog has evaporated) are sites for rapid conversion of SO_2 to SO_4^{2-} we began a study to characterize the chemical composition of fogwater. Because of the physical similarity to clouds, fog is expected to exhibit the same chemical processes occurring in clouds and to some degree aquated sub-micron aerosols. Information about the chemistry of fogwater may be applicable to the broader questions about ambient acid formation and acidic precipitation. The role of fog in the nocturnal chemistry of SO_2 has been examined by Jacob and Hoffmann [1982].

Methods

Fogwater was collected using a rotating arm collector (RAC), which was modified from an original design reported by Mack and Pilie [1975]. A 67.5 cm long Teflon-coated steel tube, which has 10 x 0.95 cm slots milled into opposite sides at each end of the tube, is rotated at 1700 rpm with a 1.5 HP induction motor. This rotation imparts a relative velocity of $\sim$ 50 m/s to the slots. Droplets impact in the slots and are driven by centrifugal force into 30 mL polyethylene bottles attached at the ends of the arms. During operation, the pivot of the arm is 1.4 m above ground level.

Based upon changes in particle-size distributions measured with a laser optical particle counter during operation in a cloud chamber, the RAC was determined to have a lower size cut of $\sim$ 8 μm [Jacob et al., 1982]. The bulk of liquid water in fogs is contributed by droplets larger than 8 μm, but droplets smaller than 8 μm may be more concentrated than those that are actually collected. Consequently, the concentration of species in fogwater may be slightly underestimated. With this design, up to 2 mL min^{-1} of fogwater has been collected during dense fog and 0.1 to 1.0 mL min^{-1} during lighter fog. Collection efficiency under these conditions is estimated to be greater than 80% based on laboratory calibration. We are currently working on a fog sampler with a lower size cut in order to characterize the chemistry of the smaller fog droplets.

Site Descriptions

Figure 1 indicates the sites at which fogwater was collected. The Pasadena site, which is located on the roof of a 4 story building on the Caltech campus, is in a predominantly residential neighborhood 25 km north of downtown Los Angeles. There are no major pollutant sources in the immediate vicinity. The Lennox site was selected because of its close proximity to both industrial and mobile pollutant sources and its high frequency of marine fog in late autumn; it is situated on the roof of a one story building at a busy intersection within 100 m of a major freeway, and 6 km from the ocean. Major point sources near the Lennox site include an oil refinery, power plant, Los Angeles International Airport, and several other industrial facilities.

The Oildale site, near Bakersfield, is in an area with high sulfur emissions from secondary oil recovery operations and subject to extensive fog ("Tule fog") that persists throughout the San Joaquin Valley during the early winter. The sampler was placed on the roof of an air quality monitoring station (about 4 m above ground). Upland is 60 km NE of downtown Los Angeles. A steel plant and several other heavy industries are located within 30 km of this site, which is also on the roof of an air quality monitoring station in a residential area.

Fog Patterns

In Los Angeles fog generally occurs during two distinct periods; November through January and April through June. At the two inland sites, Pasadena and Upland, fog occurs sporadically in the night and early morning throughout the fog seasons. Fogs along the coast tend to form repeatedly for several nights, lifting for only part of the day. In the San Joaquin Valley fog forms for extended periods during the early winter months and often persists throughout the day.

Analytical Methods

The sample-handling and analytical protocol is illustrated in Figure 2. Analysis of the sample began as soon as collection ended; measurement of pH and separation of preserved aliquots was completed within 30 minutes. In the field, samples were stored over ice, and refrigerated when they were brought back to the laboratory. pH was determined in the field with a Radiometer PHM 80 meter. Sulfite was preserved by addition of CH_2O at pH 4 to form hydroxymethanesulfonic acid (HMSA) [Dasgupta et al., 1980; Fortune and Dellinger, 1982]. 3,5-diacetyl-1,4-dihydrolutidine (DDL) formed by reaction of formaldehyde and acetyl acetone in the presence of NH_4^+ [Nash,

1953] is stable for at least 7 days [Rietz, 1980]. Sulfite is known to interfere with this reaction [Nash, 1952], but no correction was made for this. Addition of HNO_3 to achieve a concentration of 0.16 M was used to stabilize an aliquot for trace-metal analyses. Beginning with the Oildale samples, aliquots were filtered through 0.4 μm Nuclepore membranes in the field. Because of extremely high cation and anion concentrations in fogwater, samples usually had to be diluted before analysis. With sample dilution complete analyses of volumes as small as 5 ml was practicable.

Major cations were determined on a Varian AA5 atomic absorption spectrophotometer using an air-acetylene flame. Lanthanum was added to the entire aliquot used for AAS in order to release calcium and magnesium. Ammonium was determined by the phenol-hypochlorite method [Solórzano, 1967]. Anions were determined by ion chromatography (IC) using a 3 mM $NaHCO_3$/2.4 mM Na_2CO_3 eluent. Aliquots of sample were spiked to give the same HCO_3^-/CO_3^{2-} concentration as the eluent in order to eliminate the water dip that interferes with F^- and Cl^- peaks. Galloway et al. [1982] suggest that low molecular weight carboxylic acids are present in rainwater. Considering the high aldehyde concentrations observed in fogwater it is likely that the corresponding acids are present as well. If present, these acids would be a positive interference with fluoride. The absorbance of DDL formed from CH_2O was measured at 412 nm on a Beckman Acta III spectrophotometer.

The preserved solution for S(IV) was injected into the IC and eluted with 1 mM KHP [Dasgupta et al., 1980]. Because the F^- and Cl^- peaks co-eluted with the HMSA using this eluent the S(IV) in the samples could not be directly quantified. Instead S(IV) was taken as the difference between the SO_4^{2-} concentration in the preserved aliquot, and the SO_4^{2-} concentration in the unpreserved aliquot measured by the usual IC methods. The first value would be SO_4^{2-} only, the second would be the sum of SO_4^{2-} and SO_3^{2-}. After December 7, S(IV) was measured by a colorimetric method using 5,5',Dithiobis-(2-nitrobenzoic acid) DTNB [Humphrey et al., 1970]. Trace metals were determined by flameless atomic absorption (Varian AA6 equipped with a CRA 90 or Perkin-Elmer 360 with a HGA 2100). Gas phase concentrations of SO_2, NO_x and O_3 were made continuously at the Lennox, Upland, and Oildale sites by conventional instrumental methods.

Results

Table 1 describes the conditions before and during the fog sampling. Samples from Pasadena were collected both after clean air days and smoggy days. The fogs in Lennox followed smoggy days. Oildale samples were collected during a period of extensive and persistent fog in the San Joaquin Valley. Samples at Upland were collected after dawn when the haze that had been present during the night thickened enough to be collected.

The high and low concentrations of major ions, sulfite and formaldehyde in fogwater during eight fog events are presented in Table 2. Concentrations of most ions in the second set of Pasadena samples, which followed a smoggy day, were higher than in the first Pasadena fog event. At Lennox the concentrations of major ions in fog were even higher than the Pasadena samples. Some of the fog samples from

Lennox contained significant amounts of suspended solids. The greatest amount was in the final sample taken from the 7 December fog event during morning rush hour as the fog was dissipating.

The present sampling method does not differentiate between particles within droplets and particles greater than 8 μm that are independent of water droplets. Because the minimum size for activating condensation nuclei in ambient fog is much smaller than the collector cut-off size, most particles collected in fog with the exception of hydrophobic material can be assumed to be associated with droplets.

A single fogwater sample collected in Pasadena on 17 January had exceptionally high concentrations. The sulfate and nitrate concentrations were the maximum values observed in any fog. Fogwater collected in Oildale also had very high nitrate and sulfate concentrations as well as the highest NH_4^+, CH_2O and S(IV) concentrations. The Upland fog samples were also characterized by high levels of acidity and acidic anions.

Concentrations of trace metals in the fog samples were also elevated as shown in Table 3. During some of the fog events metal concentrations varied over an order of magnitude. The usual pattern was for high concentrations at the beginning and end of the event. Lead and iron concentrations exceeded 1.0 mg L^{-1} (0.01 mM) on occasion.

The anion-to-cation ratios were close to unity for most of the samples, but there were discrepancies in some samples. In light of the large dilutions necessary to bring high concentrations down into suitable analytical ranges the ion balances were reasonable. There were apparent excesses of cations in some of the samples that had large quantities of particles present. Calculation of the ion balance using the concentrations of cations in filtered aliquots yielded better results. The aliquot for anions was routinely filtered prior to injection into the IC. This does

not explain the apparent anion deficiency (or cation excess) in the fogwater samples collected from Oildale. The inclusion of SO_3^{2-} in the anion sum does not completely make up the deficit either, however, sulfite in aliquots from these samples was not measured immediately. Even though preservation techniques were used sulfite may be underestimated. Considering the high concentrations of aldehydes it is probable that the corresponding carboxylic acids were present in the fogwater; this would account for some of the apparent anion deficiency. Other factors that may contribute to poor ionic balances are losses of ions to particle surfaces via sorption and formation of adducts and complexes of indeterminant charge.

Discussion

Figure 3 presents the ionic composition of individual fog samples as a function of time. Concentrations of all ions decrease sharply during the first few hours of the fogs in Lennox; however, the ionic proportions do not change appreciably. In most cases concentrations in the fogwater rose as the fog dissipated. The short duration fogs, which were usually very light fogs that resulted in low collection rates, also had high concentrations. Physical processes of droplet growth by accretion of water vapor followed by evaporation appear to account for this pattern.

Dilution by droplet growth could take place without any appreciable change in liquid water content (LWC) if the sedimentation rate was high enough to balance the condensation rate. Work by Roach et al. [1976] suggests that a significant portion of the liquid water formed during a fog event is lost, presumably to ground surfaces. During the periods over

which concentrations were decreasing, collection rates, which are a function of LWC, remained constant. Advection of more dilute fog could account for this as well.

In Figures 4 and 5, the concentration of selected ions normalized to their initial concentration are depicted. If physical factors are responsible the patterns will be nearly identical for ions that are controlled by the same factors or have common sources. The nearly 100-fold increase in Ca^{2+} and Mg^{2+} and the concomitant drop in H^+ concentration in the final two samples collected in the 7 December fog at Lennox coincided with morning rush hour traffic, which would generate a large amount of road dust. Concentrations of other ions were increased during that period due to evaporation, but not to the extent that Ca^{2+} and Mg^{2+} increased (25 fold from their initial concentrations); $[Na^+]$ and $[Cl^-]$ increased by a factor of 5 and $[SO_4^{2-}]$, $[NO_3^-]$ and $[NH_4^+]$ returned to their initial concentrations. Acidity was nearly neutralized at the end of this fog event. In association with the increased $[Ca^{2+}]$ and $[Mg^{2+}]$, an increase in suspended particles, [Pb] and [Fe] was observed at the same time as a rise in CO levels at Lennox coinciding with the morning traffic. Transfer of gaseous NH_3 into the droplets could account for the increase in $[NH_4^+]$ and simultaneous drop in $[H^+]$ during the 7 December Lennox fog event, while the other ions were maintained at constant concentrations. However, if the NH_3 had been present when the fog formed it would have been immediately scavenged because of its high solubility at low pH. Unless there was a local source for NH_3, advective transport must be invoked to account for the apparent increase in $[NH_4^+]$.

In Pasadena $[H^+]$ and $[NO_3^-]$ simultaneously increased, while the other ions were decreasing. This may be evidence for the nocturnal formation of HNO_3 via the following reactions [Graham and Johnston, 1978]:

$$NO + O_3 \longrightarrow NO_2 + O_2 \quad (5)$$

$$NO_2 + O_3 \longrightarrow NO_3 + O_2 \quad (6)$$

$$NO_2 + NO_3 \longrightarrow N_2O_5 \quad (7)$$

$$N_2O_5 + H_2O \longrightarrow 2HNO_3 \quad (8)$$

Alternatively the increase in HNO_3 could result from scavenging or diffusion of fine aerosol to the droplets or by advection of fog with higher NO_3^- concentrations.

In nearly all the cases the dominant ions in the fog samples were NO_3^-, SO_4^{2-}, H^+ and NH_4^+, which are the major components of secondary aerosol in Los Angeles [Cass, 1979]. These ions account for over 90% of the solutes in the initial stages of the Lennox samples. The highest concentrations were observed when the fog was preceded by smoggy days. Because secondary aerosol are effective condensation nuclei [Barrett et al., 1979] they will exert a considerable influence on the composition and concentration in fogwater. When the concentration of secondary aerosol is high, the subsequent fogwater will also have high concentrations. The fraction of NO_3^- and SO_4^{2-} neutralized by NH_3 (measured in terms of NH_4^+) will largely determine the free acidity of the fog that first deliquesces. In this connection it is noteworthy that the initial fogwater samples collected at Lennox are the most acidic and subsequent samples during the event are progressively more neutral, while at Pasadena and Upland the converse is true.

If HNO_3 and NH_3 were present when the fog initially formed they would be scavenged rapidly as well and influence the fogwater composition [Jacob and Hoffmann, 1982]. However, the combination of cooler temperatures and higher humidity before the onset of fog will probably force NH_3 and HNO_3 to condense into the particulate phase [Stelson and Seinfeld, 1982; Stelson, 1982], which can be scavenged via nucleation or diffusion as the fog forms.

Figure 6 is a conceptualization of the condensation/evaporation cycle for fog droplets and illustrates the link between fogwater chemistry and the chemistry of smog and haze aerosol. High atmospheric concentrations of aerosol precursors appear to result in highly concentrated fogwater. Likewise, dissipation of highly concentrated fog results in very concentrated and reactive aerosol. The high trace-metal content in fogs would catalyze SO_2 oxidation. This link between fog and the subsequent aerosol can be seen in the correlation reported by Cass [1975] between morning fog and high humidity and high aerosol sulfate concentrations in the afternoon.

The Role of Aldehydes in Fog Droplets

Aldehydes are released as primary emissions from combustion sources and are generated photochemically from hydrocarbons [NRC, 1981]. Peroxide radical is an important byproduct of these reactions. Aldehydes are photochemically destroyed, with $OH\cdot$ and $HO_2\cdot$ as byproducts. Intermediates in aldehyde reaction pathways also play a role in the gas phase reaction networks of SO_2 and NO_x.

Concentrations of formaldehyde as high as 0.5 mM were present in the Los Angeles fogwater samples. Other aldehydes,such as acetaldehyde and benzaldehyde, are present in the Los Angeles atmosphere [NRC, 1981; Grosjean, 1982] and their presence in fogwater samples at comparable concentrations has been confirmed by the hydrazone derivatization method [Fung and Grosjean, 1981]. Aldehydes react with HSO_3^- according to the following general stoichiometry:

$$HSO_3^- + RCHO \rightleftharpoons HOCHSO_3^- \quad (9)$$

The formation constant for the formaldehyde-bisulfite addition complex, hydroxymethanesulfonic acid (HMSA), has a maximum of about 10^5 between pH 4 and 6 and drops to 10^3 at pH 9 [Dasgupta et al., 1980]. Stewart and Donnally [1932] observed a similar pattern for the formation of the benzaldehyde-S(IV) adduct. They also observed an interaction between temperature and pH. At low pH the temperature dependence of the equilibrium was stronger than at high pH. Low temperature increased the stability of the complex. The molar ratio of formaldehyde to S(IV) in the fog samples ranged from 0.9 to 17. Using Dasgupta's constants, the free S(IV) concentration in the fog ranges from 5% to 60% of the total. The equilibrium partial pressures of SO_2 and CH_2O required to achieve the S(IV) and CH_2O values measured in the fogwater were calculated from the following mass balance relationships:

$$[S(IV)] = [SO_2(aq)] + [HSO_3^-] + [SO_3^{2-}] + \sum_{i=1}^{n}[R_iCHOHSO_3^-] + \sum_{j=1}^{m}[M_jSO_3] \quad (10)$$

$$[R_i\dot{C}HO]_T = [R_iCHO] + [R_iCHOHSO_3^-] \quad (11)$$

where R_iCHO represents aldehydes forming sulfonic acid adducts and M_j represents first-row transition metals forming stoichiometric sulfite complexes. Using the appropriate conditional equilibrium expressions for the concentration of the sulfonic acid adducts of CH_2O, CH_3CHO and C_7H_6O and the sulfitoiron(III) complex and ignoring other S(IV) adducts and complexes because of their low potential concentrations gives

$$[S(IV)] = K_H P_{SO_2}\left(1 + \frac{K_{a1}}{[H^+]} + \frac{K_{a1}K_{a2}}{[H^+]^2} + \frac{K_{a1}K_{a2}\beta}{[H^+]^2}[Fe(III)] + \sum_{i=1}^{n}\frac{K_{a1}}{[H^+]}[R_iCHO]K_{Ai}\right) \quad (12)$$

$$[R_iCHO]_T = K_H^i P_{R_iCHO}\left(1 + \frac{K_{a1}K_H P_{SO_2}}{[H^+]}K_{Ai}\right) \quad (13)$$

$$[Fe(III)]_T = [Fe(III)] + [Fe(III)SO_3^-] \quad (14)$$

where β is the formation constant for an Fe(III)-S(IV) complex, K_H^i is Henry's Law constant for R_iCHO, K_H is Henry's Law constant for SO_2, K_{a1} and K_{a2} are acid dissociation constants, K_{Ai} is the bisulfite adduct formation constant, P_{R_iCHO} and P_{SO_2} are partial pressures.

Substitution of the aldehyde and metal mass balances into eqn. 12 gives

$$[S(IV)] = \frac{K_H P_{SO_2}}{[H^+]^2}\left[[H^+]^2 + K_{a1}[H^+] + \frac{K_{a1}K_{a2}\beta[Fe(III)]_T[H^+]^2}{([H^+]^2+\beta K_{a1}K_{a2}K_H P_{SO_2})} + \sum_{i=1}^{n}\frac{K_{a1}K_{Ai}[H^+]^2[R_iCHO]_T}{(H^+ + K_{a1}K_{Ai}K_H P_{SO_2})}\right] \quad (15)$$

The appropriate equilibrium constants are given in Table 4.

In the absence of adduct formation, the equilibrium partial pressures of CH_2O calculated from fogwater data range from 16 ppb to 76 ppb, which are reasonable values for the Los Angeles atmosphere [Grosjean, 1982]. Adduct formation would lower the equilibrium partial pressure. The highest values of S(IV) that were found in some fog samples can not be completely accounted for by aldehyde and iron complex equilibria alone. Measured sulfite is 4-5 times higher than the predicted equilibrium value, even with P_{SO_2} as high as 30 ppb at the Los Angeles sites or 50 ppb at Oildale, which are the highest values for those sites. The lower concentrations of S(IV), however, are comparable to the values predicted from equilibrium considerations. Stable organic and inorganic sulfite species in ambient aerosols have been demonstrated to exist [Izatt et al., 1978; Eatough et al., 1981]. Aldehydes may play an important role in the atmospheric chemistry of S(IV) as stabilizers that retard oxidation of S(IV) and possibly as sources of peroxides and free radicals through their photochemistry. More data on the aldehyde content of the atmosphere are necessary to ascertain their role in the heterogeneous chemistry of SO_2.

Nitrate to Sulfate Equivalent Ratios

As is indicated in Figure 7 [NO_3^-] in Pasadena and Lennox was about two and a half times [SO_4^{2-}]; at Oildale and Upland the ratio was closer to 1:1. The nitrate to sulfate ratios in fogwater differ markedly from that observed in Los Angeles area rainwater [Liljestrand and Morgan, 1981]. In rainwater the equivalent ratio was less than one for coastal and central Los Angeles sites and increased to unity at Riverside at the eastern edge of the basin. Fogwater exhibited the opposite trend: [NO_3^-] exceeded [SO_4^{2-}] at the coastal and central Los Angeles sites and decreased to near one at the most inland site (Upland). Besides the differences in their source strengths (NO_x emissions exceed SO_2 emissions by a factor of 2.5 in Los Angeles) there are important differences in the kinetics of their respective oxidations and scavenging processes as is discussed by Jacob and Hoffmann [1982].

Sodium Chloride Ratios

As Figure 8 illustrates, most of the fogwater samples had Na:Cl ratios near that of seawater. There were a few samples with excess Cl^- that may be due to local sources. The highest excess of Cl^- was found in Lennox fog during morning rush hour, which suggests lead bromochloride salts from automobile emissions as a possible Cl^- source. Those samples also had high [Pb]. Two of the samples with excess Na^+ were collected at the beginning of fog events and may be affected by soil and dust. However, the other samples with excess Na^+ were extremely acidic. Reaction between marine aerosol and acidic gases or aerosol may be volatilizing HCl in the fog or the preceding aerosol as suggested by Eriksson [1960] and Hitchcock [1980]. The resulting fog would be deficient in Cl^-.

Comparison to Other Data

Ionic concentrations in fog and cloudwater as high as in some of these samples have been observed previously (see Table 5). At many of the sites, pH values were in the range 3 to 4, but none were as low as the most extreme values for the Los Angeles area fogs. The concentration ranges for the cations Na^+, K^+, Ca^{2+} and Mg^{2+} in other regions overlap with the concentration ranges observed in Southern California. The extreme values reported here, which were found in light fogs and the Lennox sample that was laden with particles, are somewhat higher. Ammonium concentrations are comparable, but the extreme values observed in this study are about ten times the maxima for previously reported data. Sulfate concentrations are comparable to other reported values, while nitrate concentrations are considerably higher in the California fogs, which is to be expected because of the dominance of NO_x emissions. Furthermore, high concentrations of HNO_3, that can be easily scavenged by fogwater, have been measured in the Los Angeles atmosphere [Appel, 1982].

Dense smog as a precursor gave rise to the most highly concentrated fogwater in Los Angeles. Other areas of the world that are subject to intense air pollution may also prove to have highly concentrated fogwater. Although ionic composition in the 1952 London fog was not measured, approximate calculations based on SO_2 emission rates, measured SO_2 concentrations, droplet residence time, and liquid water content [Wilkins, 1954a,b] gives SO_4^{2-} concentrations of 11 to 46 meq L^{-1}. For comparison, the extreme value measured during the winter of 1981-1982 in Southern California was 5 meq L^{-1}.

Implications

Highly concentrated fogwater can have several important environmental effects. Sedimentation and impaction rates of fog droplets will be greater than for dry gas and aerosol. Roach et al. [1976] have calculated that up to 90% of the liquid water condensed during a fog event may sediment out on the ground. When winds accompany fog, interception of droplets by vegetation is also a major depositional pathway [Schlesinger and Reiners, 1974; Lovett and Reiners, 1982]. Measurement of rain and dry deposition fluxes alone may not adequately account for atmospheric loadings in regions where fog is frequent. Surface wetness from fog deposition may enhance deposition of SO_2 and subsequent oxidation to SO_4^{2-} (with a possible involvement of trace metals) [Lindberg et al., 1979].

Fogwater deposited on leaf surfaces is highly efficient in leaching ions from the leaves [Tukey, 1970] and may result in some plant injury. Experiments with acid mists show plant injury occurring at pH levels around 3 [Jacobson, 1980], which is typical of fogwater in parts of Southern California. Damage to building materials and metal surfaces is also possible from deposition of acidic fog. Corrosion of statuary and building materials has been observed in several locations throughout the world. The role of fog in this damage is not known, although research [Metropolitan Museum of Art, 1979] on the Horses of San Marco (c.a. 100 B.C.) in Venice, Italy, indicates that fog and high SO_2 concentrations have resulted in significant damage during the last 50 years.

Historically, fogs have been implicated in a number of severe pollution episodes that caused increased human mortality [EPA, 1971]. The most notable of these is the infamous London Fog of 1952 [Wilkins, 1954a,b], which caused 4,000 excess deaths during the 5 day episode and 12,000 excess deaths over

4 months. Further research is needed to ascertain whether fog plays a causative role in mortality or is merely a consequence of the severe inversion conditions that caused a build up of toxic air pollutants, which were the true agents of mortality. Previous analysis [Larsen, 1970] suggested that these deaths correlated well with the product of gas-phase SO_2 and particle concentrations; however, sulfuric acid mists have been implicated [Wilkins, 1954a,b].

Conclusion

Fogwater in Southern California provides a propitious environment for the scavenging of particulate and gaseous forms of S(IV), S(VI), N(V), N(-III), for the subsequent conversion of S(IV) to S(VI), and for the concomitant production of acidity. Unusually high concentrations of SO_4^{2-}, NO_3^-, NH_4^+ and H^+ were observed. The highest concentrations were observed during fog events preceded by smoggy days. Acidity due to NO_3^- and SO_4^{2-} precursors was neutralized to some extent by scavenging of NH_3 and calcareous dust.

The physical processes of condensation and evaporation along with scavenging and subsequent chemical conversion of reactive gas-phase components appear to mutualistically control the temporal trends in fogwater composition. The apparent cyclical relationship between the occurrence of smog and fog in the Los Angeles basin is a manifestation of this phenomenon. The late night and early morning fogs, which form more readily in a particle laden atmosphere, appear to accelerate and enhance smog production, visibility reduction and particulate sulfate levels during the subsequent day. This

relationship can be dubbed the smog-fog-smog cycle.

Clearly more research is needed to elucidate the mechanisms by which fog-processed aerosols become highly reactive sites for daytime photochemical transformations. The role of aldehydes and transition metals in the transport and transformation of S(IV) in atmospheric water droplets needs to be explored more intensively. Furthermore, given the millimolar concentrations of some of the metal ions in urban fog, the effect of metal ion catalysts on important chemical transformations (e.g. S(IV) to S(VI)) needs to be considered more carefully in the development of quantitative air quality models for urban airsheds.

Acknowledgements

We gratefully acknowledge the financial support of the California Air Resources Board and the invaluable assistance provided by its professional staff. Additional logistical support was provided by the South Coast Air Quality Management District. Special thanks are extended to Drs. R. C. Flagan, J. J. Morgan, D. Lawson and D. Grosjean for their contributions to the success of this research.

References

Appel, B. R., E. L. Kothny, E. M. Hoffer, and J. J. Wesolowski, Sulfate and Nitrate Data from the California Aerosol Characterization Experiment (ACHEX). Adv. Environ. Sci. Tech. 9, 315-336, 1980.

Appel, B. R., Y. Tokiwa, and M. Haik, Sampling of Nitrates in Ambient Air, Atmos. Environ. 15, 283-289, 1981.

Baboolal, B., H. R. Pruppacher, and J. H. Topalian, A Sensitivity Study of a Theoretical Model of SO_2 Scavenging by Water Drops in Air, J. Atmos. Sci. 38, 856-870, 1981.

Barrett, E., F. P. Parungo, and R. F. Pueschel, Cloud Modification by Urban Pollution: A Physical Demonstration, Meteorol. Resch. 32, 136-149, 1979.

Carlyle, D. W., A Kinetic Study of the Aquation of Sulfitoiron(III) Ion, Inorg. Chem. 10, 761-764, 1971.

Cass, G. R., Dimensions of the Los Angeles SO_2/Sulfate Problem, Environmental Quality Laboratory Memorandum No. 15, California Institute of Technology, Pasadena, California, 1975.

Cass, G. R., On the Relationship between Sulfate Air Quality and Visibility with Examples in Los Angeles, Atmos. Environ. 13, 1069-1084, 1979.

Cass, G. R., Sulfate Air Quality Control Strategy Design, Atmos. Environ. 15, 1227-1249, 1981.

Cass, G. R., and F. H. Shair, Transport of Sulfur Oxides Within the Los Angeles Sea Breeze/Land Breeze Circulation System, Proc. 2nd Joint Conf. on Application of Air Pollution Meteorology, American Meteorological Society, New Orleans, 24-27 March 1980.

Castillo, R. A., J. E. Jiusto, and E. McLaren, The pH and Ionic Composition of Stratiform Cloud Water, unpublished manuscript, 1980.

Cox, R. A., Particle Formation from Homogeneous Reactions of Sulfur Dioxide and Nitrogen Dioxide, Tellus 26, 235-240, 1974.

Dasgupta, P. K., K. De Cesare, and J. C. Ullrey, Determination of Atmospheric Sulfur Dioxide without Tetrachloromercurate(II) and the Mechanism of the Schiff Reaction, Analytical Chem. 52, 1912-1922, 1980.

Eatough, D. J., T. Major, J. Ryder, M. Hill, N. F. Mangelson, N. L. Eatough, L. D. Hansen, R. G. Meisenheimer, and J. W. Fischer, The Formation and Stability of Sulfite Species in Aerosols, Atmos. Environ. 12, 263-271. 1978.

Eriksson, E., The Yearly Circulation of Chloride and Sulfur in Nature: Meteorological, Geochemical and Pedological Implications. Part II, Tellus 12, 63-109, 1960.

Falconer, P. D., Cloud Chemistry and Meteorological Research at Whiteface Mountain: Summer 1980, Atmospheric Sciences Research Center, SUNY, ASRC Publ. 806, 1981.

Fortune, C. R., and B. Dellinger, Stabilization and Analysis of Sulfur(IV) Aerosols in Environmental Samples, Environ. Sci. Tech. 16, 62-66, 1982.

Fung, K., and D. Grosjean, Determination of Nanogram Amounts of Carbonyls as 2,4-Dinitrophenylhydrazones by High-Performance Liquid Chromatography, Anal. Chem. 53, 168-181, 1981.

Fung, K., and D. Grosjean, Determination of Nanogram Amounts of Carbonyls as 2,4-Dinitrophenylhydrazones by High-Performance Liquid Chromatography, Anal. Chem. 53, 168-181, 1981.

Galloway, J. N., G. E. Likens, W. C. Keene and J. M. Miller, The Composition of Precipitation in Remote Areas of the World, J. Geophys. Res. 87, 8771-8786, 1982.

Graham, R. A., and H. S. Johnston, The Photochemistry of NO_3 and the Kinetics of the N_2O_5-O_3 System, J. Phys. Chem. 82, 254-268, 1978.

Grosjean, D., Formaldehyde and Other Carbonyls in Los Angeles Ambient Air, Environ. Sci. Techn. 16, 254-262, 1982.

Hansen, L. D., L. Whiting, D. J. Eatough, T. E. Jensen and R. M. Izatt, Determination of Sulfur(IV) and Sulfate Aerosols by Thermometric Methods, Anal. Chem. 48, 634-638, 1976.

Hitchcock, D. R., Sulfuric Acid Aerosols and HCl Release in Coastal Atmospheres: Evidence of Rapid Formation of Sulfuric Acid Particulates, Atmos. Environ. 14, 165-182, 1980.

Hegg, D. A., and P. V. Hobbs, Cloudwater Chemistry and the Production of Sulfates in Clouds, Atmos. Environ. 15, 1597-1604, 1981.

Hoffmann, M. R., and D. J. Jacob, Kinetics and Mechanisms of the Catalytic Oxidation of Dissolved Sulfur Dioxide in Aqueous Solution: An Application to Nighttime Fog-Water Chemistry, in Acid Precipitation, V. 6, J. G. Calvert (ed.), Ann Arbor Science Publ., Michigan, 1982.

Houghton, H. G., On the Chemical Composition of Fog and Cloud Water, J. Meteor. 12, 355-357, 1955.

Humphrey, R. E., M. H. Ward, and W. Hinze, Spectrophotometric Determination of Sulfite with 4,4-Dithiopyridine and 5,5-Dithiobis(2-Nitrobenzoic acid), Anal. Chem. 42, 698-702, 1970.

Galloway, J. N., G. E. Likens, W. C. Keene and J. M. Miller, The Composition of Precipitation in Remote Areas of the World, J. Geophys. Res. 87, 8771-8786, 1982.

Graham, R. A., and H. S. Johnston, The Photochemistry of NO_3 and the Kinetics of the N_2O_5-O_3 System, J. Phys. Chem. 82, 254-268, 1978.

Grosjean, D., Formaldehyde and Other Carbonyls in Los Angeles Ambient Air, Environ. Sci. Techn. 16, 254-262, 1982.

Hansen, L. D., L. Whiting, D. J. Eatough, T. E. Jensen and R. M. Izatt, Determination of Sulfur(IV) and Sulfate Aerosols by Thermometric Methods, Anal. Chem. 48, 634-638, 1976.

Hitchcock, D. R., Sulfuric Acid Aerosols and HCl Release in Coastal Atmospheres: Evidence of Rapid Formation of Sulfuric Acid Particulates, Atmos. Environ. 14, 165-182, 1980.

Hegg, D. A., and P. V. Hobbs, Cloudwater Chemistry and the Production of Sulfates in Clouds, Atmos. Environ. 15, 1597-1604, 1981.

Hoffmann, M. R., and D. J. Jacob, Kinetics and Mechanisms of the Catalytic Oxidation of Dissolved Sulfur Dioxide in Aqueous Solution: An Application to Nighttime Fog-Water Chemistry, in Acid Precipitation: SO_2, NO and NO_2 Oxidation Mechanisms: Atmospheric Considerations, (J. G. Calvert, ed.), Ann Arbor Science, Ann Arbor, Michigan, 1982.

Houghton, H. G., On the Chemical Composition of Fog and Cloud Water, J. Meteor. 12, 355-357, 1955.

Humphrey, R. E., M. H. Ward, and W. Hinze, Spectrophotometric Determination of Sulfite with 4,4-Dithiopyridine and 5,5-Dithiobis(2-Nitrobenzoic acid), Anal. Chem. 42, 698-702, 1970.

Izatt, R. M., D. J. Eatough, M. L. Lee, T. Major, B. E. Richter, L. D. Hansen, R. G. Meisenheimer, and J. W. Fischer, The Formation of Inorganic and Organic S(IV) Species in Aerosols, Proc. 4th Joint Conf. on Sensing Environmental Pollutants, pp. 821-824, 1978.

Jacob, D. J., R. C. Flagan, J. M. Waldman and M. R. Hoffmann, Design and Calibration of Rotating-Arm Collectors for Ambient Fog Sampling, Proc. 4th International Conf. on Precipitation Scavenging, Dry Deposition and Resuspension, 29 Nov. - 3 Dec., Santa Monica, California, 1982.

Jacob, D. J., and M. R. Hoffmann, A Dynamic Model for the Production of H^+, NO_3^-, and SO_4^{2-} in Urban Fog, submitted to J. Geophys. Res., 1982.

Jacobson, J. S., Experimental Studies on the Phototoxicity of Acidic Precipitation: The United States Experience, pp. 151-160, in Effects of Acid Precipitation on Terrestrial Ecosystems, (T. C. Hutchinson and M. Havas, eds.), Plenum Press, New York, 1980.

Larsen, R. I., Relating Air Pollutant Effects to Concentration and Control, J. Air Poll. Control Assoc. 20, 214-225, 1970.

Lazrus, A. L., H. W. Baynton, and J. P. Lodge, Trace Constituents in Oceanic Cloud Water and their Origin, Tellus 22, 106-113, 1970.

Ledbury, W., and E. W. Blair, The Partial Formaldehyde Vapour Pressure of Aqueous Solutions of Formaldehyde. Part II. J. Chem. Soc. 127, 2832-2839, 1925.

Liljestrand, H. M., and J. J. Morgan, Spatial Variations of Acid Precipitation in Southern California, Environ. Sci. Tech. 15, 333-338, 1981.

Lindberg, S. E., R. C. Harriss, R. R. Turner, D. S. Shriner and D. D. Huff, Mechanisms and Rates of Atmospheric Deposition of Selected Trace Element and Sulfate to Deciduous Forest Watershed, ORNL/TM-6674, Oak Ridge National Laboratory, Oak Ridge, TN, 1979.

Lovett, G. M. and W. A. Reiners, Deposition of Cloudwater and Dissolved Ions to Subalpine Forests of New England, Proc. 4th Intl. Conf. Precip. Scav. Dry Dep. Resusp., Santa Monica, CA, Nov. 29 - Dec. 3, 1982.

Mack, E. J., and U. Katz, The Characteristics of Marine Fog Occurring off the Coast of Nova Scotia, Calspan Corp., Buffalo, New York, Report No. CJ-5756-M-1, 1976.

Mack, E. J., U. Katz, C. W. Rogers, et al., An Investigation of the Meteorology, Physics and Chemistry of Marine Boundary Layer Processes, Calspan Corp., Buffalo, New York, Report No. CJ-6017-M-1, 1977.

Mack, E. J., and R. J. Pilie, Fog Water Collector, U.S. Patent No. 3889532, 1975.

Martin, L. R., Kinetic Studies of Sulfite Oxidation in Aqueous Solution, in Acid Precipitation: SO_2, NO, NO_2 Oxidation Mechanisms: Atmospheric Considerations, J. G. Calvert (ed.), Ann Arbor Science, Ann Arbor, MI, 1982.

McMurry, P. H., D. J. Rader, and J. L. Smith, Studies of Aerosol Formation in Power Plant Plumes - I. Parameterization of Conversion Rate for Dry, Moderately Polluted Ambient Conditions, Atmos. Environ. 15, 2315-2329, 1981.

Metropolitan Museum of Art, The Horses of San Marco; Venice, J. and V. Wilton-Ely, transl., 1979.

Morgan, J. J., and H. J. Liljestrand, Measurement and Interpretation of Acid Rainfall in the Los Angeles Basin, W. M. Keck Laboratory of Hydraulics & Water Resources, California Institute of Technology, Pasadena, California, Report No. AC-2-80, 1980.

Mrose, H., Measurement of pH and Chemical Analyses of Rain-, Snow-, and Fog-Water, Tellus 18, 266-270, 1966.

Nash, T., The Colorimetric Estimation of Formaldehyde by Means of the Hantzsch Reaction, Biochem J. 55, 416-421, 1953.

National Research Council, Formaldehyde and Other Aldehydes, National Academy Press, Washington, D.C., 1981.

Oddie, B. C. V., The Chemical Composition of Precipitation at Cloud Levels, Quart. J. Roy. Meteor. Soc. 88, 535-538, 1962.

Okita, T., Concentrations of Sulfate and Other Inorganic Materials in Fog and Cloud Water and in Aerosol, J. Meteor. Soc. Japan 46, 120-126, 1968.

Petrenchuk, O. P., and V. M. Drozdova, On the Chemical Composition of Cloud Water, Tellus 18, 280-286, 1966.

Rietz, E. B., The Stabilization of Small Concentrations of Formaldehyde in Aqueous Solutions, Analytical Letters 13, 1073-1084, 1980.

Roach, W. T., R. Brown, S. J. Caughey, J. A. Garland, and C. J. Readiness, The Physics of Radiation Fog: I - A Field Study, Quart. J. Roy. Meteor. Soc. 10, 313-33, 1976.

Sander, S. P., and J. H. Seinfeld, Chemical Kinetics of Homogeneous Oxidation of Sulfur Dioxide, Environ. Sci. Tech. 10, 1114-1123, 1976.

Schlesinger, W. H., and W. A. Reiners, Deposition of Water and Cations on Artificial Foliar Collectors in Fir Krummholz of New England Mountains, Ecology 55, 378-386, 1974.

Schwartz, S. E., Gas-Aqueous Reactions of Sulfur and Nitrogen Oxides in Liquid-Water Clouds, in Acid Precipitation: SO_2, NO, and NO_2 Oxidation Mechanisms: Atmospheric Considerations, (J. G. Calvert, ed.), Ann Arbor Science Publishers, Inc., Michigan, 1982.

Sillén, L. G., and A. E. Martell, Stability Constants of Metal-Ion Complexes, Supplement No. 1, 2nd ed., The Chemical Society, London, 1971.

Smith, F. B., and G. H. Jeffrey, Airborne Transport of Sulphur Dioxide from the U.K., Atmos. Environ. 9, 643-659, 1975.

Solórzano, L., Determination of Ammonia in Natural Waters by the Phenolhypochlorite Method, Limnol. Oceanogr. 14, 799-801, 1967.

Stelson, A. W., Thermodynamics of Aqueous Atmospheric Aerosols, Ph.D. Thesis, California Institute of Technology, Pasadena, California, 127 pp, 1982.

Stelson, A. W., and J. H. Seinfeld, Relative Humidity and Temperature Dependence of the Ammonium Nitrate Dissociation Constant, Atmos. Environ. 16, 983-992, 1982.

Stewart, T. D., and L. H. Donnally, The Aldehyde Bisulfite Compounds II. The Effect of Varying Hydrogen Ion and of Varying Temperature upon the Equilibrium Between Benzaldehyde and Bisulfite Ion, J. Am. Chem. Soc. 54, 3555-3558, 1932.

Tukey, H. B., Jr., The Leaching of Substances from Plants, Ann. Rev. Plant Physiol. 71, 305-324, 1970.

U.S. EPA, Guide for Air Pollution Avoidance. Appendix B. History of Episodes. PH-22-68-32, 123-135, 1971.

Waldman, J. M., J. W. Munger, D. J. Jacob, R. C. Flagan, J. J. Morgan and M. R. Hoffmann, Chemical Composition of Acid Fog, Science 218, 677-680, 1982.

Wilkins, E. T., Air Pollution and the London Fog of December, 1952, J. Roy. Sanit. Instit. 74, 1-21, 1954a.

Wilkins, E. T., Air Pollution Aspects of the London Fog of December, 1952. J. Roy. Meteorol. Soc. 80, 267-278, 1954b.

Wilson, J. C., and P. H. McMurry, Studies of Aerosol Formation in Power Plant Plumes - II. Secondary Aerosol Formation in the Navajo Generating Station Plume, Atmos. Environ. 15, 2329-2339, 1981.

Table Captions

Table 1. Description of conditions during and before fog sample collection.

Table 2. Concentration ranges for major and minor ions, sulfite, and formaldehyde observed during fog events. The number of samples collected during each event is indicated in column 2.

Table 3. Ranges of selected trace-metal concentrations in fog samples. Number of samples per event is the same as for Table 2.

Table 4. Equilibrium constants applicable to S(IV) and aldehyde chemistry in the aqueous phase.

Table 5. Summary of fog and cloud water compositions reported by previous investigators.

Table 1

Site	Date	Sampled Interval (hrs)	Conditions During Fog	Prior Conditions
Pasadena	11/15/81	2040-0115	Light wind SSW-N; sampled beginning to end of fog.	Fair, good air quality.
Pasadena	11/23/81	2320-0130	Light S-SE wind; 14°-12°C; fog thickened to near drizzle; sampled beginning to end of fog.	Hazy and smoggy.
Lennox	12/7/81	2305-0840	Light W wind; traffic volume and ambient pollutants began to increase at 0530; missed first hour of fog, sampled until fog lifted.	Previous night foggy, smoggy during day, NO_x alert called (NO_x = 0.8 ppm).
Lennox	12/18/81	2315-0043	Light W wind; sampled from beginning of fog, fog persisted until morning.	Previous night foggy; high NO_x levels during day.
Pasadena	12/20/81	745-845	Light N wind; 10°C; fog began before 0700; sampled until fog lifted	Previous day was fair.
Oildale	1/14/82	0200-0750	Light S wind; 3°-4°C, thin fog.	Overcast all of preceeding day, dense fog on previous night.
Pasadena	1/17/82	2130-2200	Sample collected as fog dissipated.	Smog and haze during the afternoon.
Upland	5/14/82	0630-0910	Light and variable wind, 12°C, thin fog.	Low clouds and ground haze throughout night.

Table 2

Location	# Samples in Event	Date	pH	$\mu eq\ L^{-1}$										mg/L	
				H^+	Na^+	K^+	NH_4^+	Ca^{2+}	Mg^{2+}	F^-	Cl^-	NO_3^-	SO_4^{2-}	SO_2	CH_2O
Pasadena	4	11/15/81	5.25-4.74	5.6-55	12-496	4-39	370	19-360	7-153	120	56-280	130-930	62-380	--	--
Pasadena	4	11/23/81	4.85-2.92	14-1200	320-500	33-53	1290-2380	140-530	89-360	180-410	480-730	1220-3250	481-944	150-180	3.1-3.5
Lennox	8	12/7/81	5.78-2.55	2-2820	28-480	6-156	1120-4060	49-4350	17-1380	115-395	111-1110	820-4560	540-2090	30-250	4.6-12.8
Lennox	3	12/18/81	2.81-2.52	1550-3020	80-166	19-40	950-1570	73-190	43-99	180-500	90-197	2070-3690	610-1970	--	--
Pasadena	1	12/20/81	3.75	178	51	373	1773	217	78	242	161	1000	450	--	--
Oildale	3	1/14/82	3.07-2.90	850-1260	151-1220	39-224	4310-9750	165-1326	20-151	126-242	203-592	3140-5140	2250-5000	440-710	6.1-14.4
Pasadena	1	1/17/82	2.25	5625	2180	500	7960	2050	1190	637	676	12000	5060	--	--
Upland	3	5/14/82	2.88-2.22	1320-6310	1220-5200	96-482	2329-6312	596-4218	321-1816	168-342	654-1110	4240-10660	2760-4890	446-592	6.1-8.6

Table 3

$\mu g\ \ell^{-1}$

Site	Date	Fe	Mn	Pb	Cu	Ni
Pasadena	11/15/81	90-2100	18-160	250-270	1-15	2-21
Pasadena	11/23/81	920-1770	34-56	1310-2540	88-140	8-14
Lennox	12/7/81	356-23700	19-810	820-2400	9-150	2-52
Lennox	12/18/81	1020-2080	25-81	1700-2350	84-1400	32-54
Pasadena	12/20/81	340	42	156	--	--
Oildale	1/14/82	240-6400	97-800	241-366	45-401	124-586
Upland	5/14/82	--	430-570	1690-2400	156-185	155-213

Table 4

Equilibrium Constants Applicable to S(IV) and Aldehyde Chemistry

	K (M or $M\ atm^{-1}$)	ΔH°_{298} (kcal/mole)	Ref.
$SO_{2(g)} \overset{K_H}{\rightleftharpoons} SO_{2(aq)}$	1.245	-6.247	a
$SO_{2(aq)} \overset{K_{a1}}{\rightleftharpoons} H^+ + HSO_3^-$	1.290×10^{-2}	-4.161	a
$HSO_3^- \overset{K_{a2}}{\rightleftharpoons} H^+ + SO_3^{2-}$	6.014×10^{-8}	-2.23	a
$CH_2O_{(g)} \overset{K_H'}{\rightleftharpoons} CH_2O_{(aq)}$	6.3×10^3	--	b
$CH_2O_{(aq)} + HSO_3^- \overset{K_{A,1}}{\rightleftharpoons} CH_2OHSO_3^-$	$\approx 10^5$	--	c
$Fe^{3+} + SO_3^{2-} \overset{\beta}{\rightleftharpoons} FeSO_3^+$	$\approx 10^{10}$-10^{18}	--	d
$C_7H_6O + HSO_3^- \overset{K_{A,2}}{\rightleftharpoons} C_7H_6OHSO_3^-$	$\approx 10^5$	--	e
$C_2H_4O + HSO_3^- \overset{K_{A,3}}{\rightleftharpoons} C_2H_4OHSO_3^-$	$\approx 10^5$	--	f

a. Sillén and Martell [1971]

b. Ledbury and Blair [1925]

c. Dasgupta et al. [1980]

d. Carlyle [1971]; Hansen et al. [1976]

e. Stewart and Donnally [1932]

f. by extrapolation

Table 5

Summary of Fog & Cloud Water Compositions

Location	Date	Type[a]	pH	SO_4^{2-} (μeq L^{-1})	NO_3^- (μeq L^{-1})	Cl^- (μeq L^{-1})	Na^+ (μeq L^{-1})	K^+ (μeq L^{-1})	Ca^{2+} (μeq L^{-1})	Mg^{2+} (μeq L^{-1})	NH_4^+ (μeq L^{-1})	Reference
Mt. Washington, NH	1930-40	CF	3.0-5.9	4.2-1100		0-34						Houghton (1955)
Nantucket, MA	1930-40	MF	-	285-2600		650-5750						"
Brooklin, ME	1930-40	F	3.5-6.3	95-770		0-140						"
SW of London	1960	C[b]	4.4-7.2	40	19	94	95	13	66	25	22	Oddie (1962)
Germany, Baltic Sea	1955-65	MF[b]	3.8	1860	900	1740	1500	240	750		2335	Mrose (1966)
Harz Mtn.	1955-65	CF[b]	5.1	775	450	205	295	85	220		710	"
nr. Dresden	1955-65	UF[b]	4.2	3300	380	585			3180		2100	"
Kiev, USSR	12/64	C	3.4-5.4	400-2060	17-200	115-325	80-215	30-130	40-535	16-160	235-1300	Petrenchuk & Drozdova (1966)
Mt. Norikura, Japan	7/63	CF	3.4-4.3	230-1250	50-350	75-230	45-165	55-85			115-260	Okita (1968)
Mt. Tsukaba, Japan	11/63	CF	5.6-6.5	360-2065	11-75	295-1270	180-435	154			110-965	"
Puerto Rico	11-12/67	C	4.9-5.4	75-190		150-1975				20-90	35-400	Lazrus et al. (1970)
Nova Scotia	8/75	MF		54-470		14-235	880-1240	43-50	38-69	42-77	9-72	Mack & Katz (1976)
Coastal California	9-10/76	MF		77-490	24-235	96-1235	78-945	11-23	9-100	23-175	0-580	Mack et al. (1977)
Whiteface Mtn., NY	8/76	CF[c]	3.6-3.9	52-140	140-215	1.7-3.1	2.3-11	13-20	10-20	2.2-6.1	32-89	Castillo (1980)
	8/80	CF	3.2-4.0	32-806	7-192	1-14	1-7	1-6			4-197	Falconer (1981)
Los Angeles, CA	1/80	C	4.6-6.8	5-400	0-445	1-760	2-50	1-70			0-230	Hegg & Hobbs (1981)

[a]Type of sample: F = fog; C = clouds aloft; CF = intercepted clouds; MF = marine fog; UF = urban fog

[b]Mean values of samples

[c]Range of mean values; otherwise range of samples

Figure Captions

Figure 1. Map of fog sampling sites in Southern California. Los Angeles area sites are indicated on the inset.

Figure 2. A schematic flow diagram indicating fog sample-handling protocol and analytical procedures.

Figure 3. Ionic composition as a function of time in sequential fog samples. Sampling interval is indicated by the width of each bar. The times of fog formation and dissipation are indicated by arrows.

Figure 4. (a-h) Non-dimensional concentrations of individual ions in fog collected on 7-8 December 1981 at the Lennox sampling site. Concentrations are normalized for each component with respect to the concentrations in the initial sample (i.e., $\hat{C}_i = C_i/C_{i,o}$). Note the differences in scale. Sampling interval indicated by the width of each bar. NA indicates that a sample was not analyzed. Magnesium and sodium, which are not shown, were nearly identical to Ca^{2+} and Cl^-, respectively.

Figure 5. (a-h) Non-dimensional concentrations of individual ions in fog collected on 23-24 November 1981, at the Pasadena sampling site. The normalization procedure and scales are described in Figure 4.

Figure 6. A schematic diagram depicting the temperature and humidity dependence for fog formation and the apparent link between atmospheric gas phase and water phase chemistry.

Figure 7. Plot of nitrate and sulfate equivalent concentrations in fogwater. Dashed lines indicate 2.5:1 and 1:1 ratios.

Figure 8. Plot of sodium and chloride concentrations. Dashed line indicates the sea salt ratio for NaCl.

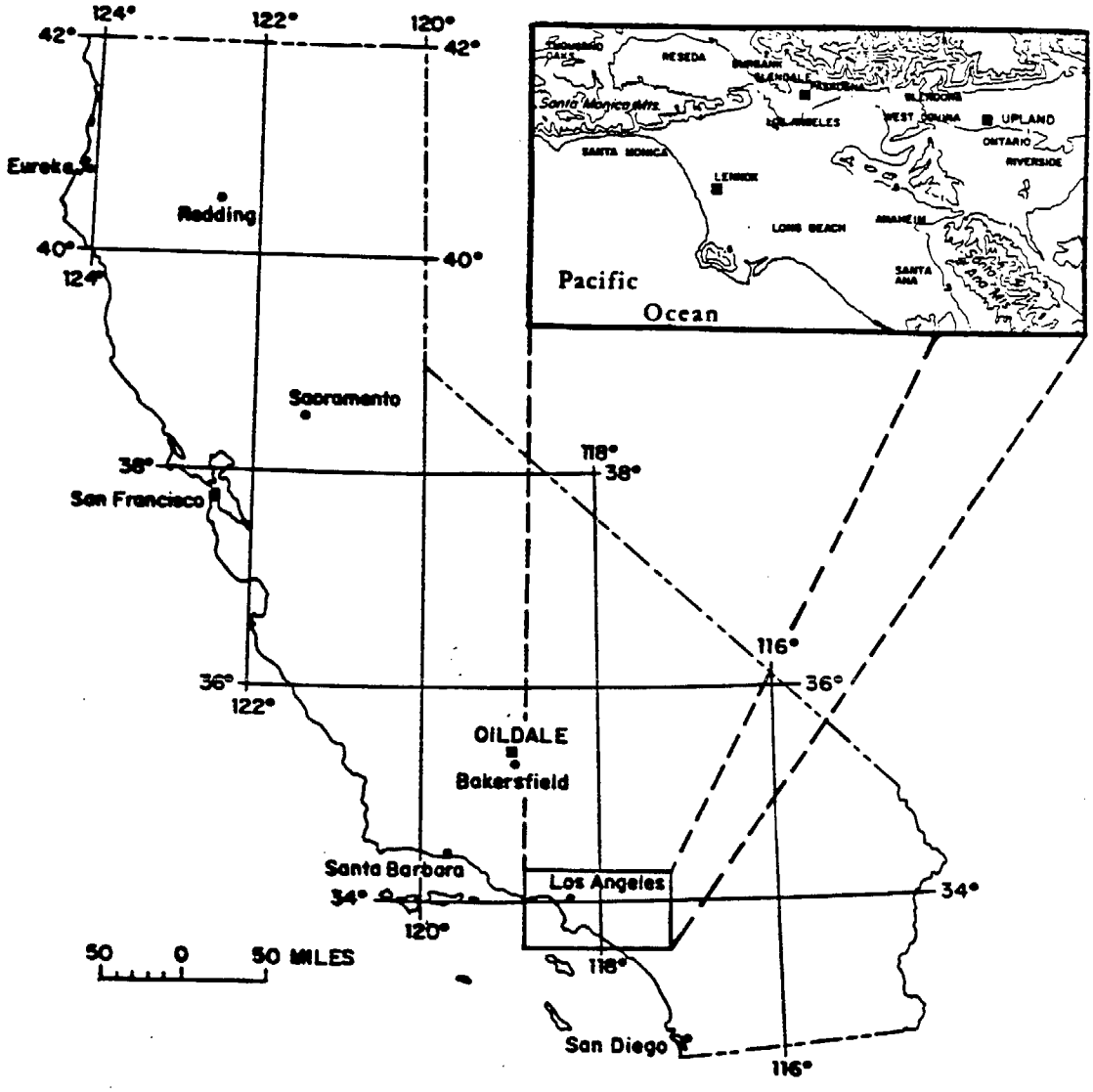
124°
122°
120°
42°
42°
Eureka
Redding
40°
124°
40°
Sacramento
38°
118°
38°
San Francisco
116°
36°
122°
36°
OILDALE
Bakersfield
Santa Barbara
Los Angeles
34°
34°
120°
118°
50 0 50 MILES
San Diego
116°
Pacific
Ocean
RESEDA
BURBANK
GLENDALE
PASADENA
Santa Monica Mts.
BLYTHE
WEST COVINA
UPLAND
ONTARIO
RIVERSIDE
SANTA MONICA
LENNOX
LONG BEACH
ANAHEIM
SANTA ANA

Figure 1

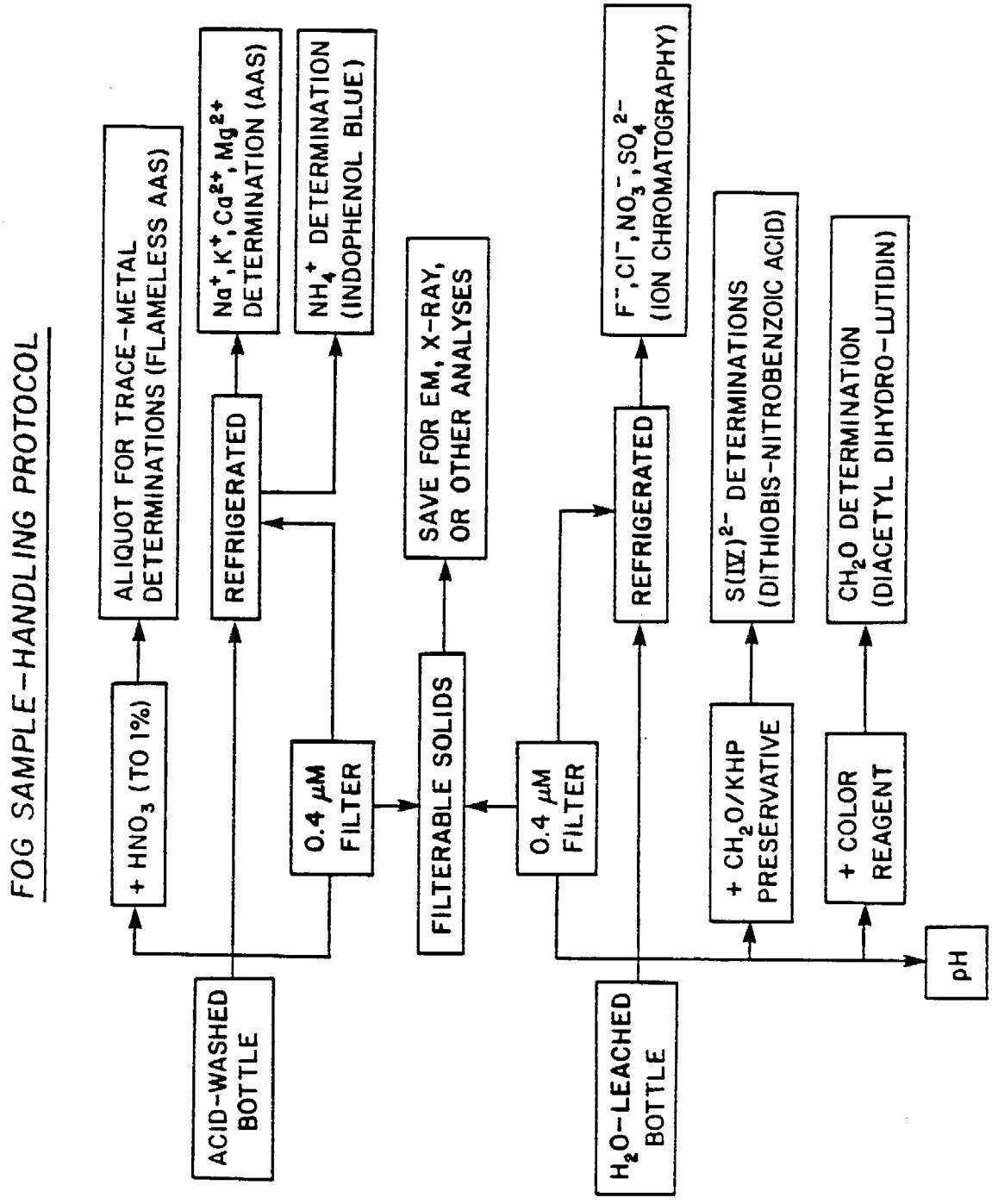
FOG SAMPLE-HANDLING PROTOCOL
ACID-WASHED BOTTLE
+ HNO_3 (TO 1%)
ALIQUOT FOR TRACE-METAL DETERMINATIONS (FLAMELESS AAS)
REFRIGERATED
$Na^+, K^+, Ca^{2+}, Mg^{2+}$ DETERMINATION (AAS)
0.4 μM FILTER
NH_4^+ DETERMINATION (INDOPHENOL BLUE)
FILTERABLE SOLIDS
SAVE FOR EM, X-RAY, OR OTHER ANALYSES
H_2O-LEACHED BOTTLE
0.4 μM FILTER
REFRIGERATED
$F^-, Cl^-, NO_3^-, SO_4^{2-}$ (ION CHROMATOGRAPHY)
+ CH_2O/KHP PRESERVATIVE
$S(IV)^{2-}$ DETERMINATIONS (DITHIOBIS-NITROBENZOIC ACID)
+ COLOR REAGENT
CH_2O DETERMINATION (DIACETYL DIHYDRO-LUTIDIN)
pH

Figure 2

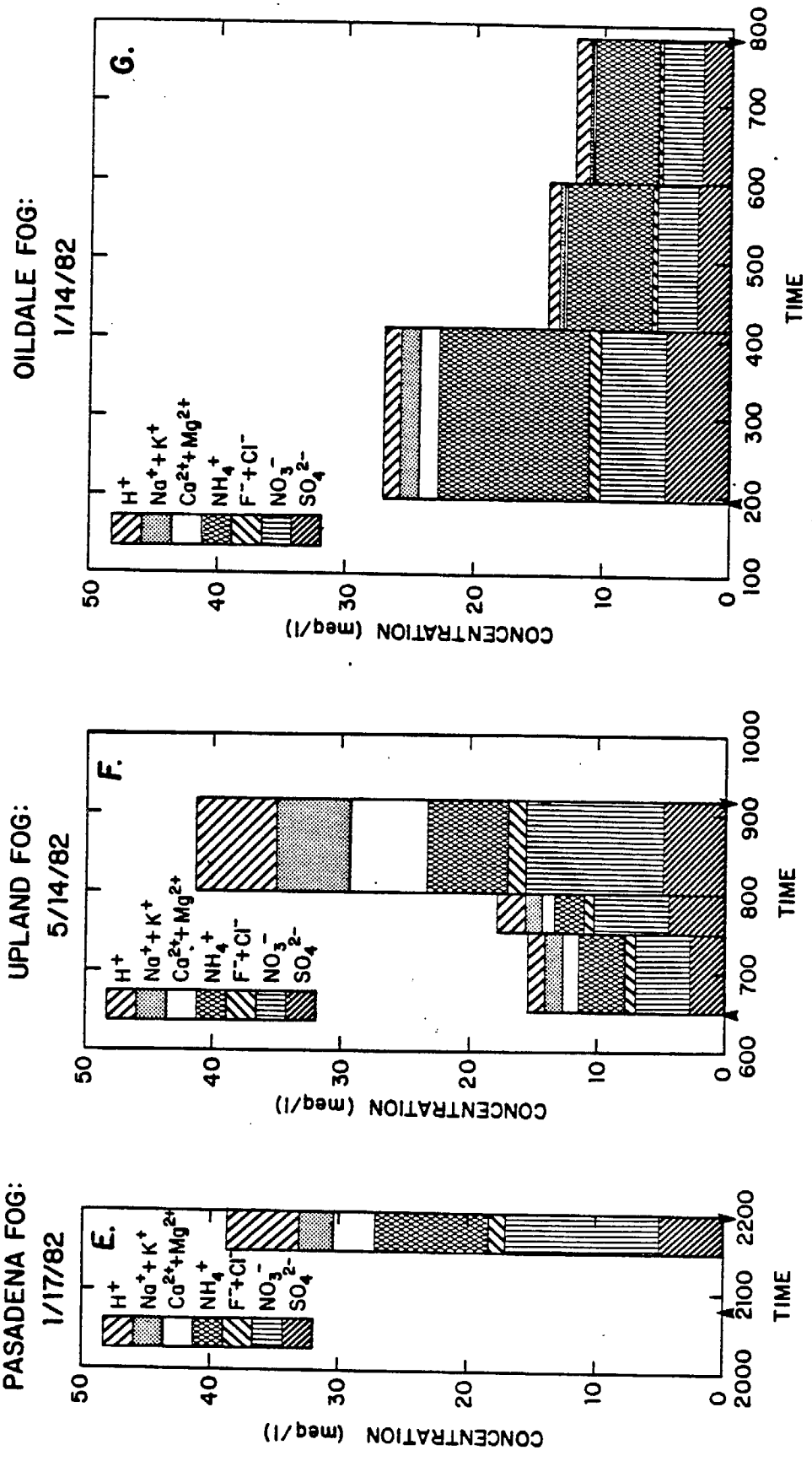
PASADENA FOG:
1/17/82
E.
UPLAND FOG:
5/14/82
F.
OILDALE FOG:
1/14/82
G.
H+
Na+ + K+
Ca2+ + Mg2+
NH4+
F- + Cl-
NO3-
SO4 2-
CONCENTRATION (meq/l)
TIME

Figure 3

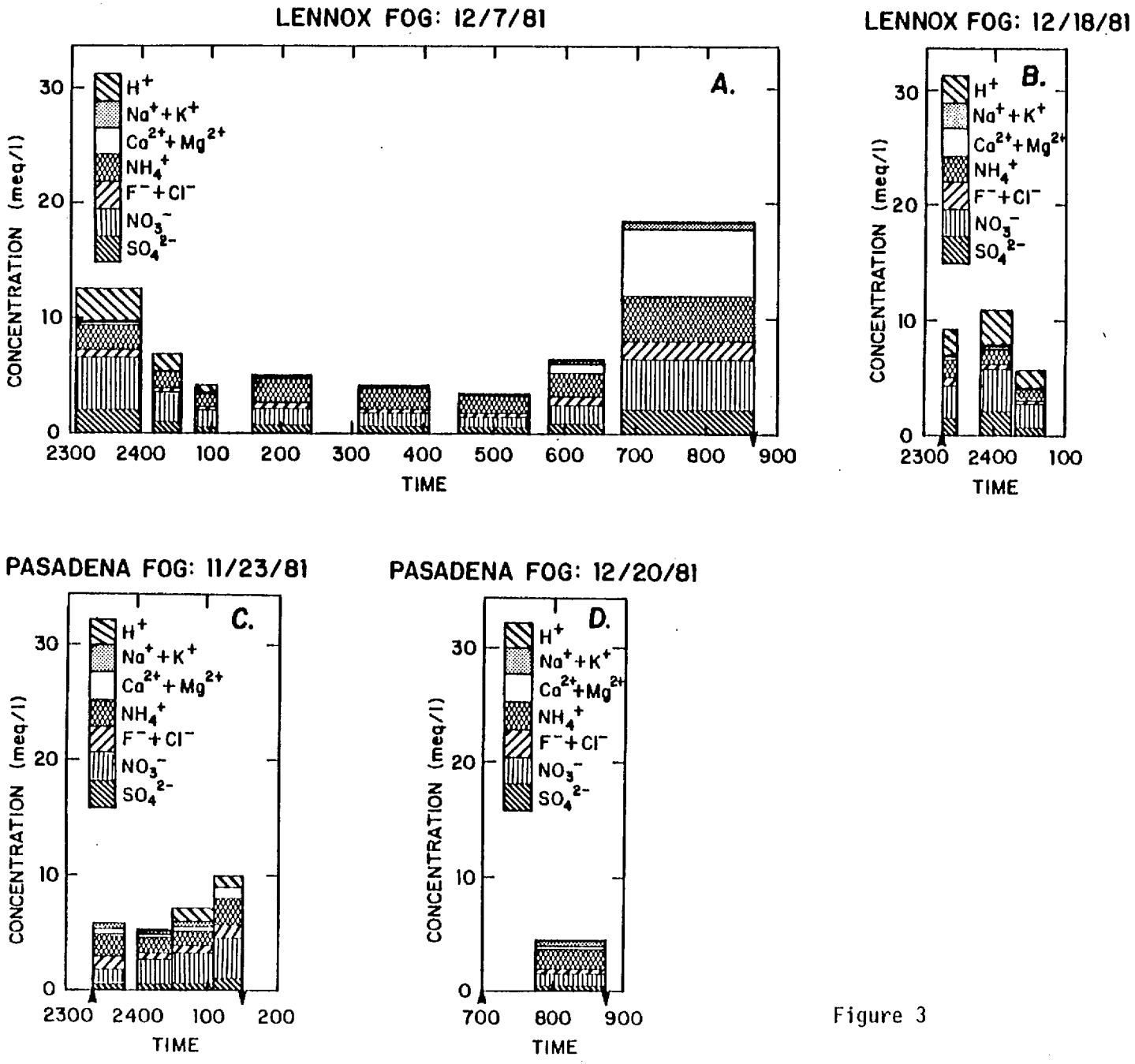
LENNOX FOG: 12/7/81
A.
LENNOX FOG: 12/18/81
B.
PASADENA FOG: 11/23/81
C.
PASADENA FOG: 12/20/81
D.
CONCENTRATION (meq/l)
TIME
H+
Na+ + K+
Ca2+ + Mg2+
NH4+
F− + Cl−
NO3−
SO4 2−
0
10
20
30
2300
2400
100
200
300
400
500
600
700
800
900

Figure 3

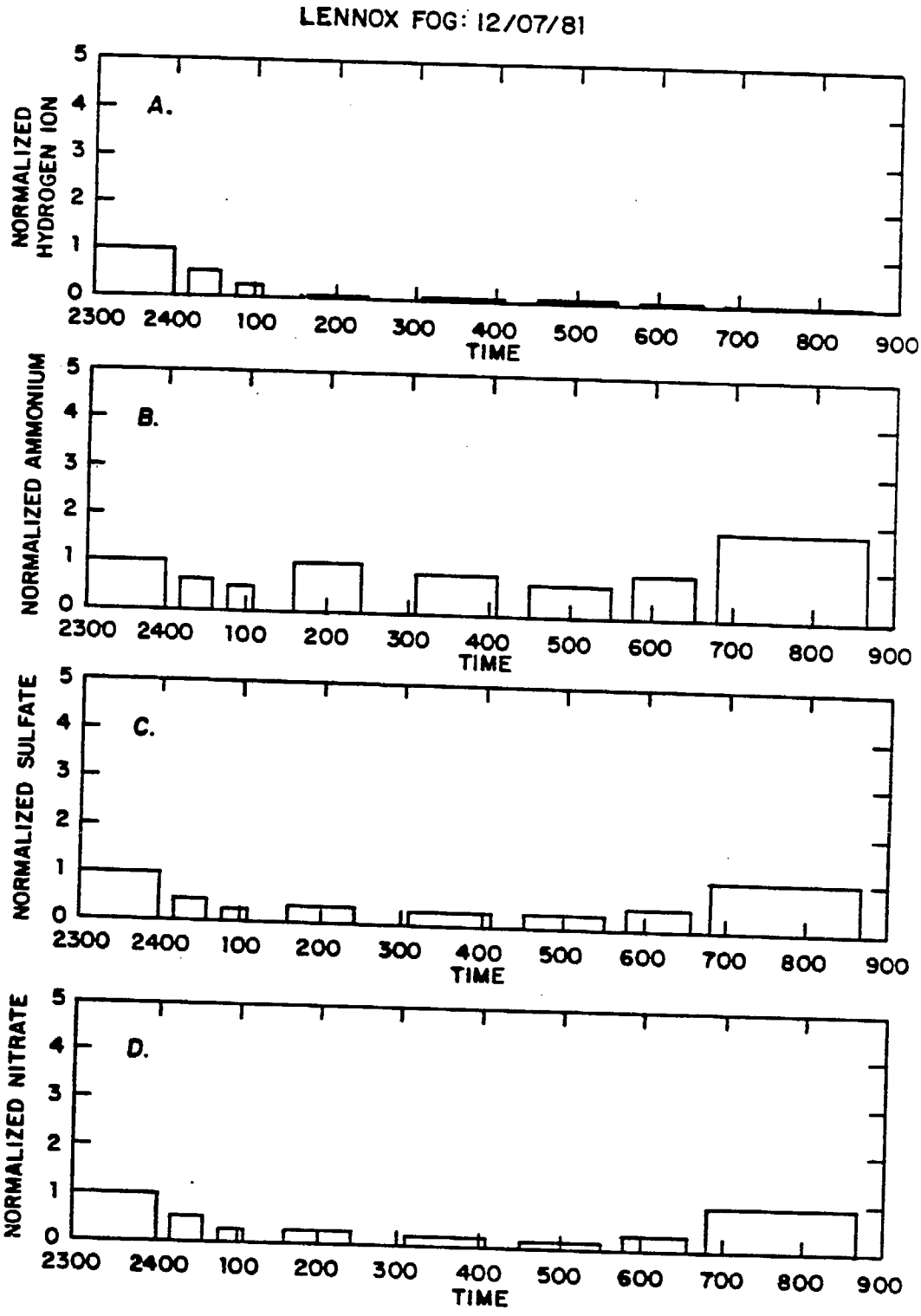
LENNOX FOG: 12/07/81
A.
NORMALIZED HYDROGEN ION
B.
NORMALIZED AMMONIUM
C.
NORMALIZED SULFATE
D.
NORMALIZED NITRATE
0
1
2
3
4
5
2300
2400
100
200
300
400
500
600
700
800
900
TIME

Figure 4

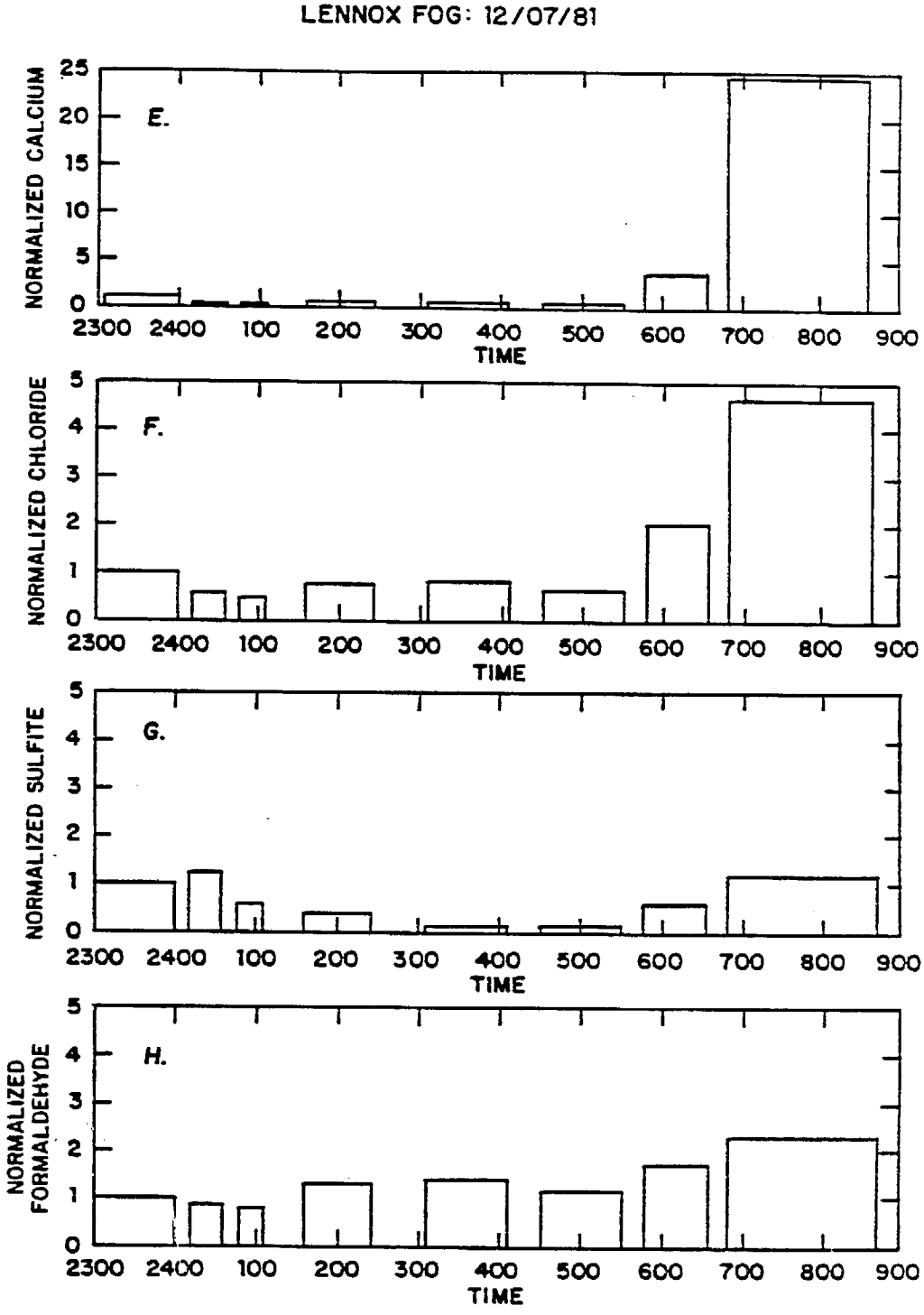
LENNOX FOG: 12/07/81
NORMALIZED CALCIUM
E.
NORMALIZED CHLORIDE
F.
NORMALIZED SULFITE
G.
NORMALIZED FORMALDEHYDE
H.
TIME
2300 2400 100 200 300 400 500 600 700 800 900

Figure 4

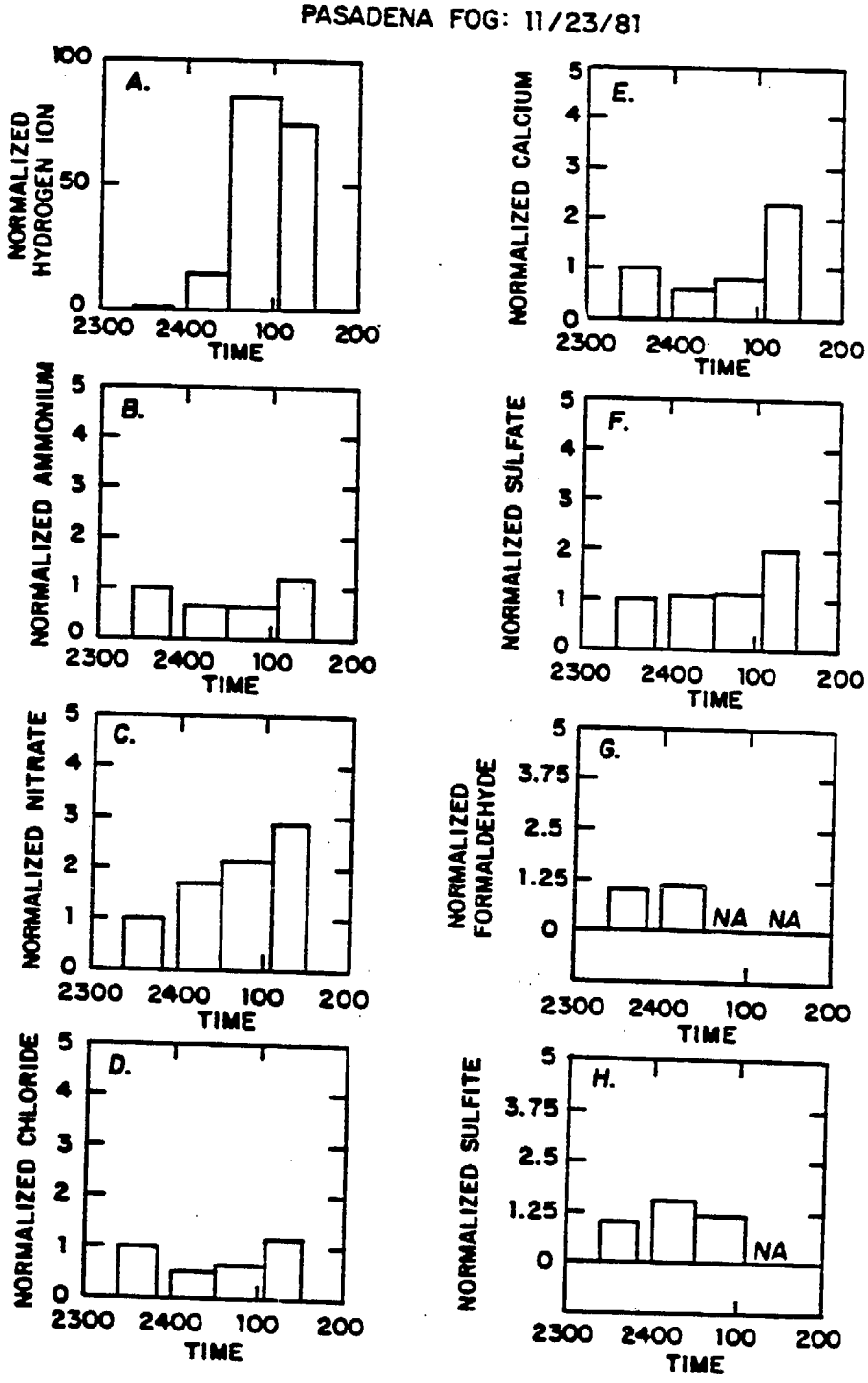
PASADENA FOG: 11/23/81
A.
NORMALIZED HYDROGEN ION
100
50
0
2300 2400 100 200
TIME
B.
NORMALIZED AMMONIUM
5
4
3
2
1
0
2300 2400 100 200
TIME
C.
NORMALIZED NITRATE
5
4
3
2
1
0
2300 2400 100 200
TIME
D.
NORMALIZED CHLORIDE
5
4
3
2
1
0
2300 2400 100 200
TIME
E.
NORMALIZED CALCIUM
5
4
3
2
1
0
2300 2400 100 200
TIME
F.
NORMALIZED SULFATE
5
4
3
2
1
0
2300 2400 100 200
TIME
G.
NORMALIZED FORMALDEHYDE
5
3.75
2.5
1.25
0
NA NA
2300 2400 100 200
TIME
H.
NORMALIZED SULFITE
5
3.75
2.5
1.25
0
NA
2300 2400 100 200
TIME

Figure 5

FOG: LINK BETWEEN ATMOSPHERIC AND WATER CHEMISTRY

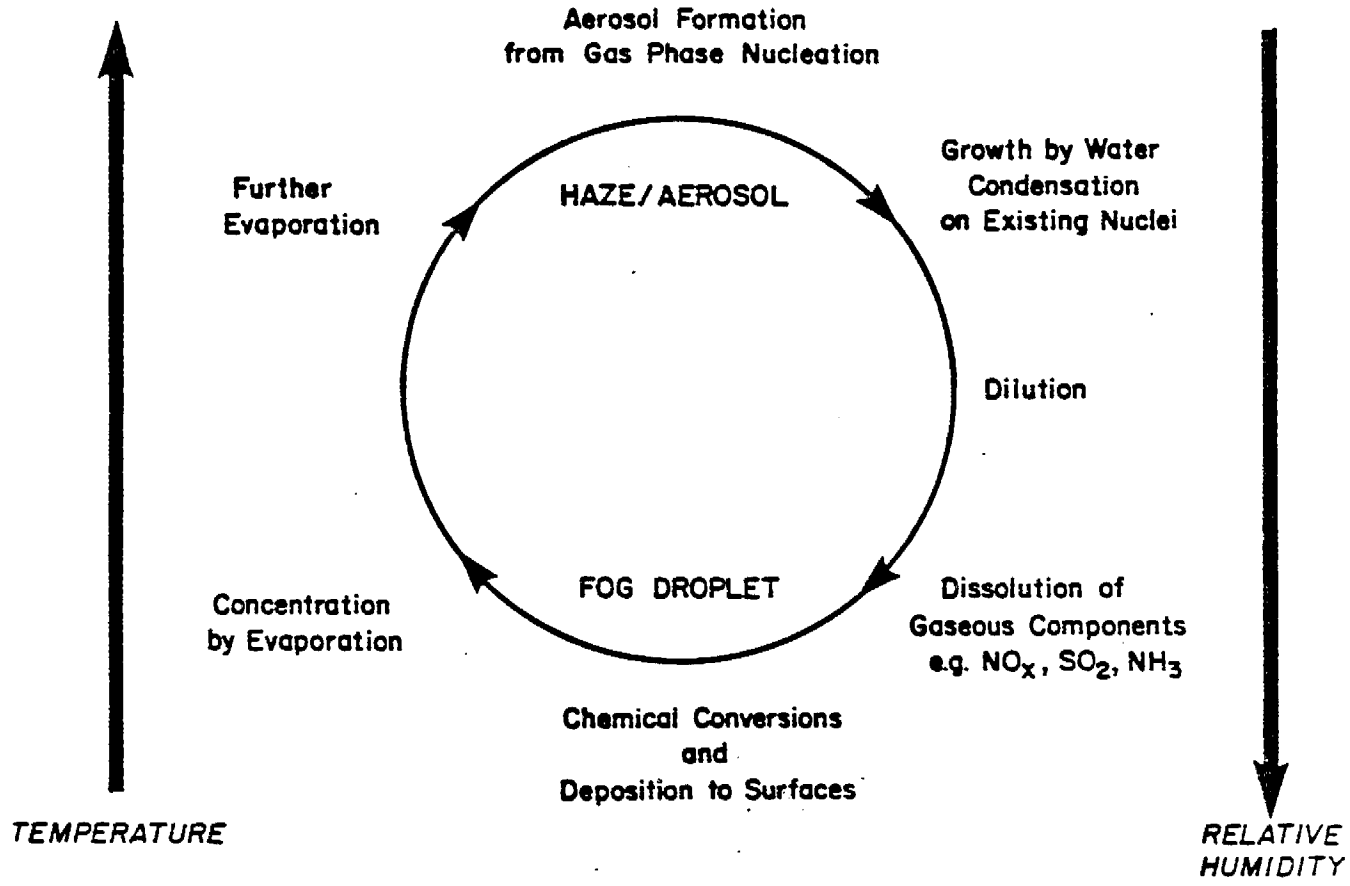

Figure 6

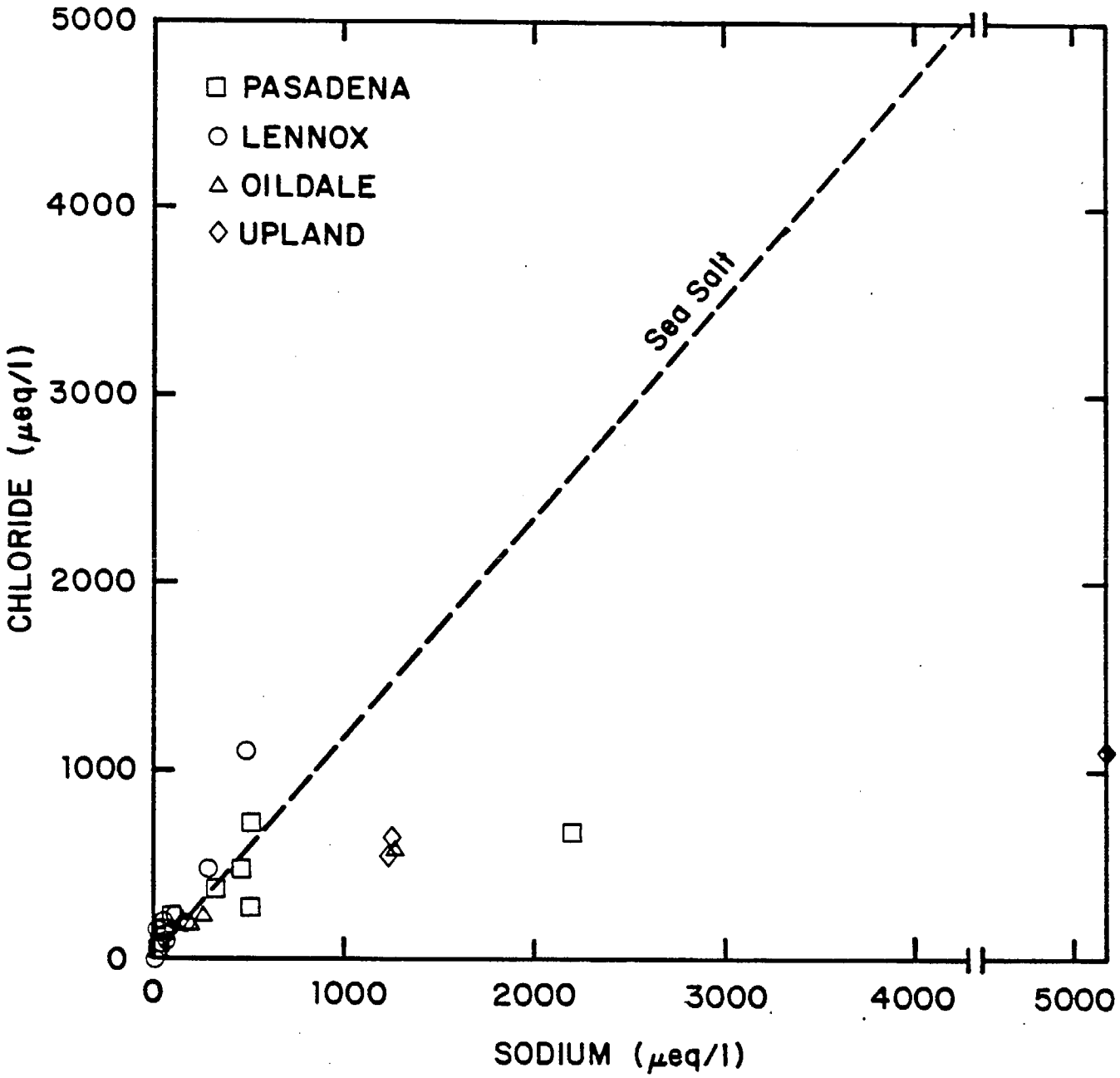
5000
4000
3000
2000
1000
0
CHLORIDE (μeq/l)
PASADENA
LENNOX
OILDALE
UPLAND
Sea Salt
0
1000
2000
3000
4000
5000
SODIUM (μeq/l)

Figure 7

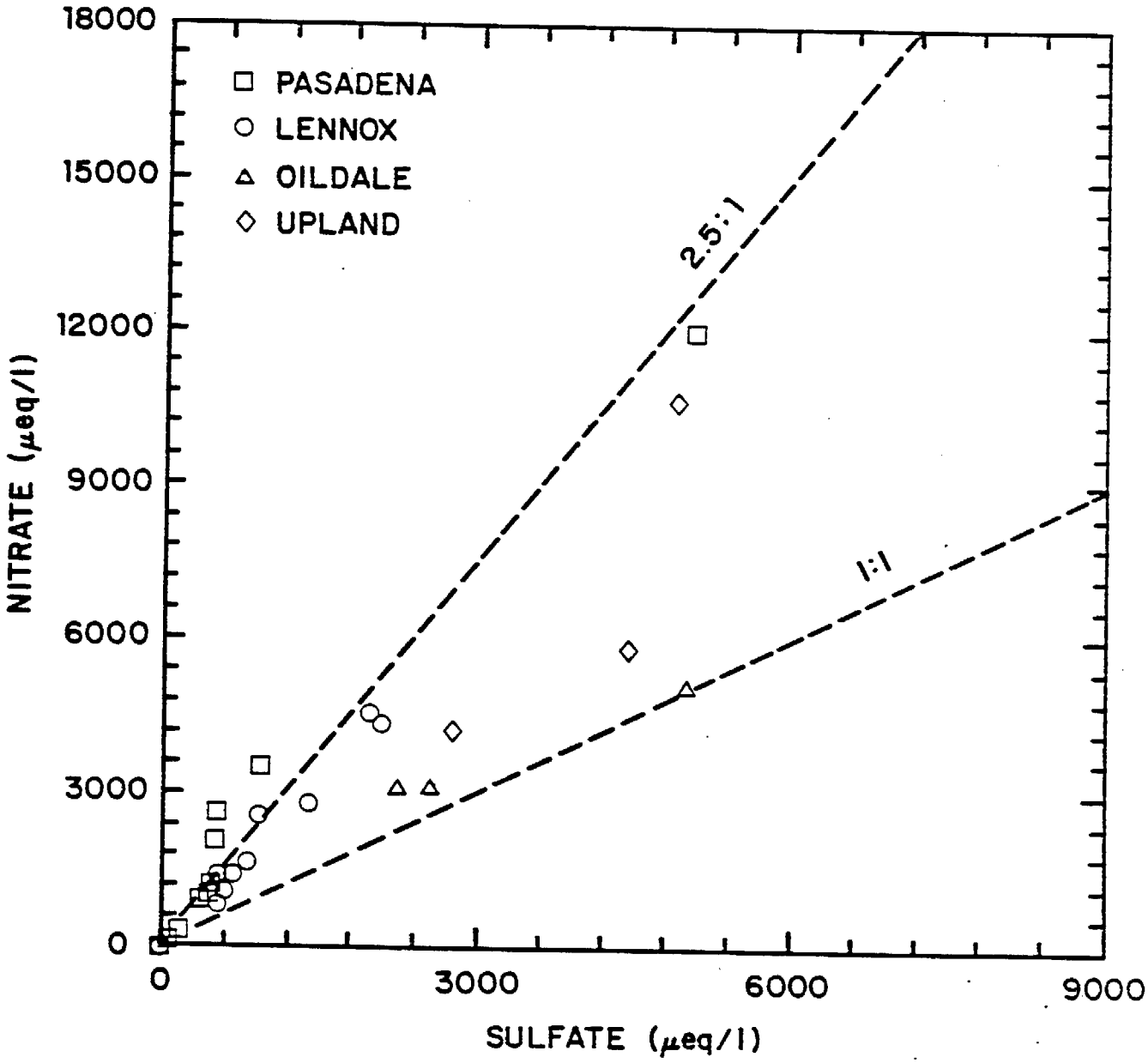
18000
15000
12000
9000
6000
3000
0
NITRATE (μeq/l)
PASADENA
LENNOX
OILDALE
UPLAND
2.5:1
1:1
0
3000
6000
9000
SULFATE (μeq/l)

Figure 8

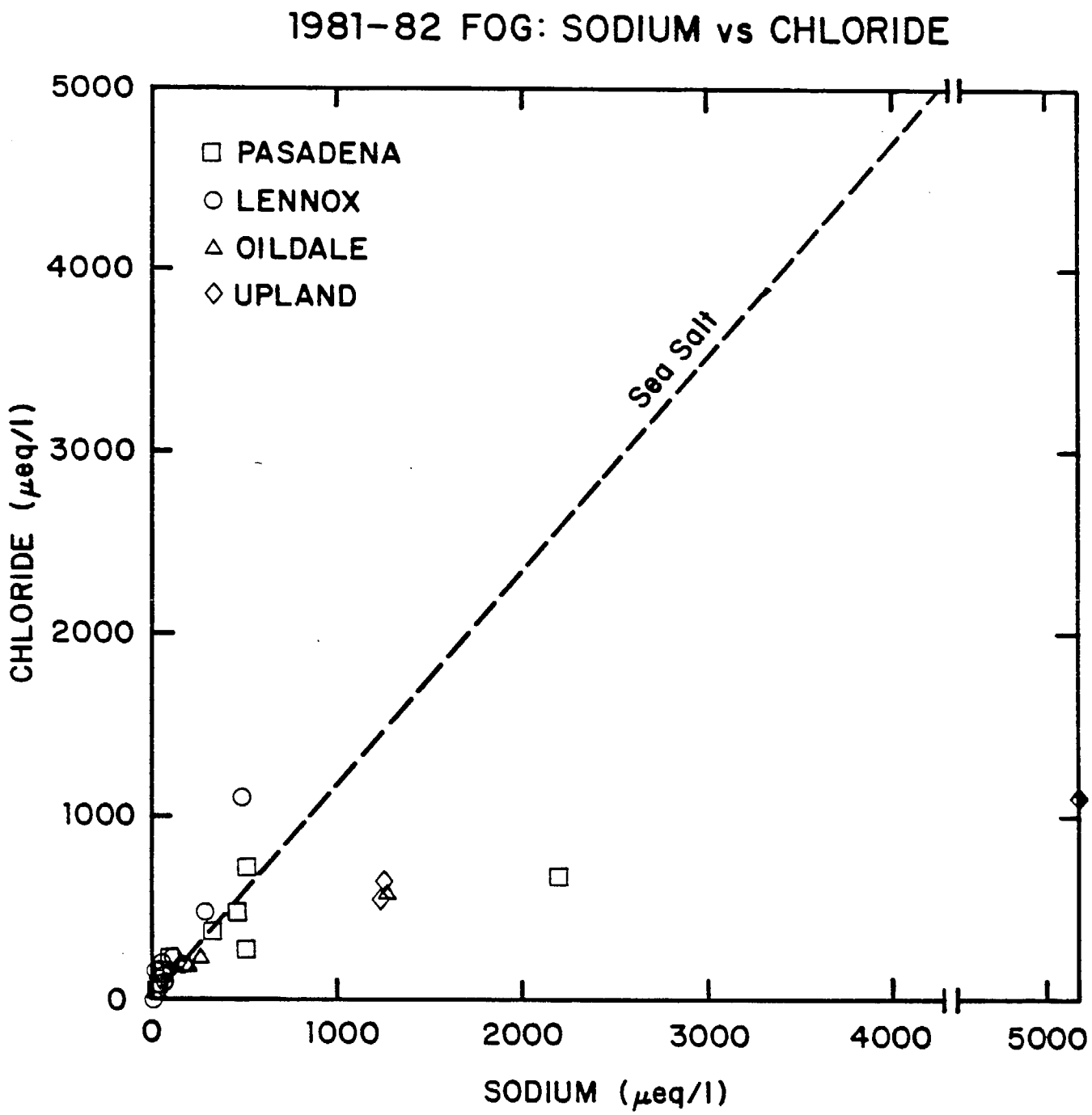
1981-82 FOG: SODIUM vs CHLORIDE
PASADENA
LENNOX
OILDALE
UPLAND
Sea Salt
CHLORIDE (μeq/l)
SODIUM (μeq/l)
0
1000
2000
3000
4000
5000

Figure 9

CHAPTER V

A DYNAMIC MODEL FOR THE PRODUCTION OF H^+, NO_3^- AND SO_4^{2-} IN URBAN FOG

by

Daniel J. Jacob and Michael R. Hoffmann*

Environmental Engineering Science
W. M. Keck Laboratories
California Institute of Technology
Pasadena, CA 91125

for

Journal of Geophysical Research
Oceans and Atmospheres

September 1982
Revised: March 1983

*To whom correspondence should be addressed.

ABSTRACT

The chemical composition of nighttime urban fog has been investigated using a hybrid kinetic and equilibrium model. Extreme acidity found in Southern California fog may be due either to condensation and growth on acidic condensation nuclei or *in situ* S(IV) oxidation. Important oxidants of S(IV) were found to be O_2 as catalyzed by Fe(III) and Mn(II), H_2O_2 and O_3. Formation of hydroxymethanesulfonate ion (HMSA) via the nucleophillic addition of HSO_3^- to $CH_2O(\ell)$ significantly increased the droplet capacity for S(IV) but did not slow down the net S(IV) oxidation rate leading to fog acidification. Gas phase nitric acid, ammonia and hydrogen peroxide were scavenged efficiently, although aqueous phase hydrogen peroxide was depleted rapidly by reduction with S(IV). Nitrate production in the aqueous phase was found to be dominated by HNO_3 gas phase scavenging. Major aqueous-phase species concentrations were controlled primarily by condensation, evaporation, and pH.

Introduction

Concentrations of major ions in non-precipitating clouds [Hegg and Hobbs, 1981] and fogs [Waldman et al., 1982; Munger et al., 1983] have been reported to be significantly higher than those commonly observed in acidic precipitation. In Los Angeles, fogwater [Waldman et al., 1982; Munger et al., 1983] was reported to have acidities 100 times higher than those observed previously in rainwater by Liljestrand and Morgan [1981]. Lower dilutions and higher scavenging efficiencies due to reduced mass transfer limitations of gas absorption and longer residence times may explain, in part, the higher concentrations found in fog (1-100 μm) than in rain (0.1-3.0 mm).

A number of rainwater and cloudwater chemistry models have been proposed recently. Adamowicz [1978] simulated the chemistry of raindrops falling through a well-mixed polluted layer with uniform and constant concentrations of SO_2, CO_2, and NH_3. Gas and aqueous-phase equilibria were established at all times and aqueous-phase transformation of S(IV) to S(VI) was allowed to proceed through the iron-catalyzed oxidation by O_2 according to the kinetic expression of Brimblecombe and Spedding [1974]. Mass transfer at the surface of the drop was modeled by two-film theory, but Baboolal et al. [1981] have since shown this simple model to be unsatisfactory since it ignores forced convection inside and outside of the falling drop. Durham et al. [1981] added NO_x to the gas phase and allowed some NO_x gas-phase chemistry, considered kinetic expressions for all reactions instead of equilibrium relationships, and assumed O_3 to be the only liquid-phase oxidant of S(IV) using the rate law of Erickson et al. [1977]. Easter and

Hobbs [1974] modeled cloudwater chemistry by using a wave cloud model, an open atmosphere with trace concentrations of CO_2, SO_2, and NH_3, and a rudimentary S(IV) oxidation rate consisting of a simple first-order dependence on sulfite. More recent models have been proposed by Middleton et al. [1980], Chameides and Davis [1982], and Carmichael et al. [1983].

With this work in mind, a dynamic model for fogwater chemistry has been developed. The model has a hybrid kinetic and equilibrium structure; reactions which rapidly come to equilibrium are considered separately from reactions that are kinetically controlled. Gas-phase chemistry, particle scavenging by droplets, evolution of the droplet microphysics and deposition were not included explicitly.

Structure of the Model

a) *aqueous-phase reactions.*

The chemical composition of a fog droplet is assumed to be determined by the following factors: (a) the composition of the activated cloud condensation nuclei (CCN) on which the droplet condenses, (b) the absorption of atmospheric gases at the droplet surface, and (c) the subsequent aqueous-phase reactions of homogeneous and heterogeneous species. Proton transfer and most ligand substitution reactions proceed extremely fast compared to the time scales of interest in this study [Hoffmann, 1981], therefore they are treated as dynamic equilibria. The same assumption is applied to gas absorption in accordance with Henry's law, although mass transfer may be retarded by the formation of an organic film at the droplet surface [Graedel et al., 1982]. Equilibrium constants, K, have been adjusted for temperature, T, with the van't Hoff relationship:

a set value which is very small. Corrections for ionic strength were made using the Davies equation [Stumm and Morgan, 1981]. The thermodynamic data base consisted of 1300 equilibria; those found to influence the droplet composition are listed in Table 1.

For slower reactions empirical rate laws were used. Specific rate laws for oxidation reactions involving N(III) and S(IV) have been incorporated in the model; they are listed in Table 2. Hydrogen peroxide, N(III) and O_3 are potentially important oxidants, and O_2 may also be important if catalyzed by active sites on soot or by transition metals such as Fe(III) and Mn(II). Iron(III) and manganese(II) are effective catalysts when dissolved as free ions or complexes [Hoffmann and Jacob, 1983] but their catalytic properties are altered if they are present as solid phases. Surface catalysis may occur but, in the absence of reliable data, it has been neglected. In the kinetic formulation of reaction (33), [Fe(III)] and [Mn(II)] represent the summation of concentrations of all dissolved iron and manganese species. It should be noted that the kinetic data for this reaction is not satisfactory around pH 4 because of the influence of $Fe(OH)_3(s)$ which starts dissolving near pH 4. Rate expressions given by Martin [1983] at high pH and low pH fail to extrapolate to the same value at intermediate pH. To minimize this problem an average of the two expressions was used near pH 4.

The reactions of absorption and aqueous-phase disproportionation of NO_x to form nitrous and nitric acid have been reviewed by Schwartz and White [1981]. These reactions could be major contributors to nitrate formation in fog droplets if allowed to reach equilibrium; however because of second-order kinetics they are too slow to be important on the time

$$\int_{K_1}^{K_2} d\ln K = \frac{\Delta H^\circ}{R} \int_{T_1}^{T_2} \frac{dT}{T^2} \qquad (1)$$

ΔH° values at 298 K were obtained from literature sources (see Table 1). The equilibrium composition was determined using a MINEQL subroutine [Morel and Morgan, 1972; Westall et al., 1976]. In MINEQL, the equilibrium constant approach is used to solve the chemical equilibrium problem which is defined by a system of mass action equations. The computed concentrations of constituents are constrained to remain positive and to satisfy mole balance relationships provided by the analytical information. Given a set of chemical constituents, which have been defined operationally as metals and ligands, along with the corresponding stoichiometric and thermodynamic data, all the possible chemical species in a model system can be defined. The concentrations of these chemical species are written as functions of the free concentrations of the constituents by mass action equations. These functions are substituted into the mole balance equations with elimination of solids. The problem is reduced to a system of non-linear equations in which the unknowns are the concentrations of the metals and ligands. This system of equations is solved by the Newton-Raphson method. The initial solution is tested against the solubility products of the solids and a new set of solids, which includes those solids with the most exceeded solubility products, is selected for the next computation. A final solution is achieved when the difference between the imposed analytical concentrations for a constituent and the sum of all individual species containing that constituent is less than or equal to

scales of concern in fog. Alternative aqueous-phase nitrate formation pathways involve the oxidation of N(III) by H_2O_2 and O_3 [Damschen and Martin, 1982].

Overall, the rate laws shown in Table 2 indicate that oxidation reactions proceed on time scales of minutes to hours under urban atmospheric conditions. These rate laws are integrated with a simple finite-difference scheme using adjustable time steps ranging from 10 sec. to 200 sec.:

$$[R_i]_{t+\Delta t} = [R_i]_t + \left(\sum_{ox} \left(\frac{d[R_i]}{dt}\right)\right)_{o_x} \Delta t \qquad (2)$$

where $[R_i]$ represents the concentration of the reduced component R_i (i.e. N(III) or S(IV)).

Of special interest in urban fog is the reaction of HSO_3^- with CH_2O and with other aldehydes, RCHO, to form hydroxymethanesulfonate ion (HMSA) and the corresponding sulfonates, $HOCHRSO_3^-$ [Munger et al., 1983]:

$$CH_2O + HSO_3^- \underset{k_r}{\overset{k_f}{\rightleftharpoons}} HOCH_2SO_3^- \qquad (3)$$

Dasgupta et al. [1980] determined a conditional equilibrium constant for HMSA to be $K_{298} = k_f/k_r = 7.04 \times 10^3\ M^{-1}$, while Boyce and Hoffmann [1983] have determined that $k_f = 3\ M^{-1}\ sec^{-1}$. Production of HMSA will contribute to the droplet acidity indirectly by producing a droplet that is supersaturated with respect to $SO_2(g)$, and, because of the slow reversibility of reaction (3), HMSA formation may inhibit the production of S(VI). Reaction (3)

is integrated at each time step by using the integrated form of the rate law:

$$\ln\left|\frac{[HSO_3^-]_{t+\Delta t}-p}{[HSO_3^-]_{t+\Delta t}-q}\right| = k_f(q-p)\Delta t + \ln\left|\frac{[HSO_3^-]_t-p}{[HSO_3^-]_t-q}\right| \quad (4)$$

$$[HMSA]_{t+\Delta t} = [HMSA]_t - ([HSO_3^-]_{t+\Delta t} - [HSO_3^-]_t) \quad (5)$$

where p and q are the solutions to the 2nd degree equation:

$$K X^2 + (K([CH_2O(\ell)]_t - [HSO_3^-]_t) + 1) X - ([HSO_3^-]_t + [HMSA]_t) = 0 \quad (6)$$

b) *Gas phase and aerosol.*

At night, the oxidation of nitrogeneous compounds and alkenes by ozone is important. The kinetics of these reactions are dependent on the downward diffusion of ozone to the boundary layer [McRae, 1982]. In the boundary layer, nitric acid may be produced [Graham and Johnston, 1978; McRae and Russell, 1982] by a variety of pathways. No attempt has been made to model gas-phase chemistry. Instead, concentrations of gases and gas-phase production rates (from emissions and homogeneous reactions) have been estimated from local field data and predictions from the Caltech air quality model for the Los Angeles basin [McRae, 1982].

The integrated mass and composition of the activated cloud condensation nuclei on which the fog droplets condense were estimated from field data. No subsequent scavenging of the interstital aerosol by diffusion or impaction was considered.

c) *Physical description.*

A parcel of air is followed in which droplets form and grow by accretion of water vapor. The droplets are assumed to remain constantly within the air parcel (i.e. sedimentation and diffusion of the droplets are ignored).

The limitation of S(IV) oxidation rates by mass transfer has been discussed by Schwartz and Freiberg [1981] and Baboolal et al. [1981]. Schwartz and Freiberg [1981] have shown that for stationary droplets smaller than 50 μm the net rate of oxidation was limited strictly by oxidation. Baboolal et al. [1981] extended this analysis to droplets larger than 50 μm. These large droplets have a significant sedimentation velocity, which drives convection both inside and outside of the droplet. This mixing effect enhances the rate of mass transfer as calculated for stationary droplets. Therefore, the chemical changes in fog droplets are most likely limited by the specific reaction rates .

Because fogs are localized events and occur on time scales of a few hours, advection of condensing and evaporating droplets can be ignored as a first approximation. Also, evolution of the droplet spectrum through coagulation can be neglected since mass transfer does not limit overall reaction rates. In this context, the liquid water content of the air parcel and its time dependency are sufficient parameters for characterizing fog microphysics.

At t = 0 droplets are assumed to condense, receive an initial chemical loading from the water-soluble fraction of the activated nuclei, and immediately react with the gaseous environment. The growth and evaporation

of the droplets is simulated by the external input of an evolving liquid water content. At each time step the equilibrium composition of the droplet is calculated along with the HMSA formation rate and the changes in component concentrations due to oxidation reactions.

Results and Discussion

a) *Sulfate and nitrate oxidation pathways.*

In this section, the relative contributions of the various S(IV) and N(III) oxidation mechanisms to the droplet chemistry are discussed. For this specific purpose a closed parcel of air with a constant liquid water content has been assumed (i.e. droplets condense on the activated condensation nuclei at t = 0 with no droplet growth or evaporation). A nighttime air mass typical of the industralized coastline of the Los Angeles basin has been chosen. Concentrations of gases and pre-existing nuclei were estimated from local field data and transport models (Table 3). Gases are depleted by absorption except for CO_2 and O_2 which are held constant at a fixed partial pressure. The liquid water content is L = 0.1 g m^{-3} and the temperature is T = 283 K.

Kinetic results shown in Figure 1 clearly show that H_2O_2 and O_2 (catalyzed by Fe and Mn) are the principal oxidants for S(VI) production *in situ*. Hydrogen peroxide is highly soluble in water and rapidly oxidizes S(IV) at low pH; however, if not replenished, it is quickly depleted from the parcel of air by reduction to water. In this case, in the absence of gas-phase or aqueous-phase H_2O_2 formation, no H_2O_2 remains in the system after ten minutes.

The catalytic effectiveness of both Fe(III) and Mn(II) is dependent on their speciation in the droplet (Figure 2). The principal manganese species are $Mn(H_2O)_6^{2+}$ and $MnSO_4(aq)$. Both of these species are assumed to be equally effective as catalysts for S(IV) autoxidation. On the other hand, Fe(III) above pH 4 is found primarily as an iron(III) hydroxide solid, which has been assumed to be catalytically inactive. As the pH decreases below 4, the solid phase dissolves and soluble Fe(III), the active catalyst, is released. The rate law indicates a decrease of the oxidation rate with pH but the dissolution of Fe(III) at low pH offsets this effect and the calculated rate actually increases between pH 4 and 3.5.

Oxidation by ozone contributes $\sim$ 4% of the total S(VI) produced after three hours of fog. This is due to the low water solubility of ozone and the reciprocal hydrogen ion dependency of its reaction rate. Therefore, little oxidation by ozone occurs below pH 4. Catalytic carbon sites in soot contribute < 5% of the total S(VI) produced, even at the high carbon levels of urban environments. Oxidation by N(III) appears to be insignificant due to the low solubility of $HNO_2(g)$ at pH < 4.

Oxidation of N(III) does not contribute appreciably to nitrate production. At t = 180 minutes, reaction with O_3 had generated less than 10^{-7} $\underline{M}$ NO_3^-, and reaction with H_2O_2 less than 10^{-10} $\underline{M}$ NO_3^-.

The aqueous-phase oxidation of S(IV) has an important consequence on the droplet acidity. Between pH 2 and 6 the principal reactive species of S(IV) is HSO_3^- [Hoffmann and Jacob, 1983]. The oxidation product, HSO_4^-, is completely dissociated above pH 3. Therefore, the oxidation directly produces one free proton. Depletion of HSO_3^- leads to further dissolution

of $SO_2(g)$ which then dissociates to give HSO_3^- and H^+ in the droplet. Because the solubility of SO_2 decreases with pH each depleted HSO_3^- molecule is not replaced in the droplet. Depending on the overall droplet chemistry, oxidation of one molar unit of S(IV) thus leads to the production of one to two-fold that molar unit of free acidity. The impact on the droplet pH is dramatic, as shown in Fig. 1(b). In the first half-hour of the fog S(VI) production is the fastest and causes a pH drop of over two units. Field observations are consistent with these predictions [Munger et al., 1983].

Components in the gas phase are scavenged by the droplets with efficiencies dependent on their Henry's law constants and aqueous-phase chemistry. Table 4 shows the fraction of each gas scavenged at t = 0, t = 30 min. and t = 180 min. It must be kept in mind that these numbers vary with the liquid water content of the fog [Schwartz, 1983]. Nitric acid is totally dissolved and dissociated, while NH_3 dissolves totally at pH < 5. These two components essentially titrate each other in the aqueous phase. Formation of HMSA over the course of a fog event was found not to significantly increase the fraction of CH_2O scavenged, therefore the CH_2O partial pressure remains approximately constant throughout the simulation. Likewise, hydroxymethanesulfonate formation cannot be a significant sink for gas phase SO_2. The solubility of SO_2 is limited, but because $SO_2 \cdot H_2O$ is a weak acid $\sim$ 5% dissolves with the formation of the fog. S(IV) oxidation reactions further increase the fraction scavenged over the lifetime of the fog. Three hours after fog formation over 80% of the initial SO_2 still remains in the gas phase, indicating that fog has little impact on the gaseous SO_2 concentration. Hydrogen peroxide is highly soluble in water.

As was discussed above, reduction of H_2O_2 in the droplet is an efficient sink which depletes H_2O_2 from the system. Ozone, on the other hand, is poorly scavenged, as is HNO_2. Both react slowly in the droplet below pH 4.

The impact of HMSA formation on the droplet chemistry is worth discussing in some detail as it has been the subject of recent interest [Munger et al., 1983; Boyce and Hoffmann, 1983]. Figure 3a shows the concentration profiles vs. time for HSO_3^- and HMSA. The formation of HMSA is rapid but still slower than S(IV) oxidation. Consequently, the amount of HMSA produced is smaller than that of sulfate. Hydroxymethanesulfonate is the most important S(IV) species in solution; if formaldehyde was not present the S(IV) concentration in the droplet would be much lower (Fig. 3(b)).

It has been suggested that HMSA may inhibit S(IV) oxidation in atmospheric droplets by limiting the availability of reactive S(IV) species. This does not appear to be the case since oxidation proceeds faster than adduct formation; furthermore, since the partial pressure of SO_2 remains approximately constant throughout the fog, the limiting concentrations of reactive S(IV) species are independent of the HMSA formation rate. However, the direct effect of HMSA on the fogwater acidity is of interest. Hydroxymethanesulfonate is the conjugate base of hydroxymethanesulfonic acid, which is a strong acid [Roberts, 1971]. Hydroxymethanesulfonate is a weak acid (see Table 1). Between pH 2 and 10, and in a system open to SO_2, HMSA is stable and complexation of HSO_3^- leads to further dissolution of SO_2, which then dissociates and releases free acidity in the droplet.

Because of the small amounts of HMSA produced with respect to the droplet $[H^+]$ concentration, this contribution is small.

In the first simulation, S(VI) formation buffered the droplet acidity at about pH 3; whereas, in some extremely polluted atmospheres, higher acidity can be imparted to the droplet at t = 0 by simple dissolution of the activated nuclei. Cass (1975) reports some cases for Los Angeles, mostly under high humidity conditions, where the aerosol sulfate concentration was as high as 75 μ gm^{-3}. A second simulation was run (Figures 4 and 5) under the same conditions as the first but with 75 μg m^{-3} SO_4^{2-} in the air mass as NH_4HSO_4 nuclei, instead of 10 μg m^{-3} SO_4^{2-} as $(NH_4)_2SO_4$.

The pH of 2.4 at t = 0 (Figure 4) indicates the impact of the acid nuclei. At this low pH there is very little S(IV) in the droplet (Figure 5) and the only S(IV) oxidation reaction to proceed at a significant rate is that with H_2O_2. Therefore, less sulfate and hydrogen ion are produced *in situ*. In the case of acidic condensation nuclei the pH of the fog may be controlled strictly by the nuclei composition instead of by S(VI) aqueous-phase production. It should be mentioned that fogwater pH in the range of 2 to 2.5 has been observed in the Los Angeles basin following heavy "smog" days. The lowest pH recorded was 1.69 in a dissipating fog along the coastline; in that case the dilution was probably less than the L = 0.1 g m^{-3} considered in the simulation.

Fog frequently forms at temperatures lower than 10°C. Radiation fogs, in particular, often form near freezing. To check the chemical sensitivity of the system to temperature a simulation was run at 1°C with L = 0.1 g m^{-3} and conditions given in Table 3. Reaction rates are slower at 1°C but gas

solubility increases. Solution equilibria are shifted in either direction depending on the sign of $\Delta H°$. The combination of these effects has an interesting impact on the sulfate production rates and the pH profile (Figure 6). The rate of S(IV) oxidation by H_2O_2 is relatively unaffected because of its low activation energy, E_a, but metal-catalyzed oxidation by O_2, which has a high E_a, is much slower at 1°C than at 10°C. Oxidation by ozone becomes appreciable at the beginning of the fog because of its low E_a and the increased ozone solubility. However, between pH 4.5 and pH 4, H_2O_2 is totally depleted and oxidation by ozone becomes insignificant; the S(IV) autoxidation reaction is also very slow. The sulfate concentration and pH profiles are almost at a plateau in this pH range. Then, as the pH drops below 4, $Fe(III)(OH)_3$ starts dissolving and the rate of oxidation by O_2 increases, such that sulfate and acidity are again produced at an appreciable rate. After three hours of fog the values for pH and sulfate concentration are close to what they were at 10°C. The speciation profile of Fe(III) (Fig. 7) is similar to that at 10°C, but dissolution of $Fe(OH)_3$ is retarded because of the slow drop in pH from 4.5 to 4. The speciation of Mn(II) is essentially the same as at 10°C.

The scavenging efficiency of gases (Table 5) reflects their increased solubility; however, because the aqueous-phase reactions are slower, little increase is seen between t = 0 and t = 30 min. After three hours the scavenging efficiency for SO_2 is similar to that at 10°C.

An interesting feature of the chemistry at 1°C is the high concentration of HMSA (Fig. 8), which is due to the increased solubility of SO_2 and CH_2O. The reaction proceeds via a nucleophillic substitution of methylene glycol [Boyce and Hoffmann, 1983] with an activation energy near 12 kcal $mole^{-1}$. Consequently, the reaction still proceeds rapidly at 1°C.

b) *Simulation of a fog event.*

The simulation with the present model of an actual fog event necessitates the knowledge of input variables such as the condensation nuclei composition, the evolution of liquid water content with time, and the gas phase concentrations. Unfortunately our field investigations [Waldman et al., 1982; Munger et al., 1983] so far have been limited to the determination of fogwater composition. Field data for the above parameters is incomplete, therefore a direct comparison of calculated and observed values is not possible at this time. In addition the current model neglects gas-phase chemistry, transport mechanisms, and aerosol scavenging by droplets.

Fogwater composition and its variation with time for fog events at Lennox, a site in an industrial area near the Los Angeles coastline, have been documented thoroughly [Waldman et al., 1982; Munger et al., 1983]. In this section, a fog occurring under conditions typical of this highly impacted site has been simulated.

A plausible scenario for the evolution of liquid water content in fogs can be obtained from existing data [Jiusto and Lala, 1983]. The liquid water content often rises linearly following fog formation (neglecting small time-scale oscillations), reaches a stable value after about an hour, and then decreases linearly as the fog evaporates. Liquid water contents range from 0.01 g m^{-3} for very light fogs to 0.5 g m^{-3} for dense fogs. The profile chosen here is shown in Figure 9.

Concentrations of condensation nuclei and atmospheric gases prior to fog formation are given in Table 3. From the discussion of the previous section, it appears that some gas-phase emissions should be included.

Hydrogen peroxide is not produced in the gas phase at night and thus actually disappears when the fog forms. Ammonia and HNO_3, which are scavenged efficiently by the droplets, are, on the other hand, continuously emitted into the atmosphere from a variety of sources. Because fog droplets are a sink for these two gases, fresh inputs into the parcel of air must be considered. At Lennox plausible values associated with an inversion height of 50 m are 0.01 ppb min^{-1} for HNO_3 [McRae and Russell, 1982] and 0.01 ppb min^{-1} for NH_3 [Russell et al., 1983]. Other gases included in the simulation are not depleted by fog, and a reasonable assumption is that their concentrations remain constant throughout the event. A constant temperature of 10°C has been chosen. Temperature changes during the course of fog events [Jiusto and Lala, 1983] are minimal.

The concentrations predicted for the major ions (Fig. 10) are in the range of those reported by Waldman et al. [1982] and Munger et al. [1983], but no precise comparison should be made because of the reasons stated at the beginning of this section. The concave profiles observed (except for $[H^+]$) confirm the important role of dilution and evaporation that was suggested initially by Waldman et al. [1982]. Aqueous-phase oxidation of N(III) to N(V) is negligible and the only nitrate source is the slow gas-phase production of HNO_3 followed by dissolution and dissociation. As a result, the nitrate concentration is controlled primarily by droplet growth. Similar behavior is predicted for ammonium ion, although in the initial stage of the fog the pH drop from a high value increases the NH_4^+ concentration. From equilibria described by equations (14) and (15), it is seen that scavenging of gaseous ammonia is highly pH-dependent over the range of

5 to 8, which is typical of fog forming in rural environments (D. J. Jacob, unpublished data, 1983) or influenced by alkaline atmospheric components [Munger et al., 1983]. In such fogs, the NH_4^+ levels are expected to be controlled by acidity as well as dilution.

Oxidation of S(IV) contributes substantially to the sulfate level and the acidity in the early stages of the fog, and in the fully developed fog 50% of the total sulfate present has been produced in the aqueous phase. During the first few minutes of the fog S(IV) oxidation is in fact rapid enough to compensate for dilution; after H_2O_2 is depleted and the pH has dropped the oxidation rate slows down and the role of dilution becomes predominant. Even with dilution, the pH of the droplets does not rise because metal-catalyzed S(IV) oxidation by O_2 produces significant acidity in the droplet; instead pH stabilizes at about 3.5. As the fog evaporates concentration leads to a further pH decrease. The speciation of Fe(III) (Fig. 11) correlates with pH in the manner discussed in the previous section. $FeSO_4^+$ becomes an important species as the fog evaporates because the sulfate concentration is so high. Speciation of Mn(II) (not shown) is similar to that in Figure 2.

An important question is: "Is the sulfate formation predicted theoretically actually seen in the field?" The data of Waldman et al. [1982] and Munger et al. [1983] do not show obvious evidence for this. However the bulk of the aqueous-phase sulfate production is predicted to occur in the first hour of the fog, so that it could not be detected given the time resolution of the field study. A way to obtain experimental confirmation of this process would be to compare the amount of sulfate

present in the atmosphere just before fog formation to that right after fog formation.

The HMSA concentration profile (Fig. 12) shows the dominant effect of droplet growth and evaporation, except in the first few minutes of the fog. Hydroxymethanesulfonate is the major S(IV) species, and its formation may explain the high S(IV) levels found in fogwater [Munger et al., 1983]. It should be noted that in addition to formaldehyde, sulfite is known to readily form sulfonates with other aldehydes, some of which have been found in fog at concentrations comparable to formaldehyde (Grosjean, personal communication). These reactions would further explain the high S(IV) concentrations observed.

Conclusion

The chemistry of fogs forming in an urban environment has been investigated using a hybrid kinetic and equilibrium model. The most important conclusions are:

a) Aqueous-phase oxidation of S(IV) is an important source of sulfate in the droplet. The principal oxidants are H_2O_2 and O_2 (catalyzed by Fe(III) and Mn(II)), although ozone can also be an important oxidant above pH 5. Oxidation by H_2O_2 is very fast but limited by its availability in the atmosphere. Most of the sulfate production occurs within the first hour following fog formation.

b) When fog condenses on alkaline to slightly acid nuclei, important acidification occurs as a result of S(IV) oxidation. In the first case simulated, the pH dropped two units from its initial value of 5.5 during the first half hour of the fog; it then stabilized around pH 3. When the fog formed on highly acidic condensation nuclei, however, the pH drop due

to S(IV) oxidation was very small because of the high acidity initially present in the droplet.

c) Oxidation of N(III) in the droplet does not lead to significant production of nitrate. Production of nitrate proceeds through gas-phase formation of HNO_3 followed by dissolution and dissociation in the droplet. Nitric acid is scavenged efficiently by the droplets as it is formed in the gas phase.

d) NH_4^+ concentration is dependent both on the liquid water content of the fog and the solubility of NH_3. Below pH 5 the droplets are essentially a total sink for NH_3 but above pH 5 the gas is partitioned between the two phases in a highly pH-dependent manner.

e) Over 90% of the S(IV) present in the droplet is complexed as HMSA, and this may explain the high S(IV) concentrations observed by Munger et al. [1983]. Formation of HMSA releases free acidity but its effect on the droplet pH is negligible.

f) Fog does not affect the SO_2 gas-phase concentrations greatly; as a result the supply of reactive S(IV) species for S(VI) and HMSA formation is determined primarily by the droplet pH. S(VI) formation proceeds faster than HMSA formation at all times, and limits HMSA formation by causing the pH to drop and thus reducing the S(IV) supply.

g) At lower temperatures (1°C vs. 10°C) metal-catalyzed oxidation by O_2 is slower and the importance of ozone as an S(IV) oxidant increases. Overall, sulfate and acidity are not produced as fast in the early stages of the fog but catch up later and become comparable in the later stage of the fog. Much more HMSA is produced at the lower temperature.

The model has thus revealed some important features of the chemistry and production of acidity in urban fogs. Gas-phase and aerosol chemistry, droplet microphysics and wind fields will have to be incorporated in future versions to give the simulations a predictive capability. These theoretical advances will have to be accompanied by concomitant sets of field measurements.

FIGURE CAPTIONS

Fig. 1: (a) Profile vs. time of total sulfate in the fogwater and of the individual contributions to the total sulfate of sulfate aerosol and different S(IV) oxidants. (b) Profile of pH vs. time. The fog formed under the conditions of Table 3, liquid water content = 0.1 g m^{-3}, temperature = 10°C.

Fig. 2: Speciation of (a) Fe(III) and (b) Mn(II) in the fogwater as a function of time under conditions of Table 3, liquid water content = 0.1 g m^{-3}, temperature = 10°C.

Fig. 3. (a) Concentrations of S(IV) species in the fogwater as a function of time under conditions of Table 3, liquid water content = 0.1 g m^{-3}, temperature = 10°C. (b) Same as (a) but with no formaldehyde in the atmosphere.

Fig. 4: (a) Profile vs. time of total sulfate and of the individual contributions to the total sulfate of sulfate aerosol and different S(IV) oxidants. (b) Profile of pH vs. time. The fog formed by condensation on highly acidic nuclei (75 μg m^{-3} NH_4HSO_4, other conditions as in Table 3), liquid water content = 0.1 g m^{-3}, temperature = 10°C.

Fig. 5: Concentration of S(IV) species in the fogwater as a function of time. The fog formed by condensation on highly acidic nuclei (75 μg m^{-3} NH_4HSO_4, other conditions as in Table 3), liquid water content = 0.1 g m^{-3}, temperature = 10°C.

Fig. 6: (a) Profile vs. time of total sulfate and of the individual contributions to the total sulfate of sulfate aerosol and different S(IV) oxidants. (b) Profile of pH vs. time. The fog formed under the conditions of Table 3, liquid water content = 0.1 g m^{-3}, temperature = 1°C.

Fig. 7: Speciation of Fe(III) in the fogwater as a function of time under conditions of Table 3, liquid water content = 0.1 g m^{-3}, temperature = 1°C.

Fig. 8: Concentrations of S(IV) species in the fogwater as a function of time under conditions of Table 3, liquid water content = 0.1 g m^{-3}, temperature = 1°C.

Fig. 9: Liquid water content profile vs. time for the fog simulated in section b.

Fig. 10: Profiles vs. time of the concentrations of the major ions in the fogwater under conditions of Table 3, liquid water content as given in Fig. 9, temperature = 10°C. (a) Nitrate and ammonium ions. (b) Total sulfate and individual contributions of the different sulfate production mechanisms. (c) pH.

Fig. 11: Speciation of Fe(III) in the fogwater as a function of time under conditions of Table 3, liquid water content as given in Fig. 9, temperature = 10°C.

Fig. 12: Concentrations of S(IV) species in the fogwater as a function of time under conditions of Table 3, liquid water content as given in Fig. 9, temperature = 10°C.

TABLE 1. HENRY'S LAW AND AQUEOUS-PHASE EQUILIBRIA RELEVANT TO THE DROPLET CHEMISTRY.

	Reaction	pK[a]	$\Delta H^\circ_{298.15}$(kcal mole^{-1})	reference[d]
1.	$H_2O(\ell) \rightleftharpoons H^+ + OH^-$	14.00	13.35	SM
2.	$SO_2(g) + H_2O \rightleftharpoons SO_2 \cdot H_2O$	-.095	-6.25	SM
3.	$SO_2 \cdot H_2O \rightleftharpoons H^+ + HSO_3^-$	1.89	-4.16	SM
4.	$HSO_3^- \rightleftharpoons H^+ + SO_3^{2-}$	7.22	-2.23	SM
5.	$HNO_3(g) \rightleftharpoons H^+ + NO_3^-$	-6.51	-17.3	SW
6.	$HNO_2(g) \rightleftharpoons HNO_2(\ell)$	- 1.7	- 9.5	SW
7.	$HNO_2(\ell) \rightleftharpoons H^+ + NO_2^-$	3.29	2.5	SW
8.	$CO_2(g) + H_2O \rightleftharpoons CO_2 \cdot H_2O$	1.47	-4.85	SM
9.	$CO_2 \cdot H_2O \rightleftharpoons H^+ + HCO_3^-$	6.37	1.83	SM
10.	$HCO_3^- \rightleftharpoons H^+ + CO_3^{2-}$	10.33	3.55	SM
11.	$CH_2O(g) + H_2O \rightleftharpoons CH_2O \cdot H_2O$	-3.85	-12.85	LB
12.	$HOCH_2SO_3H \rightleftharpoons H^+ + HOCH_2SO_3^-$	<0[c]	(b)	R
13.	$HOCH_2SO_3^- \rightleftharpoons H^+ + {}^-OCH_2SO_3^-$	11.7	(b)	SA
14.	$NH_3(g) + H_2O \rightleftharpoons NH_3 \cdot H_2O$	-1.77	-8.17	SM
15.	$NH_3 \cdot H_2O \rightleftharpoons NH_4^+ + OH^-$	4.77	.9	SM
16.	$O_2(g) \rightleftharpoons O_2(\ell)$	2.90	-3.58	P

TABLE 1 (CONTINUED)

Reaction	pK[a]	$\Delta H^\circ_{298.15}$ (kcal mole^{-1})	reference[d]
17. $H_2O_2(g) \rightleftharpoons H_2O_2(\ell)$	-4.85	-14.5	MD
18. $O_3(g) \rightleftharpoons O_3(\ell)$	2.03	-5.04	L-B
19. $CaHCO_3^+ \rightleftharpoons Ca^{2+} + HCO_3^-$	11.6	-2.78	SM
20. $CaSO_4(\ell) \rightleftharpoons Ca^{2+} + SO_4^{2-}$	2.30	-1.65	SM
21. $NaSO_4^- \rightleftharpoons Na^+ + SO_4^{2-}$	.70	-2.23	SM
22. $FeSO_4^+ \rightleftharpoons Fe^{3+} + SO_4^{2-}$	4.20	5.4	SM
23. $Fe(SO_4)_2^- \rightleftharpoons Fe^{3+} + 2SO_4^{2-}$	5.60	(b)	SM
24. $FeCl^{2+} \rightleftharpoons Fe^{3+} + Cl^-$	1.40	-7.91	SM
25. $FeOH^{2+} \rightleftharpoons Fe^{3+} + OH^-$	12.30	.04	SM
26. $Fe(OH)_2^+ \rightleftharpoons Fe^{3+} + 2OH^-$	23.3	(b)	SM
27. $Fe(OH)_3 \downarrow \rightleftharpoons Fe^{3+} + 3OH^-$	39.0	20.7	SM
28. $Fe_2(OH)_2^{4+} \rightleftharpoons 2Fe^{3+} + 2OH^-$	25.7	16.2	SM
29. $FeSO_3^+ \rightleftharpoons Fe^{3+} + SO_3^{2-}$	10.0	(b)	this laboratory
30. $MnSO_4(\ell) \rightleftharpoons Mn^{2+} + SO_4^{2-}$	2.30	-3.39	SM
31. $MnCl^+ \rightleftharpoons Mn^{2+} + Cl^-$	1.10	-8.01	SM

TABLE 1 (CONTINUED)

a) K is in $\underline{M}$ atm^{-1} or $\underline{M}^n$.

b) unknown; $\Delta H = 0$ is assumed in the calculation.

c) pK for this reaction is very low (Roberts et al., 1971). This is sufficient information at the pH's of interest in this work.

d) reference code: SM = Sillén and Martell [1964]; SW = Schwartz and White [1981]; LB = Ledbury and Blair [1925]; SA = Sørensen and Andersen [1970]; MD = Martin and Damschen [1981]; L-B = Landolt-Börnstein [1976]; R = Roberts et al. [1971]; P = Perry [1963].

TABLE 2. KINETIC EXPRESSIONS FOR THE AQUEOUS-PHASE OXIDATION REACTIONS OF S(IV) TO S(VI) AND N(III) TO N(V).

Reaction	Rate ($M\ sec^{-1}$) at 25°C	activation energy (kcal $mole^{-1}$)	reference (d)
32. $S(IV) + H_2O_2$	$\frac{d[S(VI)]}{dt} = \frac{8\times10^4[H_2O_2(\ell)][SO_2(\ell)]}{.1 + [H^+]}$	7.3	M
33. $S(IV) + O_3$	a) pH < 3		
	$\frac{d[S(VI)]}{dt} = \frac{1.9 \times 10^4[SO_2(aq)][O_3(\ell)]}{[H^+]^{1/2}}$ (a)	6	M
	b) pH > 3		
	$\frac{d[S(VI)]}{dt} = 4.19\times10^5\left(1+\frac{2.39\times10^{-4}}{[H^+]}\right)[O_3(\ell)][SO_2(aq)]$	6	Ma
34. $S(IV) + O_2$ (with Fe(III) and Mn(II))	a) $[SO_2(aq)] > 10^{-5}$, pH < 4		
	$\frac{d[S(VI)]}{dt} = \frac{4.7[Mn(II)]^2}{[H^+]} + \left(\frac{.82[Fe(III)][SO_2(aq)]}{[H^+]} \times \left(1 + \frac{1.7\times10^3[Mn(II)]^{1.5}}{6.3\times10^{-6} + [Fe(III)]}\right)\right)$	21.8	M
	b) $[SO_2(aq)] < 10^{-5}$, pH < 4		
	$\frac{d[S(VI)]}{dt} = 3\left(5000[Mn(II)][HSO_3^-] + \frac{.82[Fe(III)][SO_2(aq)]}{[H^+]}\right)$	21.8	M

TABLE 2 (CONTINUED)

Reaction	Rate($M\ sec^{-1}$) at 25°C	activation energy (kcal $mole^{-1}$)	reference (d)
	c) $[SO_2(aq)] > 10^{-5}$, pH > 4		
	$\frac{d[S(VI)]}{dt} = \frac{4.7[Mn(II)]^2}{[H^+]} + 1\times10^7[Fe(III)][SO_2(aq)]^2$	27.3	M
	d) $[SO_2(aq)] < 10^{-5}$, pH > 4		
	$\frac{d[S(VI)]}{dt} = 5000\ [Mn(II)][HSO_3^-]$	27.3	M
35. S(IV) + O_2 (with soot)	$\frac{d[S(VI)]}{dt} = 2.54\times10^7[O_2(\ell)]^{.69}\ Cx\ \frac{[SO_2(aq)]^2}{1+3.06\times10^6[SO_2(aq)]+1.5\times10^{12}[SO_2(aq)]^2}$ (b)	11.7	B
36. S(IV) + N(III)	a) pH < 3		
	$\frac{d[S(VI)]}{dt} = 142\ [H^+][HNO_2(aq)][SO_2(aq)]$	12(c)	M
	b) pH > 3		
	$\frac{d[S(VI)]}{dt} = 2.2\ [HNO_2(\ell)][HSO_3^-]$	12(c)	O
37. N(III) + H_2O_2	$\frac{d[S(VI)]}{dt} = 4.6\times10^3\ [H^+][H_2O_2(\ell)][HNO_2(\ell)]$	13.2	DM
38. N(III) + O_3	$\frac{d[S(VI)]}{dt} = 5\times10^5\ [O_3(\ell)][NO_2^-]$	13.8	DM

TABLE 2 (CONTINUED)

(a) $[SO_2(aq)] = [SO_2(\ell)] + [HSO_3^-] + [SO_3^{2-}]$; $[HNO_2(aq)] = [HNO_2(\ell)] + [NO_2^-]$.

(b) C_x is the concentration of active carbon in g ℓ^{-1}.

(c) Assumed.

(d) Reference code: M = Martin [1982]; Ma = Maahs [1982]; B = Brodzinsky et al. [1980]; O = Oblath et al. [1981]; DM = Damschen and Martin [1982].

Reaction Stoichiometries

reaction number

32. $HSO_3^- + H_2O_2(\ell) \longrightarrow HSO_4^- + H_2O$

33. $HSO_3^- + O_3(\ell) \longrightarrow HSO_4^- + O_2$

34. $HSO_3^- + 1/2\ O_2(\ell) \longrightarrow HSO_4^-$

35. id.

36. $2HNO_2(\ell) + H_2O{\cdot}SO_2 \longrightarrow 2NO + H^+ + HSO_4^- + H_2O$

$2HNO_2(\ell) + 2H_2O{\cdot}SO_2 \longrightarrow 2SO_4^{2-} + N_2O + H_2O + 4H^+$

37. $HNO_2(\ell) + H_2O_2(\ell) \longrightarrow NO_3^- + H_2O + H^+$

38. $NO_2^- + O_3(\ell) \longrightarrow NO_3^- + O_2$

Table 3. Composition of the air mass (trace gases and condensation nuclei) prior to fog formation at a polluted site. The air mass is typical of the industrial coastline of the Los Angeles basin for an inversion height of about 50 m. P_{O_2} = .21 atm, P_{CO_2} = 330 ppm.

Atmospheric Trace Gases

	concentration (ppb)	reference
SO_2	20	SCAQMD data[a]
HNO_2	1	Hanst et al. [1982]
HNO_3	3	id.
NH_3	5	id.
CH_2O	30	Grosjean [1982]
O_3	10	SCAQMD data
H_2O_2	1	Graedel et al. [1976]

Condensation Nuclei[b] (references: Gartrell et al. [1980]; Appel et al. [1980])

	concentration ($\mu g\ m^{-3}$)		concentration ($\mu g\ m^{-3}$)
SO_4^{2-}	10	NH_4^+	6.65
NO_3^-	10	Na^+	.61
Cl^-	1.1	Fe(III)	.5
CO_3^{2-}	1.83	Mn(II)	.02
C_x (soot)	30	Ca^{2+}	1.22

(a) data from the permanent records of the South Coast Air Quality Management District.

(b) $(NH_4)_2SO_4$, NH_4NO_3, NaCl, $CaCO_3$, metal oxides, and soot.

TABLE 4. SCAVENGING OF GASES BY FOG DROPLETS UNDER CONDITIONS OF TABLE III, LIQUID WATER CONTENT = 0.1 g m^{-3}, TEMPERATURE = 283K.

	Fraction scavenged from gas phase (%)		
Gas	t = 0	t = 30 min.	t = 180 min.
HNO_3	100	100	100
NH_3	43.9	99.5	100
CH_2O	5.0	5.3	5.3
SO_2	2.7	11.8	17.5
H_2O_2	32.1	100	100
O_3	0.0	1.5	1.5
HNO_2	3.8	0.0	0.0

TABLE 5. SCAVENGING OF GASES BY FOG DROPLETS UNDER CONDITIONS OF TABLE III, LIQUID WATER CONTENT = 0.1 g m^{-3}, TEMPERATURE = 274K.

	Fraction scavenged from gas phase (%)		
Gas	t = 0	t = 30 min.	t = 180 min.
HNO_3	100	100	100
NH_3	76.0	97.0	100
CH_2O	9.8	10.3	10.5
SO_2	10.7	13.0	18.2
H_2O_2	58.0	100	100
O_3	0.0	4.2	4.2
HNO_2	10.2	3.4	0.0

REFERENCES

Adamowicz, R. F., A model for the reversible washout of sulfur dioxide, ammonia and carbon dioxide from a polluted atmosphere and the production of sulfates in raindrops, Atmos. Environ. 13, 105-121, 1979.

Appel, B. R., E. L. Kothny, E. M. Hoffer, and J. J. Wesolowski, Sulfate and nitrate data from the California Aerosol Characterization Experiment (ACHEX), Adv. Env. Sci. Technol. 9, 315-335, 1980.

Baboolal, L. B., H. R. Pruppacher, and J. H. Topalian, A sensitivity study of a theoretical model of SO_2 scavenging by water drops in air, J. Atm. Sci. 38, 856-870, 1981.

Boyce, S. D. and M. R. Hoffmann, Kinetics and mechanisms of the formation of hydroxymethanesulfonic acid, to be submitted to Environ. Sci. Technol.

Brimblecombe, P. and D. J. Spedding, The catalytic oxidation of micromolar aqueous sulphur dioxide, Atmos. Environ. 8, 937-945, 1974.

Brodzinsky, R., S. G. Chang, S. S. Markowitz, and T. Novakov, Kinetics and mechanism for the catalytic oxidation of sulfur dioxide on carbon in aqueous suspensions, J. Phys. Chem. 84, 3354-3358, 1980.

Carmichael, G. R., T. Kitada, and L. K. Peters, The effects of in-cloud and below-cloud scavenging on the transport and gas phase reactions of SO_x, NO_g, HC_x, H_xO_y, and O_3 compounds, 4th Int'l. Conference on Precipitation Scavenging, Dry Deposition, and Resuspension, Santa Monica, Dec. 1982, Elsevier, Netherlands publ. (in press).

Cass, G. R., Dimensions of the Los Angeles SO_2/Sulfate Problem, Environmental Quality Laboratory Memorandum No. 15, California Institute of Technology, Pasadena, California, 1975.

Chameides, W. L. and D. D. Davis, The free radical chemistry of cloud droplets and its impact upon the composition of rain, J. Geophys. Res. 87, 4863-4877, 1982.

Damschen, D. E. and L. R. Martin, Aqueous aerosol oxidation of nitrous acid by O_2, O_3, and H_2O_2, Atmos. Environ. (in press).

Dasgupta, P. K., K. De Cesare, and J. C. Ullrey, Determination of atmospheric sulfur dioxide without tetrachloromerurate(II) and the mechanism of the Schiff reaction, Anal. Chem. 52, 1912-1922, 1980.

Durham, J. L., J. M. Overton, and V. P. Aneja, Influence of gaseous nitric acid on sulfate production and acidity in rain, Atmos. Environ. 15, 1059-1068, 1981.

Easter, R. C. and P. V. Hobbs, The formation of sulfate and the enhancement of cloud condensation nuclei in clouds, J. Atm. Sci. 31, 1586-1594, 1974.

Erickson, R. E., L. M. Yates, R. L. Clark, and D. McEwen, The reaction of sulfur dioxide with ozone in water and its possible atmospheric significance, Atmos. Environ. 11, 813-817, 1977.

Gartrell, G., Jr., S. L. Heisler, and S. K. Friedlander, Relating particulate properties to sources: the results of the California Aerosol Characterization Experiment, Adv. Env. Sci. Technol. 9, 665-713, 1980.

Graedel, T. E., L. A. Farrow, and T. A. Weber, Kinetic studies of the photochemistry of the urban atmosphere, Atmos. Environ. 10, 1095-1116, 1976.

Graedel, T. E., P. S. Gill, and C. J. Wechsler, Effects of organic surface films on the scavenging of atmospheric gases by raindrops and aerosol particles, 4th Intl. Conference on Precipitation Scavenging, Dry Deposition, and Resuspension, Santa Monica, Dec. 1982, Elsevier, Netherlands publ. (in press).

Graham, R. A. and H. S. Johnston, The photochemistry of NO_3 and the kinetics of the N_2O_5-O_3 system, J. Phys. Chem. 82, 254-268, 1978.

Grosjean, D., Formaldehyde and other carbonyls in Los Angeles ambient air, Environ. Sci. Technol. 16, 254-262, 1982.

Hanst, P. L., N. W. Wong, and J. Bragin, A long-path infra-red study of Los Angeles smog, Atmos. Environ. 16, 969-981, 1982.

Hegg, D. A. and P. V. Hobbs, Cloudwater chemistry and the production of sulfates and clouds, Atmos. Environ. 15, 1597-1604, 1981.

Hoffmann, M. R., Thermodynamic, kinetic and extrathermodynamic considerations in the development of equilibrium models for aquatic systems, Environ. Sci. Technol. 15, 345-353, 1981.

Hoffmann, M. R. and D. J. Jacob, Kinetics and mechanisms of the catalytic oxidation of dissolved sulfur dioxide in aqueous solution: an application to nighttime fogwater chemistry, in Acid Precipitation, J. G. Calvert (ed.), Ann Arbor Science Publ., Ann Arbor, MI (in press).

Jiusto, J. E. and G. G. Lala, Radiation fog field programs - recent studies, ASRC-SUNY publ. no. 869, 1983.

Landolt-Börnstein, Zahlenwerte und Funktionen. Gleichgewicht der Absorption von Gasen in Flüssigkeiten von niedrigem Dampfdruck, 6th ed., vol. 4, part 4, sect. C, Springer Verlag, Heidelberg, W. Germany, 1976.

Ledbury, W. and E. W. Blair, The partial formaldehyde vapour pressure of aqueous solutions of formaldehyde. Part II. J. Chem. Soc. 127, 2832-2839, 1925.

Liljestrand, H. M. and J. J. Morgan, Spatial variations of acid precipitation in Southern California, Environ. Sci. Technol. 15, 333-339, 1981.

Maahs, H. G., The importance of ozone in the oxidation of sulfur dioxide in nonurban tropospheric clouds, 2nd Symposium on the Composition of the Nonurban Troposphere, American Meteorological Soc., Williamsburg, VA, 1982.

Martin, L. R., Kinetic studies of sulfite oxidation in aqueous solution, in Acid Precipitation, J. G. Calvert (ed.), Ann Arbor Science Publ., Ann Arbor, MI (in press).

McRae, G. J., Mathematical modeling of photochemical air pollution, Ph.D. thesis, California Institute of Technology, Pasadena, CA, 1981.

McRae, G. J. and A. G. Russell, Dry deposition of nitrogen containing species, in Acid Deposition: Wet and Dry, Vol. 6, B. B. Hicks (ed.), Ann Arbor Science Publ., Ann Arbor, MI (in press).

Middleton, P., C. S. Kiang, and V. A. Mohnen, Theoretical estimates of the relative importance of various urban sulfate aerosol production mechanisms, Atmos. Environ. 14, 463-472, 1980.

Morel, F. and J. J. Morgan, A numerical method for computing equilibria in aqueous chemical systems, Environ. Sci. Technol. 6, 58-67, 1972.

Munger, J. W., D. J. Jacob, J. M. Waldman, and M. R. Hoffmann, Fogwater chemistry in an urban atmosphere, J. Geophys. Res. (in press).

Oblath, S. B., S. S. Markowitz, T. Novakov and S. C. Chang, Kinetics of the formation of hydroxylamine disulfonate by reaction of nitrite with sulfites, J. Phys. Chem. 85, 1017-1021, 1981.

Perry, J. M., Chemical Engineer's Handbook, 4th ed., McGraw-Hill, New York, 1963.

Roberts, J. D., R. Stewart, and M. C. Caserio, Organic Chemistry, W. A. Benjamin publ., Menlo Park, CA, 1971.

Russell, A. G., G. J. McRae, and G. R. Cass, Mathematical modeling of the formation and transport of ammonium nitrate aerosol, Atmos. Environ. (in press).

Schwartz, S. E. and J. E. Freiberg, Mass-transport limitation to the rate of reaction of gases in liquid droplets: application to oxidation of SO_2 in aqueous solutions, Atmos. Environ. 15, 1129-1144, 1981.

Schwartz, S. E. and W. H. White, Solubility equilibria of the nitrogen oxides and oxyacids in dilute aqueous solution, Adv. Env. Sci. Eng. 4, 1981.

Schwartz, S. E., Gas-aqueous reactions of sulfur and nitrogen oxides in liquid-water clouds, in Acid Precipitation, J. G. Clavert (ed.), Ann Arbor Science Publ., Ann Arbor, MI (in press).

Sillén, G. L. and A. E. Martell, Stability Constant of Metal-Ion Complexes, Chemical Society, London, special publ. no. 17, 1964.

Sørensen, P. E. and V. S. Andersen, The formaldehyde-hydrogen sulphite system in alkaline aqueous solution. Kinetics, mechanisms, and equilibria, Act. Chem. Scand. 24, 1301-1306, 1970.

Stumm, W. and J. J. Morgan, Aquatic Chemistry, 2nd Ed., Wiley-Interscience New York, 1981.

Waldman, J. M., J. W. Munger, D. J. Jacob, R. C. Flagan, J. J. Morgan, and M. R. Hoffmann, Chemical composition of acid fog, Science 218, 677-680, 1982.

Westall, J. C., J. L. Zachary and F. M. Morel, MINEQL, a computer program for the calculation of chemical equilibrium composition of aqueous solutions, Tech. Note 18, Dept. of Civil Eng., Massachusetts Institute of Technology, Cambridge, MA, 1976.

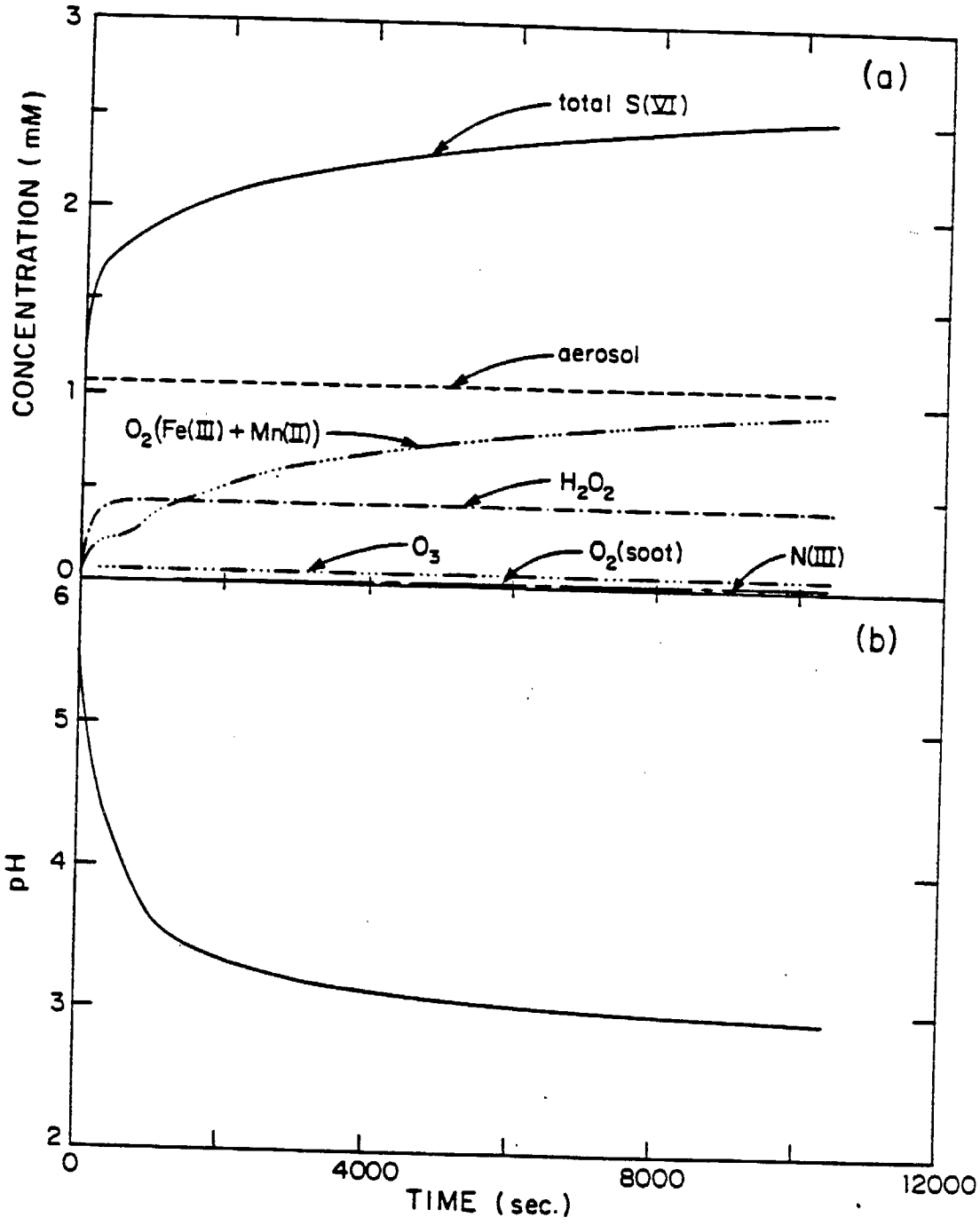
(a)
total S(VI)
aerosol
O_2(Fe(III) + Mn(II))
H_2O_2
O_3
O_2(soot)
N(III)
CONCENTRATION (mM)
3
2
1
0
(b)
pH
6
5
4
3
2
0
4000
8000
12000
TIME (sec.)

Figure 1.

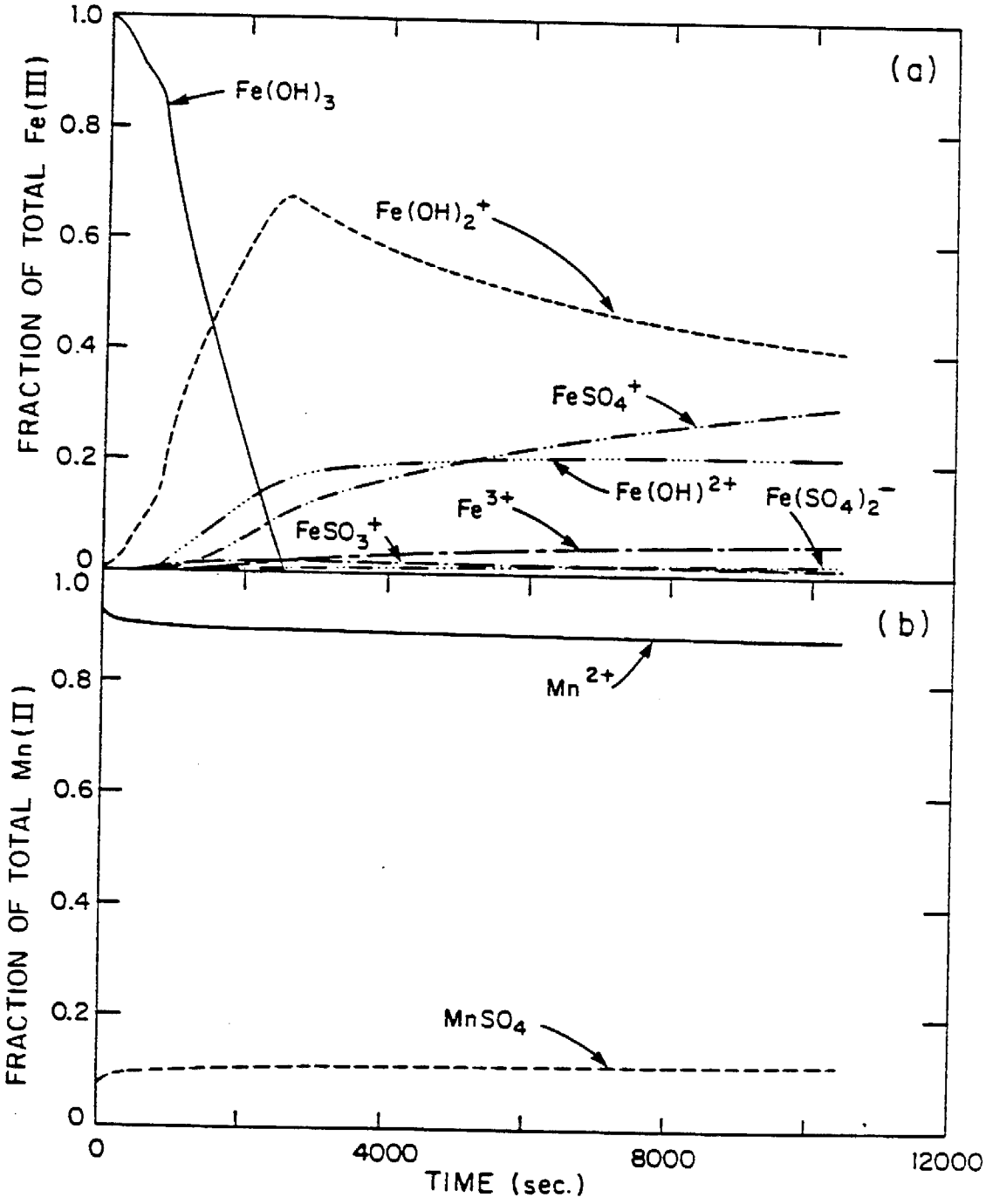
(a)
FRACTION OF TOTAL Fe(III)
1.0
0.8
0.6
0.4
0.2
0
Fe(OH)3
Fe(OH)2+
FeSO4+
Fe(OH)2+
Fe(SO4)2-
Fe3+
FeSO3+
(b)
FRACTION OF TOTAL Mn(II)
Mn2+
MnSO4
0
4000
8000
12000
TIME (sec.)

Figure 2.

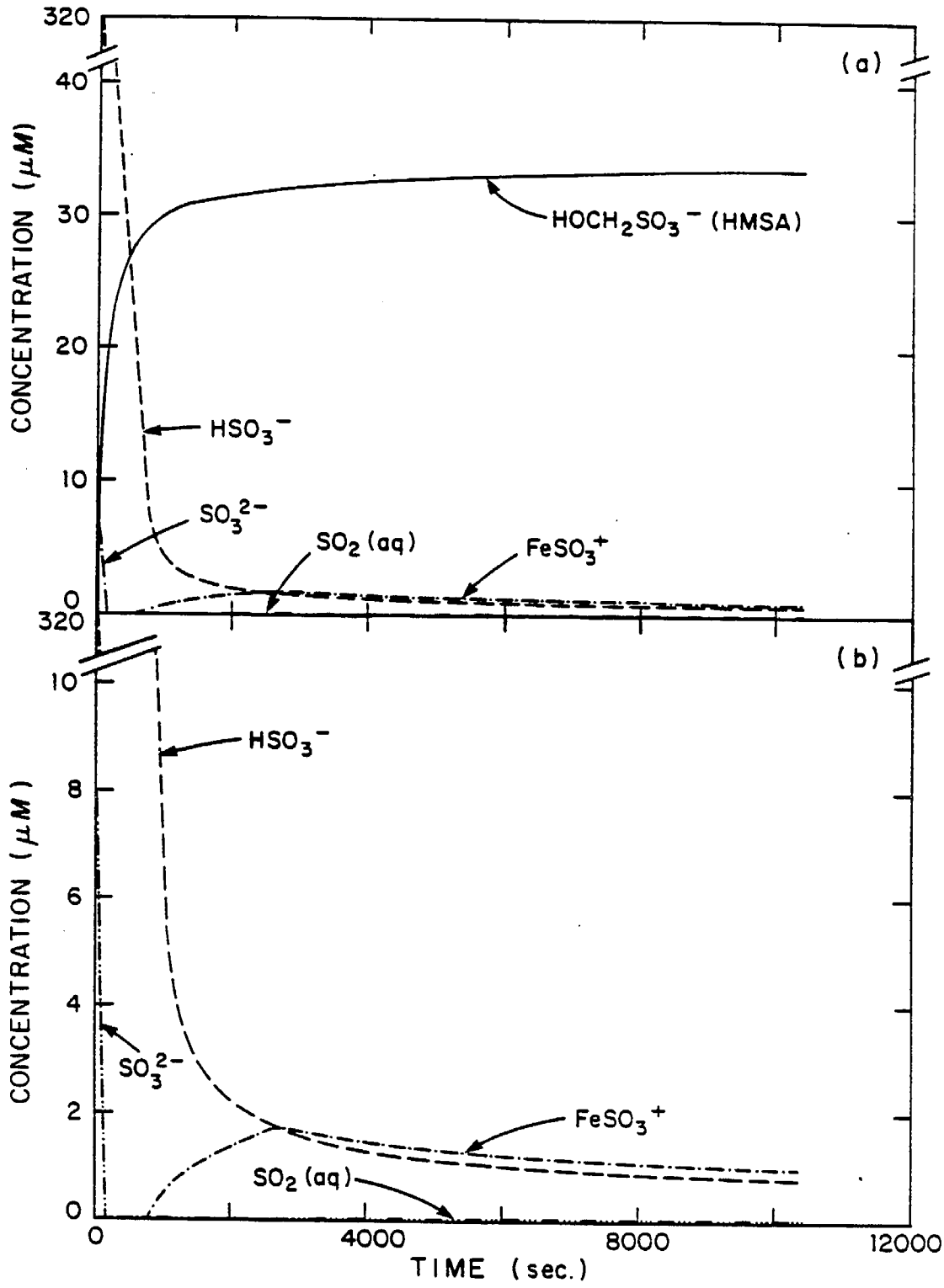
320
40
30
20
10
0
320
(a)
CONCENTRATION (μM)
HOCH2SO3− (HMSA)
HSO3−
SO3 2−
SO2 (aq)
FeSO3+
10
8
6
4
2
0
(b)
HSO3−
SO3 2−
FeSO3+
SO2 (aq)
0
4000
8000
12000
TIME (sec.)

Figure 3.

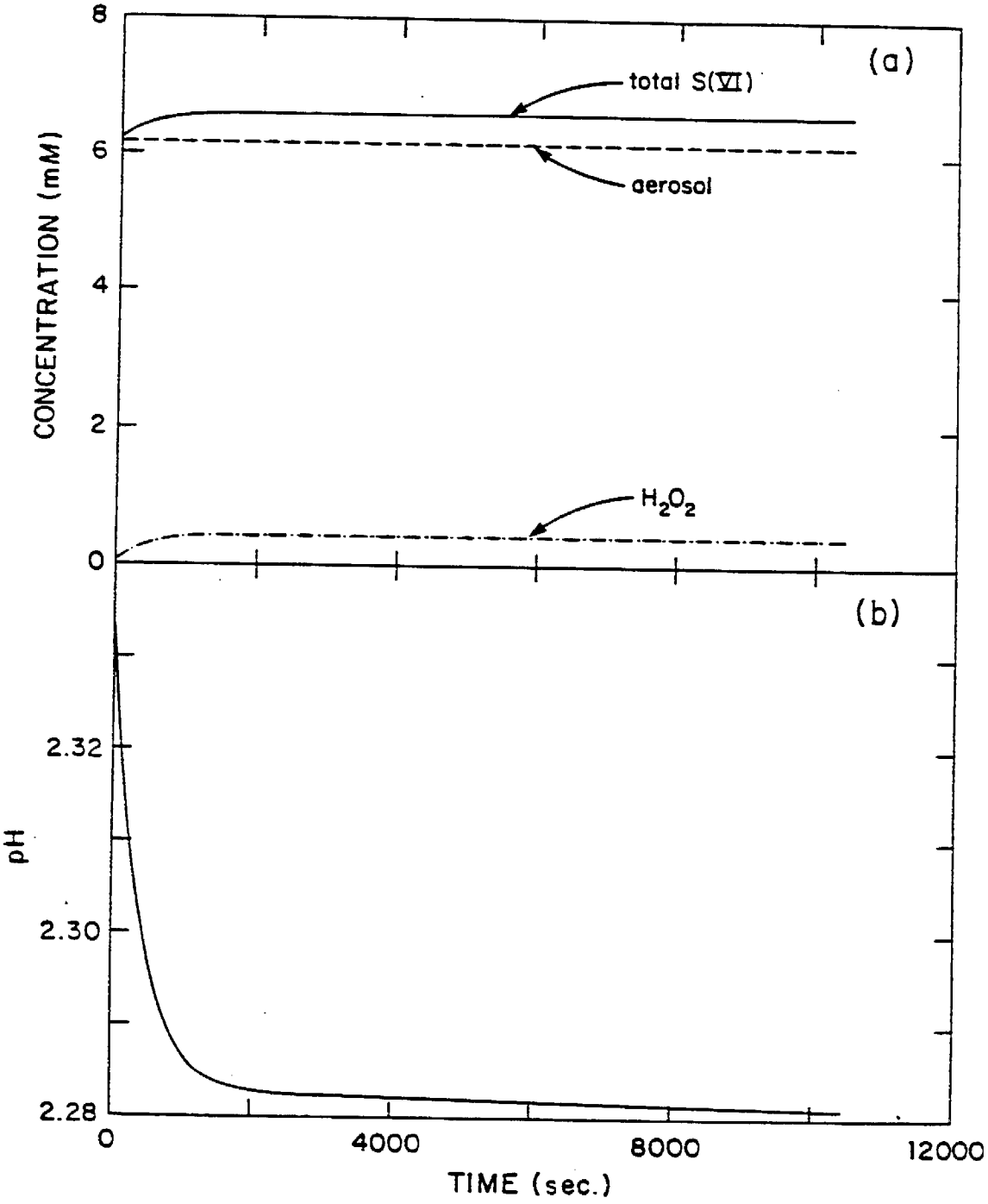
(a)
total S(VI)
aerosol
H_2O_2
CONCENTRATION (mM)
8
6
4
2
0
(b)
pH
2.32
2.30
2.28
0
4000
8000
12000
TIME (sec.)

Figure 4.

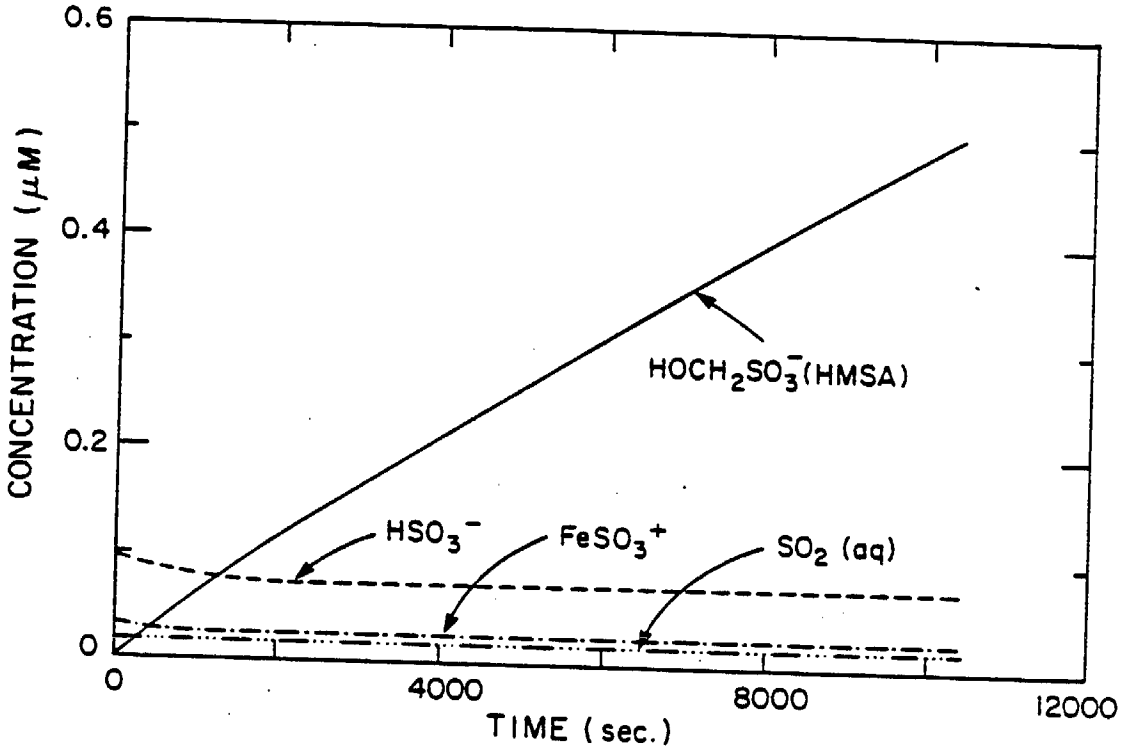
0.6
0.4
0.2
0
CONCENTRATION (μM)
HOCH2SO3−(HMSA)
HSO3−
FeSO3+
SO2 (aq)
0
4000
8000
12000
TIME (sec.)

Figure 5.

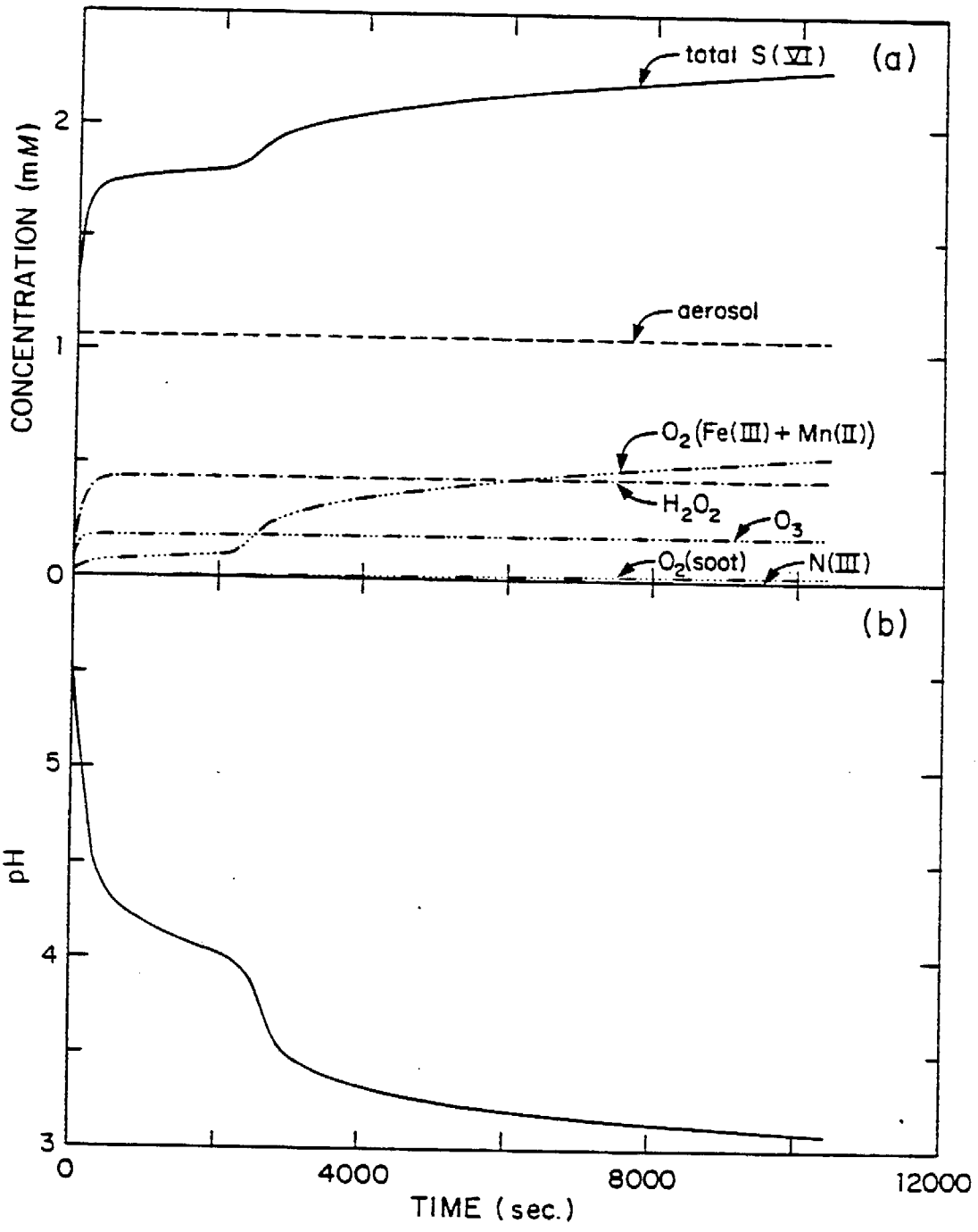
total S(VI)
(a)
aerosol
O_2(Fe(III) + Mn(II))
H_2O_2
O_3
O_2(soot)
N(III)
(b)
CONCENTRATION (mM)
pH
TIME (sec.)
0
4000
8000
12000
1
2
3
4
5

Figure 6.

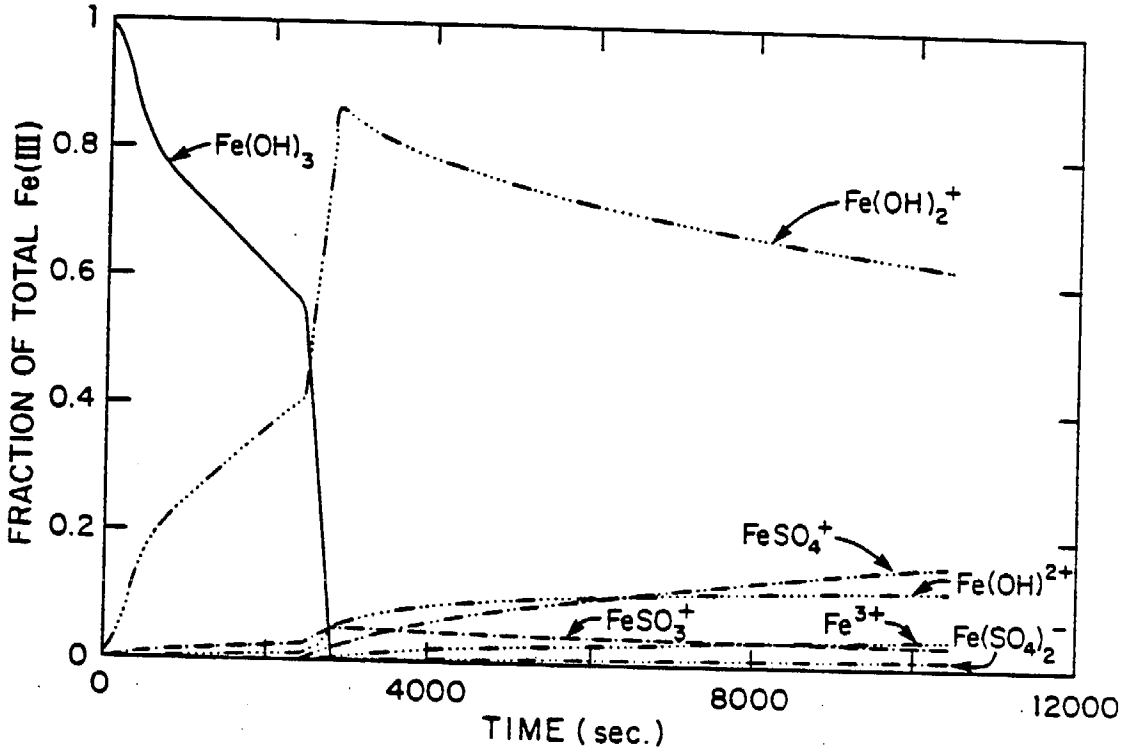
FRACTION OF TOTAL Fe(III)
1
0.8
0.6
0.4
0.2
0
0
4000
8000
12000
TIME (sec.)
Fe(OH)3
Fe(OH)2+
FeSO4+
Fe(OH)2+
FeSO3+
Fe3+
Fe(SO4)2-

Figure 7.

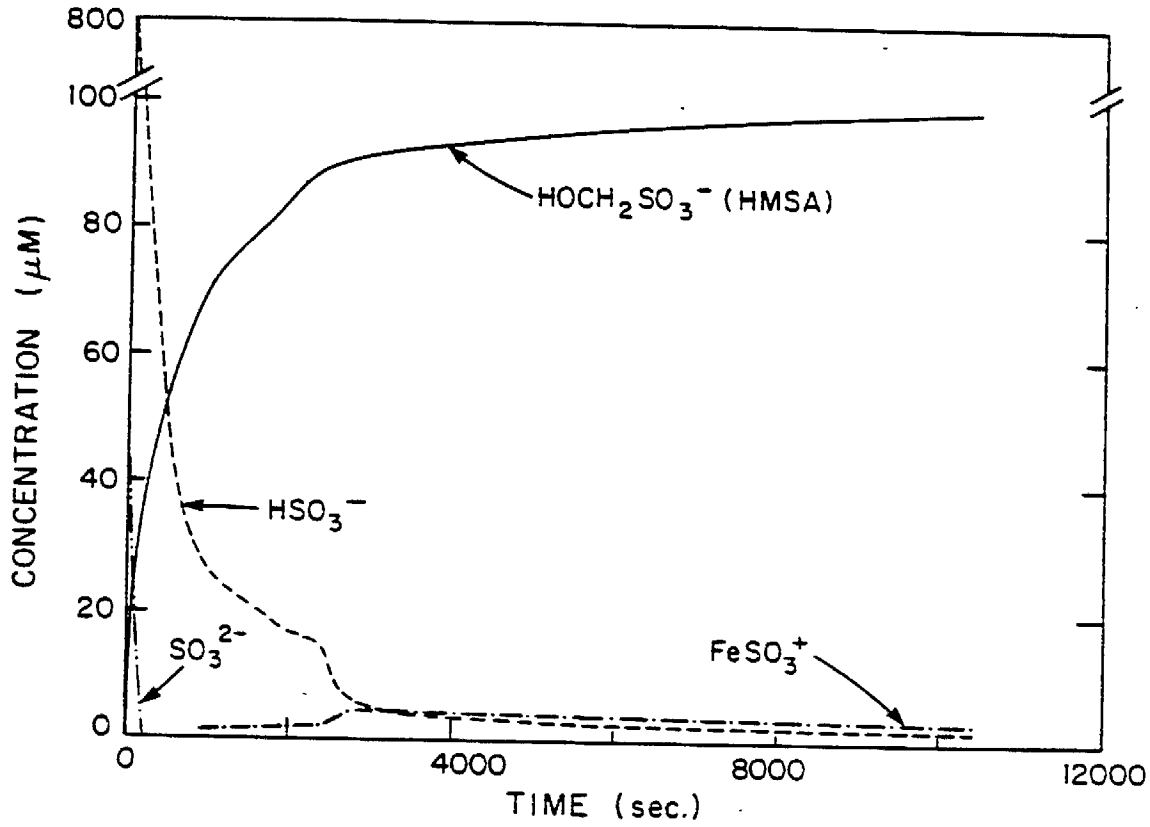
800
100
80
60
40
20
0
CONCENTRATION (μM)
HOCH2SO3− (HMSA)
HSO3−
SO3 2−
FeSO3+
0
4000
8000
12000
TIME (sec.)

Figure 8.

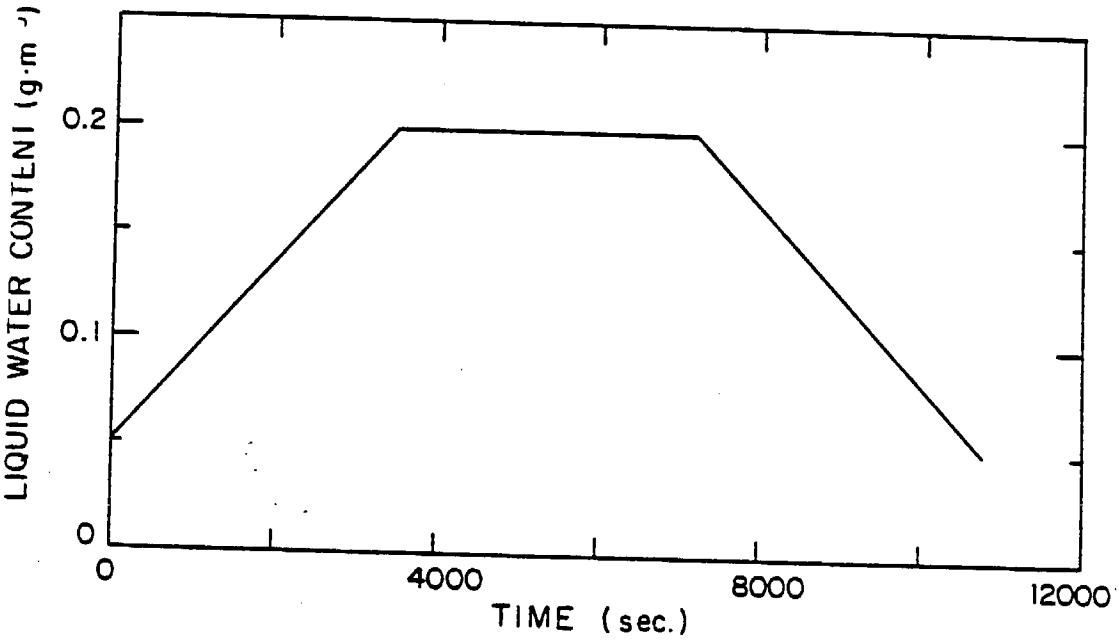

Figure 9.

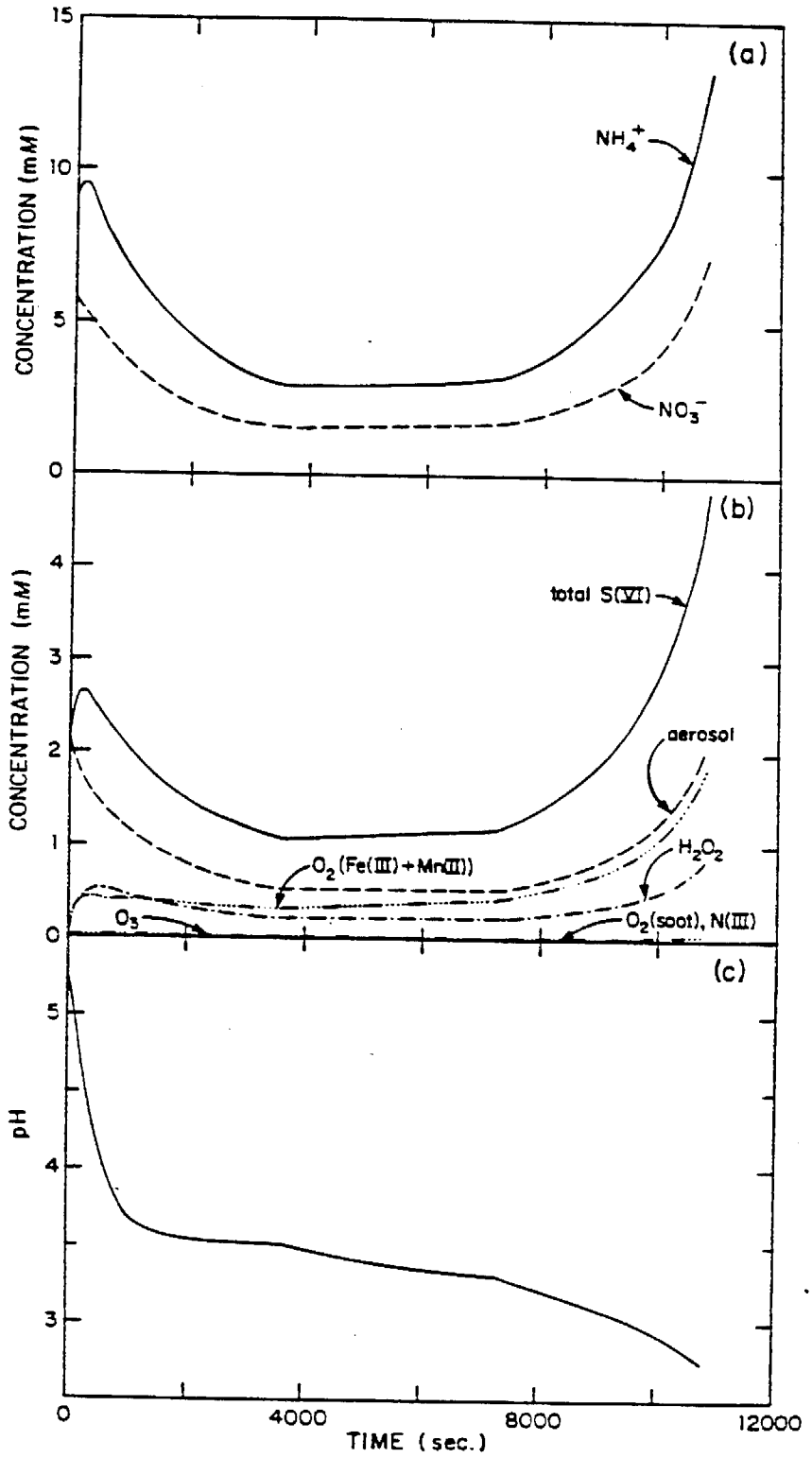
(a)
CONCENTRATION (mM)
15
10
5
0
NH_4^+
NO_3^-
(b)
CONCENTRATION (mM)
4
3
2
1
0
total S(VI)
aerosol
H_2O_2
O_2(Fe(III)+Mn(III))
O_3
O_2(soot), N(III)
(c)
pH
5
4
3
0
4000
8000
12000
TIME (sec.)

Figure 10.

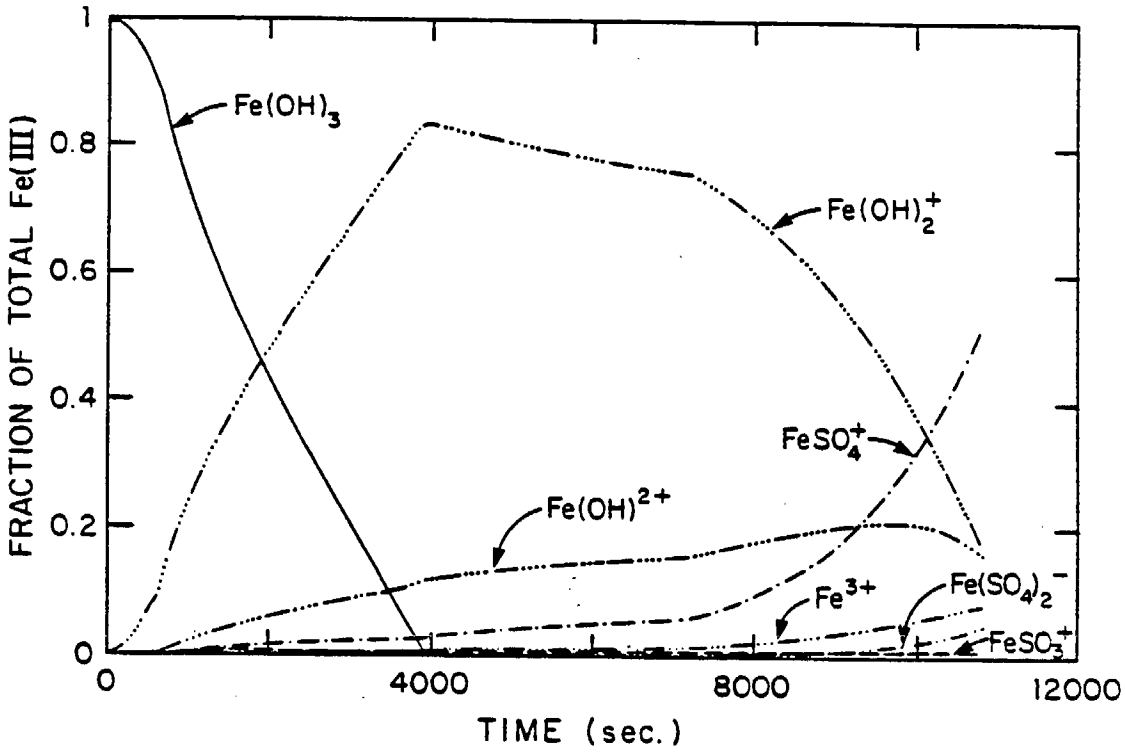
FRACTION OF TOTAL Fe(III)
1
0.8
0.6
0.4
0.2
0
0
4000
8000
12000
TIME (sec.)
Fe(OH)3
Fe(OH)2+
FeSO4+
Fe(OH)2+
Fe3+
Fe(SO4)2-
FeSO3+

Figure 11.

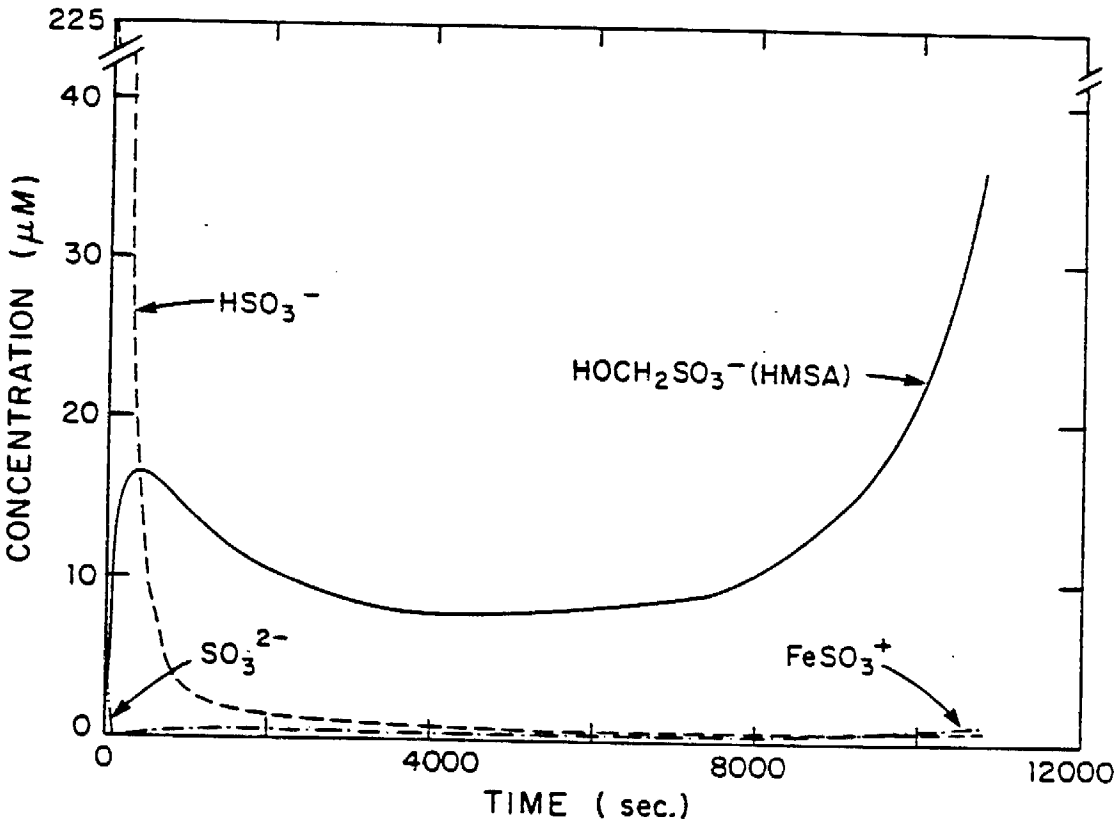
225
40
30
20
10
0
CONCENTRATION (μM)
HSO3−
HOCH2SO3− (HMSA)
SO3 2−
FeSO3+
0
4000
8000
12000
TIME (sec.)

Figure 12.

CHAPTER VI

DESIGN AND CALIBRATION OF A ROTATING ARM COLLECTOR FOR AMBIENT FOG SAMPLING.*

DANIEL J. JACOB, RICHARD C. FLAGAN, JED M. WALDMAN, AND
MICHAEL R. HOFFMANN
W. M. Keck Engineering Laboratories
California Institute of Technology
Pasadena, California 91125

INTRODUCTION

Recent reports of extremely high acidities in fogs and non-precipitating clouds[1,2] have shown the need for a reliable method to collect fogwater for chemical analysis. The large water droplets which grow by condensation on the activated cloud condensation nuclei in the atmosphere are sites for aqueous-phase reactions leading to the production of strong acids;[3] they also deposit efficiently on the ground and on surfaces by sedimentation and impaction. A fog sampler must differentiate between these large droplets and the ambient submicron aerosol, and collect volumes large enough for thorough chemical characterization.

A number of devices have been operated in past investigations.[2,4-6] May[4] used a grid of vertical 1 mm wires arranged across a wind tunnel. Droplets impact on the wires and flow by gravity in collection bottles at the base of the grid. Falconer and Falconer[2] used a multi-directional collector in which droplets impact freely on 0.4 mm Teflon fibers and flow by gravity in a bottle. Katz[5] constructed a rectangular jet impactor with slowly rotating Teflon rollers as impaction surfaces. The rollers maintain contact with a stationary Teflon rod and fogwater is collected at the contact point. Mack and Pilie[6] developed a rotating arm collector in which fog droplets impact a rotating slotted tube and are collected by centrifugal force in small vials mounted at the ends of the tube.

An improved rotating arm collector was developed at the California Institute of Technology for its fogwater chemistry research program. The purpose of this paper is to present criteria for fog sampling and to discuss the design and characterization of the Caltech rotating arm collector.

FOG SAMPLING CONSIDERATIONS AND COLLECTOR DESIGN CRITERIA

Fog droplets form and grow by condensation of water vapor on the larger hygroscopic particles of the aerosol. They range in size from 1 to 100 μm, with a mass median diameter typically of the order of 10 to 20 μm. An example of a

*Proc. 4th International Congress on Precipation Scavenging, Dry Deposition and Resuspension, 29 Nov. - 3 December, Santa Monica, CA (1982).

size distribution for San Francisco fog is shown in Fig. 1.[7] The droplet chemistry is size-dependent, mostly because of the dilution associated with droplet growth. It is, thus, important to collect all fog droplets with uniform efficiency to obtain a representative sample. The submicron aerosol, which has different chemical and physical characteristics, must not be collected as part of the fog sample.

Inertial impaction of the fog droplets on a surface is one way to collect the large particles while excluding the smaller particles. When a particle is projected into a stationary fluid with a velocity U it travels a finite distance before coming to rest. The distance the particle penetrates is given by

$$s = \frac{\rho_p d_p^2 U}{18\mu} \tag{1}$$

where

ρ_p = density of the particle

d_p = particle size

μ = viscosity of air

The ratio of this stop-distance to a characteristic length L of the impacting surface is the dimensionless Stokes' number:

$$St = \frac{\rho_p d_p^2 U}{18\mu L} \tag{2}$$

The characteristic length scale for the impaction system, L, is the diameter of the wires in a grid collector or the width of the impacting jet in a rectangular jet impactor. Ideally, particles for which the Stokes' number is larger than a certain value St^* (of order unity) will deviate from the fluid streamlines around the collector and impact on its surface. Conversely, particles for which the Stokes' number is smaller than St^* will follow the streamlines around the collector and avoid impaction. St^* is function of the geometry of the collector and the Reynolds' number.

Equation (2) may be rearranged to determine the minimum size of particles, d_p^*, which will be collected by a given sampler.

$$d_p^* = \sqrt{\frac{18\mu St^* L}{\rho_p U}} \tag{3}$$

In order to achieve sharp, well-defined size resolution with a fog sampler both U and L must be constant throughout the sampling event. This excludes static grid or wire collectors[2] because of the variability of the ambient wind speed. It also excludes small impaction substrates, e.g., wires or fibers in screen collectors[4] if accumulated droplets modify the apparent geometry of the impaction substrate. One approach to maintaining a constant d_p^* is to achieve an impaction velocity U which is much larger than the fluctuating, ambient wind speed.

In order to collect sufficient volumes of fogwater to satisfy the requirements for chemical analysis, a large volume of air must be sampled. Since a typical fog loading is 0.3 g/m^3, about 100 m^3 of air must be sampled to collect 30 cc of fog water. For sampling with a time resolution of 30 minutes in order to study the dynamics of fog chemistry, the desired sampling rates become quite large, about 3-4 m^3/min. While this large volume of air is being sampled, the collected fog must be sheltered from changing air masses promptly after impaction in order to avoid sample contamination and evaporation. Here again, grid collectors with slow, gravitational flow into bottles may lead to problems.

Both rotating arm collectors and jet-impactors with a rapid water storage system can be designed to satisfy these criteria for fogwater sampling. The rectangular jet impactor designed by Katz[5] has the further advantage of using a standard impaction design for which detailed theoretical treatments are available.[8] The rotating arm collector was, however, selected for the field operations of the present fogwater chemistry program because it is rugged and simple, inexpensive to build, and allows a higher sampling rate. In the following sections design and calibration of this instrument are discussed.

DESIGN OF ROTATING ARM COLLECTORS

The rotating arm collector is an external impactor which sweeps through the air at a high velocity in order to collect large particles. Rotating arm collectors have been used for many years to collect biological particles on adhesive coated surfaces.[9-11] Mack and Pilie[6] modified the solid arm collectors, introducing a slot in the leading edge of a hollow arm. Particles which impact into the tube flow to a vial at the end of the arm due to the centrifugal acceleration. Recently, a rotating arm virtual impactor has been developed to minimize sampling biases in the collection of filter samples of large atmospheric particles.[12]

Although rotating arm collectors have been used in numerous studies, collection characteristics are not well documented, particularly for the instruments which rely on impaction of particles through an opening in the leading edge of a rotating tube. Since the cut-off diameter is weakly dependent on the cut-off Stokes number, i.e., $d_p^* \propto St^{*1/2}$, and St^* is expected to be of order unity, we based our design on $St^* = 1$. Calibration data are, therefore, essential to the determination of the precise cut-off diameter.

In order to differentiate between the fog and the precursor aerosol, a cut-off diameter of about 5 μm was selected. The rotation speed, ω, the length of the arm, R, and the width of the collector, L, must be selected to yield this value of d_p^* and the desired fogwater collection rate. Several additional considerations enter into the design, including: (i) the power required to drive the collector; (ii) the maximum velocity at the collector tip which must be limited in order to minimize excessive aerodynamic heating of the samples. Aerodynamic heating becomes a factor as the velocity approaches the speed of sound. As long as the Mach number of the rotating arm is kept below about 0.3, this effect should be relatively minor. The power requirements are a more serious problem as will be discussed below.

The geometry of the rotating arm collector used for the Caltech fogwater chemistry program is illustrated in Figure 2. A motor drives a stainless steel solid rod of radius R. Each end of the arm has a slot milled into its leading edge. Standard 30 ml VWR Nalgene bottles are mounted at the ends of the arm to collect the water which impacts in the slots (Fig. 2(c) and (d)). Threaded Teflon tubes screwed on the end of the arm and extending inside the collection bottles prevent the collected fogwater from running out after the instrument is stopped. Deflectors prevent water which impacts on the solid part of the arm from entering the slot since the collection of this water would bias the sample toward large particle sizes. Small fins are welded to the back of the arm for extra strength. The entire arm is Teflon-coated to prevent chemical contamination and facilitate cleaning.

The power required to drive a rotating arm collector is determined by the aerodynamic drag of the arm. The arm consists of cylindrical sections and a two dimensional cup. The drag coefficients C_D of these shapes at high Reynolds numbers are 1 and 2, respectively.[13] The power required to rotate the arm at a rotating speed ω is given by

$$P = 2\int_0^R \frac{dF_{drag}}{d_r} U(r)dr \qquad (4)$$

This may be separated into the components for the solid rod ($r < R_1$), the slot ($R_1 < r < R_2$), the bottle cap ($R_2 < r < R_3$), and the bottle ($R_3 < r < R$), i.e.,

$$P = 2\sum_{1}^{4}\int_{R_{i-1}}^{R_i} \frac{dF_{drag}}{dr}\, U(r)dr \tag{5}$$

with $R_o = 0$ and $R_4 = R$. Noting that the drag force is given by

$$F_{drag} = C_D A\rho \frac{U^2}{2} \tag{6}$$

where A is the projected area of the shape and ρ is the density of the gas, we find

$$P = 2\sum_{1}^{4}\int_{R_{i-1}}^{R_i} C_{D_i} L_i \rho \frac{(2\pi r\omega)^3}{2}\, dr \tag{7}$$

where the L_i's are the widths of the corresponding portions of the arm. By integration,

$$P = 2\rho\pi^3\omega^3\sum_{1}^{4} C_{D_i} L_i (R_i^4 - R_{i-1}^4) \tag{8}$$

The power required to drive the arm is, thus, a strong function of the arm dimensions and the rotation frequency. In order to facilitate operation using readily available electrical circuits, the size and speed must be limited. The Caltech rotating arm collector was designed to achieve an acceptable sampling rate and size cut, while not requiring more than a 110V, 15A circuit to drive the sampler. From Fig. 2 and (8) the power requirement of the Caltech collector rotating at 1700 rpm is calculated (Table 1).

TABLE 1

POWER REQUIREMENT OF THE CALTECH ROTATING ARM COLLECTOR

Solid rod	34 W
Slots	247 W
Bottle caps	168 W
Bottles	448 W
Total power required	897 W (1.2 HP)

A 1 1/2 HP motor is required to drive the collector. This is still compatible with the standard power supply installations used in the field. The dimensions of the slot were chosen to achieve a high sampling rate while following the criteria for the size cut discussed in the previous section; the average slot velocity is 47 m s^{-1} and the corresponding calculated size cut is 8 μm. The slot velocities range from 38 m s^{-1} to 56 m s^{-1}, which allows an acceptable 10% spread for d_p^*. If the component of the wind speed facing the collector is at least 0.054 m s^{-1} the air sampled is renewed at every half-rotation of the arm. The sampling rate is then 5 m^3 of air per minute. Assuming 100% efficiency for fogwater collection a collection rate of 0.5 ml min^{-1} would be achieved in a fog of 0.1 g m^{-3} liquid water content. In the field collection rates of up to 2 ml min^{-1} have been obtained. The size cut obtained is a little higher than would be optimally desired. Since air compressibility is not expected to interfere with the sampling below U = 0.3 Mach a lower size cut could be obtained by cutting down drag and increasing the size of the collector. As seen from Table 1 the main contributors to the drag are the collection bottles because of their large diameter and high velocity. The use of smaller bottles would require shorter sampling intervals and the accumulation of sequentially obtained samples to carry out a thorough chemical analysis; although this was rejected up to now as being too inconvenient, it may be a valid alternative. Streamlining appears to be promising; aerodynamic bottles and bottle casings are being considered for future instrument versions.

Safety must be a primordial concern for a large diameter device rotating at such high speed. The collector must be carefully balanced to prevent vibrations and securely mounted to a rigid stand. The mechanisms for mounting the bottles must be able to withstand the loads due to high acceleration. Stainless steel caps with close tolerance threads, shown in Figure 2(c) and (d) were found to be satisfactory in laboratory tests. Finally, because the rotating arm cannot be protected with a shroud without interfering with fog collection, the operating site must be carefully selected and supervised to minimize the hazard.

CHARACTERIZATION OF THE COLLECTOR

The size cut of the collector was estimated experimentally. An atomizer (nozzle diameter .067", operating pressure 103 psi) generated a polydisperse water aerosol in a 220 x 170 x 200 cm chamber. Droplets were circulated by a system of fans inside the chamber and exited through an outlet at the bottom of the chamber.

A forward light scattering aerosol spectrometer (Particle Measurement Systems FSSP-100) monitored the droplet size distribution in the 1-45 μm range; measurements were taken every 10 seconds. A stable droplet size distribution was reached after about 1 minute. The droplets were in the size range 1-40 μm with a mass median diameter of about 20 μm which is representative of typical ambient fog distributions.[7,14]

The collector was then started inside the chamber; after about 1 minute a new stable droplet size distribution was reached. Figure 4 compares the two size distributions before and after the collector is started. No significant droplet shattering is observed. Droplets above 10 μm are depleted in their quasi-totality while very few droplets below 5 μm are collected. Ignoring impaction on the walls of the chamber, this indicates a relatively sharp size cut at 8 μm for the collector, which corresponds to a cut-off Stokes' number $St^* = 0.98$ (considering the velocity at the middle of the slot). Because the number of times the droplet-laden air crosses the sampler path before being sized by the probe is not known, it is not possible to infer from these measurements the usual collection efficiency vs. $St^{1/2}$ curve. Wind tunnel testing with a monodisperse aerosol is planned in the future to obtain a more detailed calibration.

CONCLUSION

The design of the collectors to sample ambient fog for chemical analysis has been discussed. A rotating arm collector where droplets impact at high speed in slots milled into the leading edges of a rotating rod was found to satisfy criteria for fog sampling. The experimentally determized size cut is 8 μm, which excludes the submicron aerosol from the sample while collecting most fog droplets with high efficiency. The sampling rate is 5 m^3 min^{-1}, and collection rates up to 2 ml min^{-1} have been obtained in the field.

A lower size cut could be achieved by using a longer arm and thus increasing the impacting speed of the droplets. This implies the use of airfoil shapes or smaller collection bottles to cut down drag. Such prototypes are being built at Caltech but have not yet been tested in a wet environment.

ACKNOWLEDGEMENTS

This research was supported by the State of California Air Resources Board (A2-048-32) and the President's Fund of the California Institute of Technology.

REFERENCES

1. Waldman, J. M., Munger, J. W., Jacob, D. J., and Hoffmann, M. R. (this volume).
2. Falconer, R. E. and Falconer, P. D. (1980) J. Geophys. Res., 85, 7465-7470.
3. Jacob, D. J. and Hoffmann, M. R. (this volume).
4. May, K. R. (1961) J. R. Met. Soc., 87, 535-548.
5. Katz, U. (1980) in Communications de la 8eme Conference sur la Physique des Nuages, Clermont-Ferrand, 15-19 July 1980.
6. Mack, E. and Pilie, R. (1975) U.S. Patent No. 3889532.
7. Goodman, J. (1977) J. Appl. Met., 16, 1056-1067.
8. Mercer, T. T. and Chow, H. Y. (1968) J. Colloid. Interface Sci., 27, 75-83.
9. Durham, O. C. (1947) J. Allergy, 18, 231-238.
10. Perkins, W. A. (1957) "The Rotorod Sampler", 2nd semi-annual rept., Aerosol lab., Dept. Chem. & Chem. Eng., Stanford Univ., CML-186, 66 pp.
11. Asai, G. N. (1960) Phytopathology, 50, 535-541.
12. McMurry, P. H., personal communication.
13. Hoerner, S. (1965) Fluid-dynamic drag, published by author, Midland Park, NJ.
14. Mallow, J. V. (1975) J. Atm. Sci., 32, 440-443.

Figure Captions

Figure 1. Typical size distribution of San Francisco fog (from Goodman[7]).

Figure 2. The Caltech rotating arm collector: (a) design, (b) general view, (c) and (d) detailed views of the collection mechanism.

Figure 3. Size distributions of a polydisperse water aerosol generated in a continuous-flow stirred tank before and during operation of the Caltech rotating arm collector.
Δ: aerosol spectrometer range 1-15 μ, 0 = aerosol spectrometer range 3-45 μm. Droplets above 8 μm are collected with high efficiency.

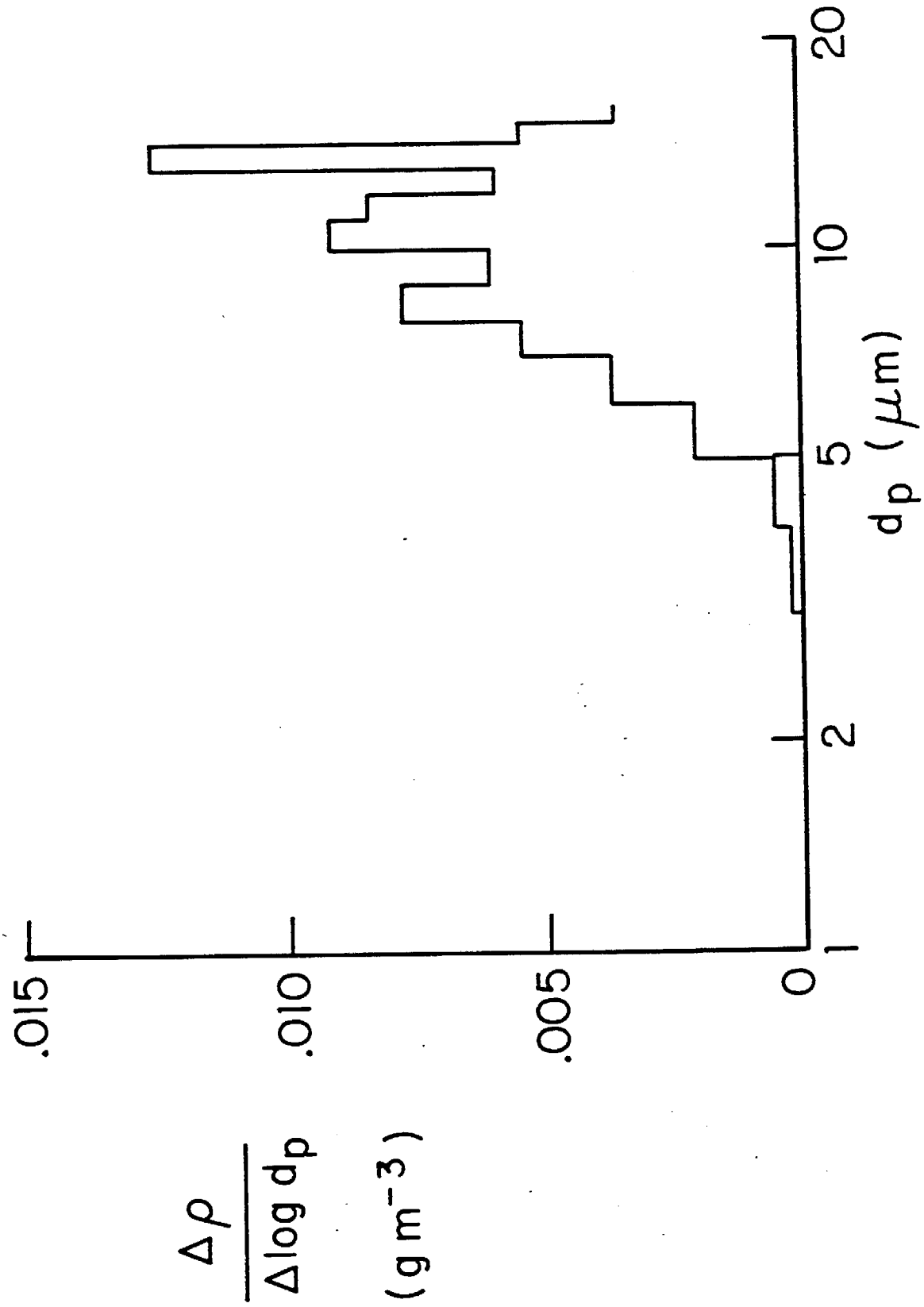

Figure 1.

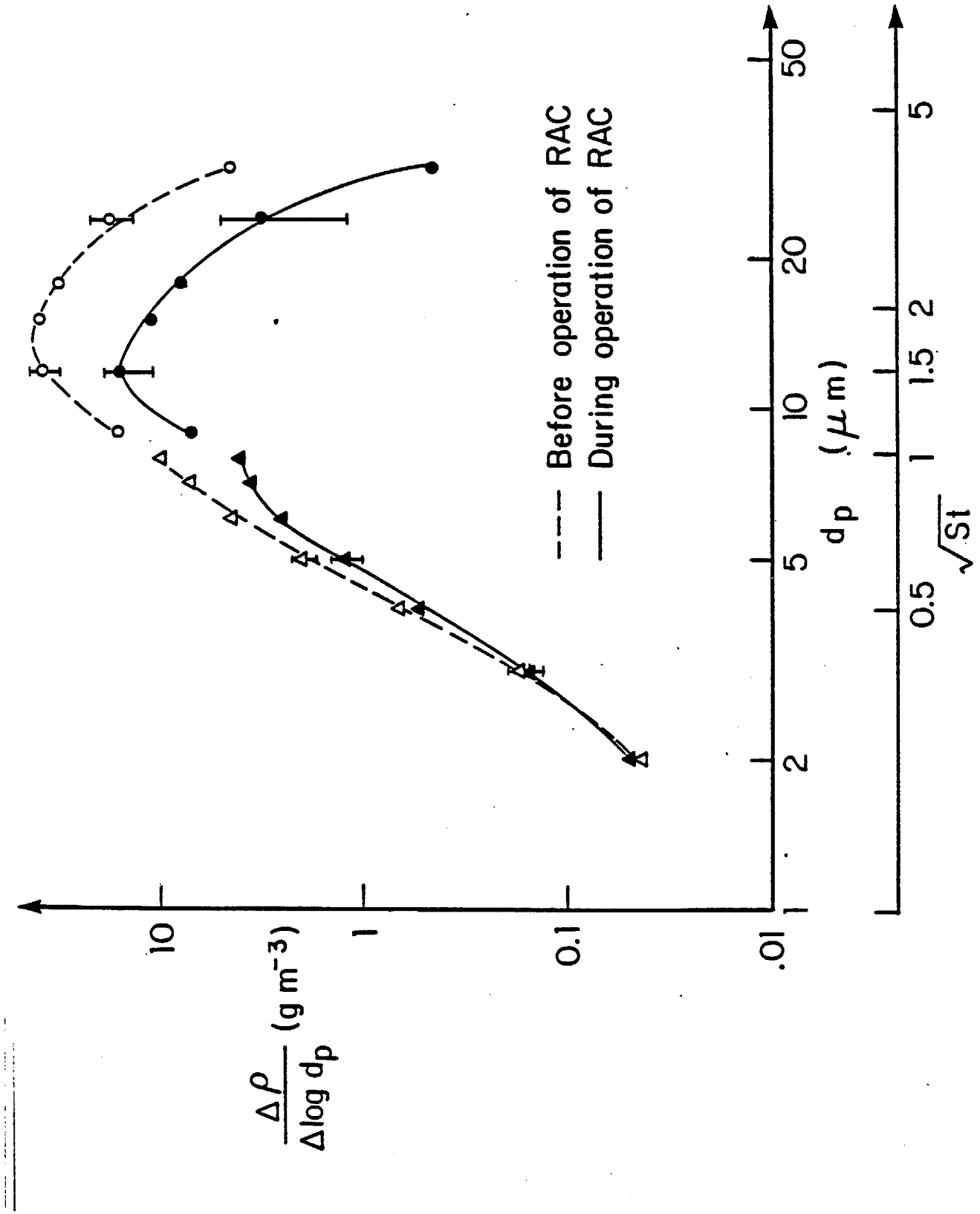
Before operation of RAC
During operation of RAC
$\frac{\Delta \rho}{\Delta \log d_p}$ (g m^{-3})
10
1
0.1
.01
1
2
5
10
20
50
d_p (μm)
0.5
1
1.5
2
5
$\sqrt{St}$

Figure 3.

CHAPTER VII

VERTICAL VARIABILITY AND SHORT-TERM TEMPORAL TRENDS IN PRECIPITATION AND CHEMISTRY.*

J. W. MUNGER, J. M. WALDMAN, D. J. JACOB, AND M. R. HOFFMANN
W. M. Keck Laboratories
California Institute of Technology
Pasadena, California 91125

INTRODUCTION

Recent evidence[1] indicates that precipitation in the Los Angeles basin is as acidic as precipitation over eastern North America. In the East, storm systems transport SO_2, NO_x, and their oxidation products, H_2SO_4 and HNO_3, for long distances before depositing them in precipitation.[2] In Los Angeles, however, storm systems originate over the Pacific Ocean and have little or no contact with polluted air masses until they reach the Los Angeles basin. In addition to the Pacific cyclonic storms, which provide the majority of the precipitation in Los Angeles, stratus clouds forming at the top of the marine layer may thicken enough to produce light drizzle. This drizzle exhibits very high concentrations of H^+, NH_4^+, NO_3^-, and SO_4^{2-}, but it is only a minor contributor to the total precipitation budget in the basin.[3]

If the storm systems responsible for most of the Los Angeles area precipitation are in fact originally clean, then a significant portion of the H^+, NH_4^+, NO_3^-, and non-marine SO_4^{2-} would be incorporated into precipitation by below-cloud scavenging (BCS). In-cloud scavenging would be a more important process for the drizzling stratus clouds, which form nearer the ground below the inversion layer.

The relative contributions of in-cloud and below-cloud scavenging can be estimated by comparing the concentrations in precipitation and cloudwater at high elevations with concentrations at lower elevations. Increases in concentration from sites near the cloud base to lower sites would indicate BCS. Pasadena and the adjacent mountain slopes, where a 1500 m vertical gradient is achieved over an 11 km horizontal span (see Fig. 1), are ideal for a study of elevational gradients in precipitation composition.

Methods. During the 1981-82 wet season wet only precipitation collectors[4] were operated at Mt. Wilson and Pasadena. During a rain event, the initial 1.8 mm of precipitation are collected in a separate bottle; two additional bottles collect 27 mm increments. A second collector at Pasadena collects the first five 0.34 mm increments sequentially. Stratus clouds were sampled during June 1982 at Henninger Flats with a rotating arm collector.[5] The analytical methods have been described elsewhere.[6]

*Proc. 4th International Congress on Precipitation Scavenging, Dry Deposition and Resuspension, 29 Nov. - 4 Dec., Santa Monica, CA (1982).

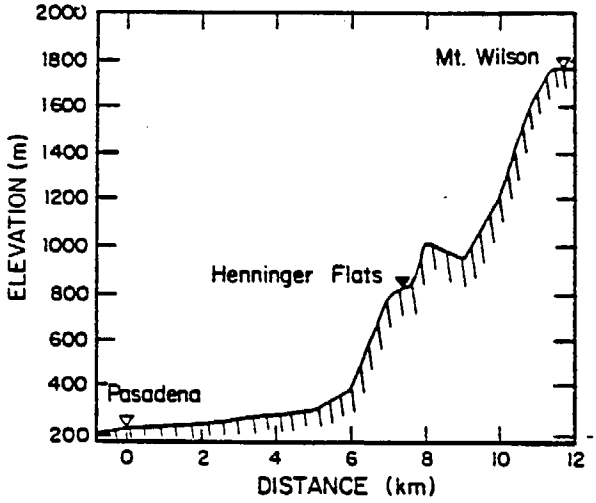

Fig. 1. Profile of San Gabriel Mountain slopes adjacent to Pasadena. Vertical exaggeration ∿ 3.3:1. The locations of rain collectors ∇ and fog sampling site ▼ are indicated. During winter rains the cloud base is frequently below Mt. Wilson. Stratus forms during the spring at the level of Henninger Flats and above; Henninger Flats is usually towards the bottom of the stratus layers, which do not reach Mt. Wilson.

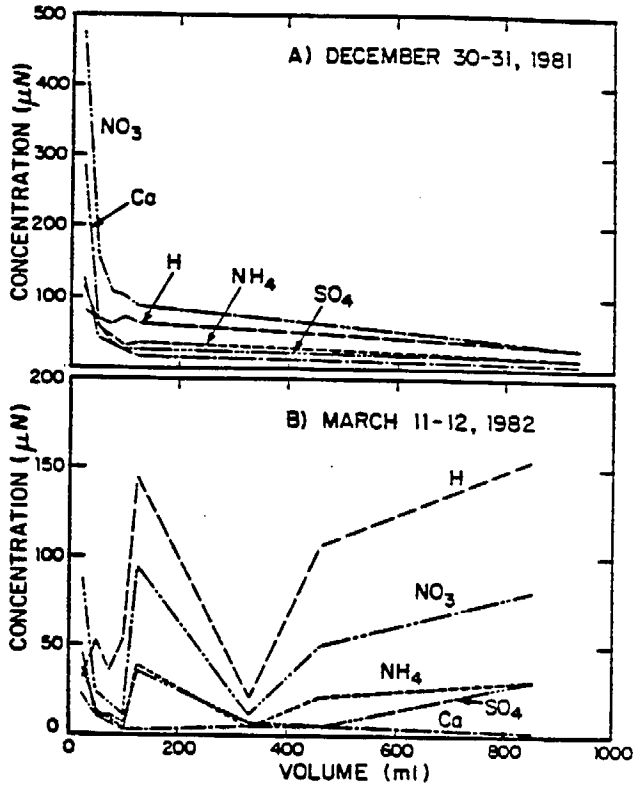

Fig. 2. Concentrations of ions in serial fractions of rainwater at Pasadena. A. Storm on 12/30-31, 1981. B. Storm on 3/11-12, 1982. The sharp decline suggests rapid depletion of gases and large aerosol. Subsequent increases suggest replenishment during the course of the storm.

RESULTS

Temporal Trends. The data from the small-increment collector (see Fig. 2) indicate a rapid depletion of solutes during the beginning of storms, the first 75 ml of rain correspond to 15 minutes or less. This rapid drop in concentration suggests removal of the readily scavengeable gases and large aerosol. During some storms there is an apparent replenishment of the ions that have anthropogenic sources, H^+, NH_4^+, NO_3^-, and SO_4^{2-}; the March 11 storm presented in Fig. 2B is the most dramatic example of this.

Vertical Variations. Of the thirteen precipitation events that occurred during the period December 1981 through May 1982, six yielded samples at both Pasadena and Mt. Wilson. Events for which precipitation was predominantly snow at Mt. Wilson were excluded because of incomplete collection.

The differences between deposition of major ions at Pasadena and at Mt. Wilson (see Table 1) indicate that a significant amount of material is added to precipitation below Mt. Wilson. The slight increase in $[K^+]$ at Mt. Wilson is probably due to

contamination by small amounts of debris from nearby vegetation at that site. The December 30-January 2 storm had a surplus of Na^+, Ca^{2+}, Mg^{2+}, Cl^-, and SO_4^{2-} at Mt. Wilson, which suggests either a local source, such as soil dust, for these ions at Mt. Wilson or that local updrafts over the mountains mix ground-level pollutants up to the clouds.

TABLE 1

COMPARISON OF PASADENA AND MT. WILSON WET DEPOSITION DURING 1981-82.

	← μeq m^{-2} →									mm
Dates	H^+	Na^+	K^+	NH_4^+	Ca^{2+}	Mg^{2+}	Cl^-	NO_3^-	SO_4^{2-}	H_2O
12/30-1/2	522	-118	-28	141	-106	-29	-38	304	-205	-9.2
1/5	258	17	- 4	84	39	15	2	571	225	-3.8
3/11-3/15	631	178	-22	176	- 27	49	246	252	212	-21.
4/12	634	88	1	-	73	28	98	131	483	2.3
5/8	867	5.7	-53	378	118	36	114	1280	376	10.3

Differences in wet deposition of individual ions and precipitation amount during storm events at Pasadena and Mt. Wilson. ($\Delta F = F_p - F_w$). Positive values (i.e., greater deposition at Pasadena) suggest below-cloud scavenging.

The volume-weighted mean concentrations and sum of deposition for the six events considered (see Table 2) indicate that BCS makes a significant contribution to the composition of precipitation at Pasadena. This fraction ranges from near 50% for H^+, NH_4^+, and NO_3^- to about 10% for Na^+ and Ca^+. Some ions have higher concentrations at Mt. Wilson than would be due to marine aerosol alone. This suggests that the meteorology near the mountains may be more complicated than we assumed or that there is some mixing of the Los Angeles air mass with the cloud layer, but that does not detract from the validity of the BCS estimates for this pair of sites.

Potential increases in precipitation concentration due to BCS can be calculated using equilibrium chemistry, aqueous-phase oxidation rates and aerosol scavenging theory. We assume an open system that is well mixed. A typical size raindrop (R_p = 0.5 mm, terminal velocity, V_t = 4 m s^{-1}) is allowed to scavenge SO_2, HNO_3, NH_3 and any aerosol present in a layer 1500 m deep. Droplets are assumed to be in equilibrium with ambient trace gases at all times (i.e. diffusion does not limit the oxidation kinetics). Rate constants and activation energies for the oxidation of S(IV) to S(VI) are given by Martin.[7] Adjusting to 4°C and combining constants gives:

$$v_t \frac{d[S(VI)]}{dz} = 2.0 \times 10^{10} P_{H_2O_2} P_{SO_2} \quad (1)$$

$$v_t \frac{d[S(VI)]}{dz} = 3\left[\frac{6.48\times10^{-2}[Fe^{3+}]P_{SO_2}(1.31\times10^{-2}+[H^+])}{[H^+]^2} + \frac{2.58[Mn^{2+}]P_{SO_2}}{[H^+]}\right] \quad (2)$$

Non-reactive gases and aerosol are scavenged by impaction and diffusion according to (3)

$$\frac{dC_p^i}{dz} = \frac{3E^i C_a^i}{4R_p} \quad (3)$$

Where C_p^i and C_a^i are concentrations of component i in precipitation and air. The scavenging efficiency, E, is set at 1 for diffusion of soluble gases and varied according to particle size for impaction. Calculations of E based on aerosol impaction theory[8] predict that particles with diameter $\geq$ 3 um will impact to some extent on the falling drops, but most of the SO_4^{2-} and NO_3^- aerosol in Los Angeles is below this size range[9] and will not be effectively scavenged by falling drops.

At $[H^+]$ = 50 μN, the average observed in Pasadena, equilibrium with 5 ppb SO_2 would yield 3 μN of S(IV) in the rain that would be free to oxidize to S(VI) during storage. At typical concentrations of Fe and Mn (0.73 μM and 0.026 μM [1]) and the average $[H^+]$, catalytic oxidation of 5 ppb SO_2 would yield a [S(VI)] increase of 3 μN. Oxidation of 5 ppb SO_2 by 0.5 ppb H_2O_2 could increase [S(VI)] by 38 μN. These calculations are based on averages, but they suggest that even low concentrations of gaseous pollutants could account for the 17 μN average increase in SO_4^{2-} observed. Sulfate aerosol is unlikely to contribute significantly to the increase in SO_4^{2-} concentration because it is too small to be scavenged by impaction.

Nitric acid and ammonia are very soluble in the pH range 2-6, and will be rapidly removed from the atmosphere by precipitation. In order to account for the average increase observed in the initial concentrations of NO_3^- and NH_4^+ between Mt. Wilson and Pasadena, gas phase concentrations of 1.0 ppb (2.8 μg m^{-3}) and 0.22 ppb (0.18 μg m^{-3}) are required for HNO_3 and NH_3, respectively.

The impact of BCS should be most pronounced during the initial moments of a storm, when the atmosphere is most heavily laden with gases and aerosol. Data on concentrations in the initial fractions of precipitation at Pasadena and Mt. Wilson are sparse but in most cases Pasadena had higher concentrations (see Table 3). However, February 10 was a notable exception; cations at Mt. Wilson exceeded the concentrations at Pasadena by factors of 4.5 to 10.5. In most of the storms considered $[Na^+]$ and $[Cl^-]$, which

are derived from sea salt, tended to be nearly equal at the two sites or have a slight excess at Mt. Wilson.

TABLE 3

RATIO OF CONCENTRATIONS IN FIRST FRACTIONS AT MT. WILSON AND PASADENA.

Date	H^+	Na^+	K^+	NH_4^+	Ca^{2+}	Mg^{2+}	Cl^-	NO_3^-	SO_4^{2-}
12/30	0.02	8.6	6.2	0.35	1.35	0.91	-	-	-
1/5	0.18	0.89	1.0	0.27	0.30	0.40	0.27	0.28	0.36
2/10	6.61	9.2	4.5	8.7	6.86	10.5	-	-	-
3/11	0.19	1.09	2.69	0.57	0.59	0.53	5.26	0.47	0.70
5/8	0.01	1.64	1.50	0.35	0.77	1.15	3.89	0.33	0.72

Ratios are calculated as $R = C_w/C_p$. Ratios will be less than 1 when the concentrations at Pasadena are greater than at Mt. Wilson. Initial fractions contain the first 1.8 mm of precipitation. - indicates missing data.

TABLE 4

COMPARISON OF HENNINGER FLATS CLOUD AND PASADENA RAIN.

	← μeq ℓ^{-1} →								
	H^+	Na^+	K^+	NH_4^+	Ca^{2+}	Mg^{2+}	Cl^-	NO_3^-	SO_4^{2-}
Pasadena rain	794	112	16.9	492	168	51	63.1	1093	621
Henninger Flats Cloud	224	11.6	3.8	145	17.8	3.8	21.4	191	128
Henninger Flats	← μeq ℓ^{-1} →								
6/21 2130-2200	1380	116	31.5	1030	203	5.7	70.4	936	894
6/22 540-605	398	19.3	8.8	226	12.8	5.5	45.6	411	225

Concentrations in rain collected at Pasadena during the morning of June 7 and in stratus water collected at Henninger Flats from 9:30 to 10:00 a.m. on June 7. The additional data for Henninger flats are for cloud in the evening and again the following morning; drizzle fell at that site between the sampling periods.

Stratus Precipitation. Only one attempt was made to collect stratus cloudwater at Henninger Flats while it was raining at Pasadena. The majority of the rain fell before the cloud sampling began. Contrary to our expectation that most of the solute content of drizzle would be due to scavenging in the stratus, we observed higher concentrations in the rain than in the cloudwater. Concentrations in the first stratus sample and the last fraction of rainwater, the samples most nearly simultaneous, are presented in Table 4. However, subsequent sampling at Henninger Flats indicated that concentrations in the cloudwater decrease sharply during periods of drizzle, so it is possible that cloudwater concentrations in the stratus were initially as high as in the rainwater on June 17.

CONCLUSION

The series of precipitation collectors in Pasadena and the adjacent mountain slopes are ideal for testing scavenging models. Relatively clean air masses in Pacific storms interact with the polluted air in the Los Angeles basin. Contact time between the two airmasses is short. Pollutants in Los Angeles are either mixed rapidly into the overlying clouds, where the aerosol may act as condensation nuclei, or they are removed by below-cloud scavenging, which is most effective for gases and large particles. Data collected so far suggest that BCS, primarily of gases, accounts for up to half of the H^+, NH_4^+, and NO_3^- present in Los Angeles area precipitation.

Dissolution of SO_2 and oxidation to H_2SO_4 within the falling raindrops also appears to be important. The concentrations observed in high altitude precipitation suggest that some mixing of pollutants into the clouds must occur. The present data are insufficient to judge the relative importance of in-cloud and below-cloud scavenging for stratus-cloud precipitation.

ACKNOWLEDGEMENTS

We gratefully acknowledge the financial support of the California Air Resources Board (A2-048-32) for this research.

REFERENCES

1. Liljestrand, H. M., and Morgan, J. J. (1981) Environ. Sci. & Technol. 15, 333-338.
2. Husar, R. B. and Patterson, D. E. (1980) Ann. NY Acad. Sci. 338, 399-417.
3. Morgan, J. J. and Liljestrand, H. M. (1980) Measurement and Interpretation of Acid Rainfall in the Los Angeles Basin. W. M. Keck Laboratory, Report No. AC-2-80, California Institute of Technology, Pasadena, California.

4. Liljestrand, H. M. (1980) Atmospheric Transport of Acidity in Southern California by Wet and Dry Mechanisms. Ph.D. thesis, California Institute of Technology, Pasadena, California.
5. Jacob, D. J. et al. (1982) This volume.
6. Munger, J. W., Jacob, D. J., Waldman, J. M., and Hoffmann, M. R. (1982) submitted to J. Geophys Res.
7. Martin, L. R. (1982) in Acid Precipitation, Calvert, J. G., ed., Ann Arbor Science, Ann Arbor, Michigan.
8. Friedlander, S. K. (1977) Smoke, Dust, and Haze. John Wiley & Sons, New York, 317 pp.
9. Appel, B. R. et al. (1980) in the Character and Origins of Smog Aerosols, Hidy, G. M., Mueller, P. K., Grosjean, D., Appel, B. R. and Wesolowski, J. J., eds., John Wiley & Sons, New York, pp. 315-335.

TABLE 2

COMPARISON OF VOLUME-WEIGHTED MEAN CONCENTRATION AND SUM OF WET-DEPOSITION FOR SIX PRECIPITATION EVENTS AT MT. WILSON AND PASADENA DURING THE PERIOD DECEMBER 1981 THROUGH MAY 1982.

	Concentration $\mu eq\ L^{-1}$									
	H^+	Na^+	K^+	NH_4^+	Ca^{2+}	Mg^{2+}	Cl^-	NO_3^-	SO_4^{2-}	H_2O
Pasadena	52.3	13.3	1.5	19.9	13.4	4.9	14.9	45.1	32.9	-
Mt. Wilson	17.7	8.4	1.9	7.7	9.0	2.8	7.9	18.1	17.2	-

	Mass $meq\text{-}m^{-2}$									$L\text{-}m^{-2}$ (mm)
Pasadena	5.48	1.40	0.16	2.08	1.40	0.51	1.56	4.73	3.45	104.9
Mt. Wilson	2.56	1.22	0.27	0.94	1.31	0.40	1.14	2.61	2.49	144.8

CHAPTER VIII

"PREPRINT EXTENDED ABSTRACT"
Presented before the Division of Environmental Chemistry
American Chemical Society
Washington, D.C. September 1983

URBAN CLOUDWATER AND ITS POTENTIAL FOR POLLUTANT DEPOSITION IN A LOS ANGELES PINE FOREST

Jed M. Waldman, J. William Munger, Daniel J. Jacob and Michael R. Hoffmann

Environmental Engineering Science
California Institute of Technology
Pasadena, CA 91125

In addition to the orographic enhancement of precipitation at mountain sites, cloud droplet capture, primarily by wind-driven interception, can lead to greater solute deposition relative to the surrounding lowlands. The enhancement of water catchment in coastal and mountain forests has been reported with values as high as 1 inch/day for precipitation collectors located beneath trees exposed to fog-laden winds (1). Using artifical foliar collectors in the White Mountains of N.H., Schlesinger and Reiner (2) found the enhancement of cation deposition to exceed that for water catchment, which itself averaged 4.5 times greater than for open buckets.

Cloud droplet capture has been determined to be an important hydrological input for some ecosystems (3). In light of recent measurements of highly concentrated and acidic fogwater in the Los Angeles area (4), there appears to be potential for enhanced pollutant deposition in adjacent mountain forests. Furthermore, exposure to concentrated acid solutions may lead to damage of plant tissue (5). In this paper, we report the composition of cloudwater samples collected in a Los Angeles pine forest.

During the spring of 1982, dense fog caused by stratus cloud interception was observed 12 times in May and 18 times in June at Henninger Flats, a campground and tree nursery located at approximately 730 m MSL on the southern slope of Mount Wilson, 25 km northeast of Los Angeles. Collection of cloudwater was performed on June 11-15,17,21 and 22, using the Caltech rotating-arm-collector (6). On most dates sampling occurred from the time fog had formed at the site to the time it had dissipated. Immediately after each sample was collected (intervals were generally 30 to 60 min.), pH was measured, and aliquots were preserved for analysis of major ions, formaldehyde, S(IV) and trace metals. Sample handling and analytical procedures have been given elsewhere (7).

Results of the chemical analyses are summarized in Table I. The median and range of values for each of the major chemical species are indicated. For comparison, values are given for the volume-weighted mean concentrations of Pasadena and Mt. Wilson rainfalls. With the exception of Na^+, the median values for Henninger Flats cloudwater concentrations are more than 10 times those for local rainwater - indicative of the severity of fogwater composition relative to the alternative source of moisture (i.e. precipitation).

The concentrations of hydrogen, ammonium, nitrate and sulfate comprise the majority of the ionic composition in most samples (Figure 1). Gaseous ammonia (NH_3) as well as alkaline particles can be scavenged by droplets and neutralize the nitric and sulfuric acid fractions. The free acidity (H^+) shows a broad distribution with extreme values comparable to the nitrate and sulfate. These extreme values occur because there is insufficient ambient base to balance the acid. The low levels of sodium indicate that the bulk of sulfate is not from the seasalt.

The high concentrations of sulfate and nitrate in the fogwater reflect the degree of regional pollutant transport to the mountain slopes of the basin. The nitrate-to-sulfate equivalent ratio for these samples was approximately 2:1, similar to fogwater samples collected in the Los Angeles basin but markedly different than rainwater collected in adjacent areas. The basinwide ratio for emissions is also close to 2:1 (8).

The sampling intervals on June 17 and 22 were preceded by rainfall at the site. In both cases, these cloudwater samples showed the lowest ionic concentrations (c.f. Figure 1b). This is consistent with the notion that precipitation scavenging will effectively remove airborne pollutants to the ground surface. While there is some deposition at the surface, much of the solutes in the cloudwater remains in the airshed after it evaporates. Interestingly, the lowest nitrate-to-sulfate ratios occurred in these samples.

Cloudwater capture may represent a more severe threat to plant tissue than deposition accompanying rainfall, since plant surfaces are subjected to much higher concentrations and acidity. To better understand the nature of its interaction with plant tissue, cloudwater was removed from pine needles where it had been naturally collected. One important observation was that these solutions were significantly more concentrated than the suspended cloudwater (Table I). We believe this can be attributed to one or more of these three causes: a) accumulated dry deposition is dissolved by cloudwater which collects on the plant surfaces; b) cloudwater solution causes leaching from internal plant tissue; c) evaporation of the deposited solution as the cloud dissipates leaves a concentrated residue. This residue is only removed by rainfall or leaf "drip". Note the lower concentrations for the June 22 sample. A second point of interest is that some of these samples had higher pH than cloudwater collected during the same interval. This suggests that either impacted cloudwater leached nutrients from the plant tissue or, alternatively, the previously deposited material was more alkaline.

The liquid water content (LWC) of the cloud was not measured directly at the collector site. Estimated from the collection rate, the LWC was consistently in the 0.05 to 0.10 g m^{-3} range. With the cloudwater composition, this gives nitrate and sulfate values of 2 to 20 $\mu g\ m^{-3}$ air. While this is comparable to the pollutant levels for dry days, the shift of particle size is significant: mass mean diameters for dry nitrate and sulfate aerosol are 0.2 to 0.5 micron versus 10 to 20 microns for cloud droplets. The commensurate increase in the deposition velocity associated with droplet sedimentation and impaction can lead to far greater deposition rates compared to dry deposition. As a representative calculation, a water deposition rate of 0.2 mm hr^{-1} for cloudwater with 1000 $\mu eq\ l^{-1}$ acid gives a rate equal to 200 meq m^{-2} hr^{-1}. This is the same rate as for an ambient nitrate aerosol concentration of 10 $\mu g\ l^{-1}$ with a deposition velocity of 34 cm s^{-1}. While wet (rain) deposition rates can be higher, rainfall washes over the plant surfaces, removing most of the solute to the ground. At leaf surfaces, concentrated cloudwater plus dissolution of accumulated dry aerosol leads to a most severe and potentially harmful micro-environment.

ACKNOWLEDGEMENTS

We are grateful to the Los Angeles Fire Department Forestry Bureau for notifying us of the situation at Henninger Flats and for allowing us to conduct our field sampling at the site. This research has been supported by a contract with the California Air Resources Board.

Table I

MEDIAN AND RANGE OF CONCENTRATIONS FOR CLOUDWATER AT HENNINGER FLATS, JUNE 1982

		Cloudwater [a] This study	Rainwater [b] Pasadena	Mt. Wilson	Tree "drip" [c] June 12	June 22
pH		2.86 2.06-3.65	4.4	5.0	3.12	2.90
H^+		1365 224-8710	39	10	760	1260
Na^+		143 5-2465	24	26	14500	950
K^+		17.5 1.2-161	1.7	1.7	1625	750
NH_4^+		576 128-3130	21	36	5650	2400
Ca^{2+}		132 5.3-975	6.7	9.3	11700	1300
Mg^{2+}	μeq/l	53.7 1.6-762	7.2	6.6	6170	425
Cl^-		125 21-1965	28	28	2000	960
NO_3^-		1435 191-9500	31	23	19900	1260
SO_4^{2-}		617 128-7310	39	40	5910	880
S(IV)		14.5 7-85	na	na	na	na
CH_2O	μmol/l	66 34-920	na	na	na	na
Fe		1055 200-6880	223	28	na	na
Pb	μg/l	346 80-2780	na	na	na	na

a. Median and range for 38 samples.
b. Volume-weighted mean value for 1978-79 (9).
c. Samples removed from pine needles by shaking branch; filtered prior to ion analysis.

REFERENCES

(1) Oberlander,G.T. (1956) Summer fog precipitation on the San Francisco pennisula. Ecology 37, 851-852.
(2) Schlesinger,W.H. and W.A. Reiners (1974) Deposition of water and cations on artificial foliar collectors in fir krummholz of New England mountains. Ecology 55, 378-386.
(3) Lovett.G.M., W.A. Reiners and R.K. Olson (1982) Cloud droplet deposition in subalpine balsam fir forests: hydrological and chemical inputs. Science 218, 1303-1304.
(4) Waldman,J.M., J.W. Munger, D.J. Jacob, R.C. Flagan, J.J. Morgan and M.R. Hoffmann (1982) Chemical composition of acid fog. Science 218. 677-680.
(5) Tukey,Jr.,H.B. (1970) The leaching of substances from plants. Ann.Rev.Plant Physiol. 71, 305-324.
(6) Jacob.D.J., R.C. Flagan, J.M. Waldman and M.R. Hoffmann (1982) Design and calibration of a rotating-arm-collector for ambient fog sampling. 4th Int.Conf.on Precipitation Scavenging,Dry Deposition and Resuspension, (Santa Monica, CA) Elsevier-Netherlands (in press).
(7) Munger.J.W., D.J. Jacob, J.M. Waldman and M.R. Hoffmann (1983) Fogwater chemistry in an urban atmosphere. J. Geophys. Res. (in press).
(8) McRae, G.J., W.R. Goodin and J.H. Seinfeld (1982) Mathematical Modeling of Photochemical Air Pollution. EQL Report No.18 (Calif. Inst. Tech., Pasadena, CA).
(9) Liljestrand.H.M., and J.J. Morgan (1981) Spatial variations of acid precipitation in Southern California. Environ. Sci. Tech. 15, 333-338.

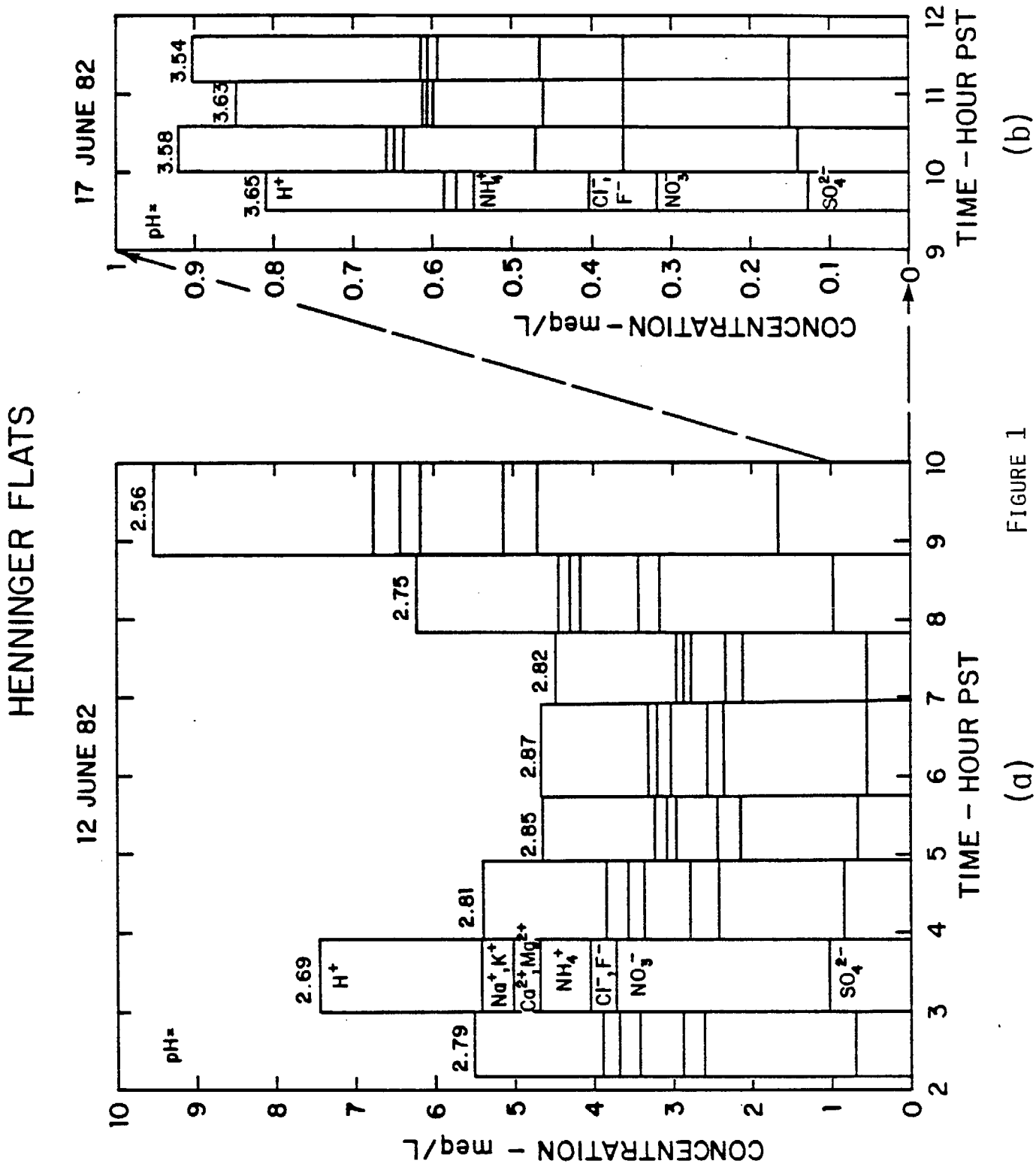
HENNINGER FLATS
12 JUNE 82
17 JUNE 82
pH=
2.79
2.69
2.81
2.85
2.87
2.82
2.75
2.56
3.65
3.58
3.63
3.54
H+
Na+,K+
Ca2+,Mg2+
NH4+
Cl-,F-
NO3-
SO4 2-
CONCENTRATION - meq/L
TIME - HOUR PST
(a)
(b)

FIGURE 1

CHAPTER IX

DRAFT: to appear in Atmospheric Chemistry, E.D. Goldberg, ed. Dahlem Konferenzen. Springer-Verlag, 1982

FACTORS GOVERNING THE pH, AVAILABILITY OF H^+, AND OXIDATION CAPACITY OF RAIN

J. J. Morgan
Environmental Engineering Science
California Institute of Technology
Pasadena, California 91125 U.S.A.

Abstract. The acidity of rain is coupled to redox reactions in air and in atmospheric water. The pH, an intensive quantity, needs to be distinguished from the base neutralizing capacity. For acid rain observed at most locations H_2SO_4, HNO_3, NH_3 and $CaCO_3$ are dominant components. Their local availability or production rates govern net acidity. pH is thus almost entirely determined by these major "strong" components imposed on a CO_2 background, with some influence by $SO_2(aq)$, smaller concentrations of HNO_2 and weak organic acids and minor bases, e.g., Fe_2O_3, yielding acid aquo metal ions. Total global emissions to the atmosphere of H_2SO_4 precursors outweigh those of HNO_3 by a factor 2-3 on an equivalent basis. In specific settings HNO_3 may be comparable to H_2SO_4 in rain. Total atmospheric acidity appears to be a useful quantity for estimating potential acidity of rain at different locations. There are indications in photochemical models of HNO_3 and H_2SO_4 that feedback among S and N species may be important. Heterogeneous oxidations of SO_2 in cloud, fog, and rain play important roles in the acidification process. "Background" acidities of rain appear to be highly variable; pH values are expected to range from below 5 to above 6. Present day SO_2 and NO_x fluxes account for a pH lowering of $\sim$ 0.5 to 1.5, depending upon source location and transport-conversion rates.

INTRODUCTION

Acidity (base-neutralizing capacity) and alkalinity (acid-neutralizing capacity) are complementary concepts. The acidity versus alkalinity balance of rain (and drizzle, snow, fog and

clouds) is intrinsically coupled to oxidation-reduction reactions in the air and in atmospheric water. Sillén (17) likened the geochemical evolution of the earth's atmospheric-ocean system to a set of gigantic, somewhat coupled acid-base and oxidant-reductant titrations in which the "volatiles," acids from the earth's interior (H_2O, HCl, SO_2, CO_2 and others) were titrated by bases from the rocks and in which reduced components (H_2, NH_3, Fe_3O_4, C) were titrated by the O_2 of the evolving atmosphere-biosphere system. As a result of such global titrations we arrive at a present-day atmosphere which is 20% O_2, 79% N_2, and 0.03% CO_2, a world ocean with a pH of 8 and alkalinity of 2.3 meq/ℓ. The system is not a stationary equilibrium, of course. It is open, with high fluxes. Still, the titration metaphor may be useful in thinking about the state of the atmosphere-hydrosphere-biosphere system today, on global, regional and local scales. Evidence over the last century shows increased emissions of strongly acidic precursors such as sulfur dioxide and nitric oxide to the atmosphere. Fossil fuel burning has also led to an increase of global atmospheric CO_2 by some 15%. These emissions, through photochemical and chemical reactions in the atmosphere, lead to an increase in the total acidity of the atmosphere and consequent increases in local and regional fluxes of acidity to the earth's surface through rainfall of increased acid content and lower pH (wet deposition) and through absorption and fallout of gases and aerosols (dry deposition). Present fluxes of acidity and possible future increases have important implications for aquatic and terrestrial ecosystems, water resource systems, weathering of natural and man-made environments, and for the longer-term chemical state of atmosphere-water systems locally and regionally, if not globally.

Concepts of H^+ Availability and Acidity

Acids are proton donors; bases are proton acceptors. In water as a solvent the "strong" acids, e.g., HNO_3 donate protons to water essentially completely.

$$HNO_3 + H_2O \rightleftharpoons H_3O^+ + NO_3^-$$

the equilibrium acidity constant, K_a, is the measure of acid strength. Here, $K_{a,HNO_3} = 1$ for the standard state conventions adopted. The aquated proton, H_3O^+, is the strongest acid that can exist in water. Aqueous CO_2 is a weak acid. The reaction

$$CO_2(aq) + H_2O \rightleftharpoons H_3O^+ + HCO_3^-$$

has an effective acidity constant $K_{a,CO_2} = 10^{-6.4}$ at 25°C. Bases, e.g., OH^- ion, CO_3^{2-} ion or NH_3 are similarly strong or weak. For example, the strengths of OH^-, CO_3^{2-} and NH_3 as bases can be ranked by their acceptance of protons (19)

$$OH^- + H_3O^+ \rightleftharpoons 2H_2O$$

$$CO_3^{2-} + H_3O^+ \rightleftharpoons HCO_3^- + H_2O$$

$$NH_3 + H_3O^+ \rightleftharpoons NH_4^+ + H_2O$$

with respective equilibrium constants $10^{14} > 10^{10.3} > 10^{9.2}$ at 25°C.

The concentrations or activities of a given acid are readily linked to those of related components in the gas phase or in solid phases by appropriate two-phase constants, e.g., Henry's law and solubility equilibrium constants. Similarly, acids and bases can be formed from precursors by overall oxidation-reduction processes, e.g., $N_2 + \frac{5}{2} O_2 + H_2O = 2HNO_3$.

Four key concepts which define the resultant acid-base characteristics of rain are: (i) energetics, i.e., equilibrium properties of component acids and bases and acid-base precursors; (ii) the total acid or base neutralizing capacity with respect to some proton reference level, i.e., a specified acid-base solution; (iii) the aqueous proton concentration, $[H_3O^+] \equiv [H^+]$, or activity, $\{H^+\}$, related intensity factors representing free aqueous protons or immediately available protons, (Bates (1) refers to proton activity, proton availability, and degree of acidity synonymously); (iv) kinetics of reactions and transfer processes leading to production of acids or bases in rain.

It is essential to distinguish between $H_3O^+(aq)$ and a base neutralizing capacity, or reservoir of ultimate H^+ availability. These notions can be illustrated by means of simple examples for various component acids at concentration levels like those in rain. A group of acids of different strengths (see Figure 3, below) and concentrations was selected. Initial pH values (neglecting minor activity coefficient corrections) and base neturalizing capacities have been calculated. No redox changes have been assumed. The solution is closed to the atmosphere. The results are shown in Table 1.

TABLE 1 - Available H^+ (pH) and Base Neutralizing Capacities of Dilute Acid Solutions.

Acid	Conc μM	pH (25°C)	Base Neutralizing Capacity $\mu eq\ell^{-1}$	
			to pH	BNC#
H_2SO_4	10	4.7	7.0	20
	50	4.0	7.0	100
HNO_3	10	5.0	7.0	10
	50	4.3	7.0	50
$SO_2(aq)$	10	5.0	6.1	10
			8.1	20‡
CH_3COOH	10	5.1	7.1	10
	50	4.7	7.3	50
NH_4NO_3	10	7.0	8.9	10
	50	6.8	9.4	50
$CO_2(aq)$	10	5.7	7.6	10
			9.0	20‡

#BNC with respect to least-protonated level is also known as TOTH. ‡Least-protonated level of weak diprotic acid.

Some points can be noted. Comparing equimolar (10 μM) solutions one at a time we see that pH values range from 4.7 (H_2SO_4) to neutral (for the weak acid NH_4NO_3), whereas the total acidity (TOTH) is the same on an equivalent basis (H_2SO_4, hydrated SO_2 and hydrated CO_2 are diprotic). As remarked by Odén (14), for strong acid solutions (e.g., H_2SO_4 and HNO_3), the total concentrations of these acids fix the pH value, hence the H^+ activity or availability. For a weak acid

such as CH_3COOH, with $pK_a = 4.7$, a dilute solution leads to extensive dissociation and pH 5.1. If CO_2 at 10 μM is titrated to pH ∿ 9, 20 μeq^{-1} of acidity will be measured. We notice that SO_2 with $pK_a = 1.8$ is effectively a "strong" acid at these concentrations.

At five-fold higher concentrations of H_2SO_4, HNO_3 or CH_3COOH pH is lowered considerably. If H_2SO_4, HNO_3, CH_3COOH and NH_4NO_3 were mixed at 50 μM concentrations levels, the resulting pH would be approximately 3.8. The CH_3COOH dissociation would contribute only about 6 $\mu eq\ell^{-1}$ to the free acidity (available protons). The NH_4NO_3 contributes nothing. The base neutralizing capacity with respect to a CO_2/H_2O two phase system (with aqueous CO_2 = 10 μM) would be 195 $\mu eq\ell^{-1}$ (because 10% of the 50 μM weak acid CH_3COOH remains undissociated at pH 5.7).

Were NH_3 rather than NH_4NO_3 introduced at 50 μM, the basicity of NH_3 would lead to the reaction $NH_3 + H^+ = NH_4^+$ and the acidity would decrease by 50 $\mu eq\ell^{-1}$, the pH rising to 4.0. If 50 μM NH_3 were oxidized to HNO_3 (in a receiving ecosystem): $NH_3 + 2O_2 \longrightarrow H^+ + NO_3^- + H_2O$, the base neutralizing capacity would increase by 100 $\mu eq\ell^{-1}$, or about 50% of the original 195 $\mu eq\ell^{-1}$. If H_2SO_4 would be reduced (in an anoxic sediment environment) to H_2S ($pK_a = 7$), the base neutralizing capacity towards CO_2/H_2O would decrease by almost 100 $\mu eq\ell^{-1}$. Oxidation of all the CH_3COOH to CO_2 would decrease BNC by 45 $\mu eq\ell^{-1}$ with respect to the original CO_2/H_2O reference level. Finally, if SO_2 were present at 10 μM, oxidation of SO_2: $SO_2 + \frac{1}{2} O_2 \longrightarrow H_2SO_4$, would increase the BNC towards CO_2 by 10 $\mu eq\ell^{-1}$, lowering pH slightly but leaving TOTH unchanged. It is clear that the acid-base and oxidant-reductant states of precipitation are strongly related.

ACIDITY, ALKALINITY AND pH

The earliest known quantitative description of the chemistry of rain and its acidity was given for the United Kingdom by Smith in his book Air and Rain, in 1872 (18). His analysis

included acidity (as H_2SO_4), ammonia, nitrate, sulfate, chloride and organic matter. Arrhenius' theory of electrolytic dissociation came 15 years later; Smith's acidity corresponded to, roughly, $[H^+]$ of 200 μM. Sorenson introduced the pH scale in 1909; Smith's rain had a pH of perhaps 3.7. Thinking in terms of the components required to establish the rain composition which Smith analyzed at Manchester (5) we could choose H_2O, H_2SO_4, HNO_3, HCl, NH_3, NaCl and Na_2SO_4 (the latter two for the marine component). The approximate charge-balance relationship in the rain water would than be $[H^+] + [NH_4^+] + [Na^+] = 2[SO_4^{2-}] + [NO_3^-] + [Cl^-]$. We now recognize that this chemical balance is incomplete. Later rainfall analyses (e.g., Gorham (4),Junge (8), and Granat (6,7)) reveal that the following ions are nearly always found in acidic rainfall in significant concentrations, the relative importance depending on provenance: SO_4^{2-}, NO_3^-, Cl^-, NH_4^+, Na^+, K^+, Ca^{2+}, Mg^{2+} and H^+. For weakly acidic and alkaline precipitation HCO_3^- ion is an important species. Table 2 shows ion concentration data and pH for acidic rainfall at three locations.

TABLE 2 - Chemical Analyses of Acidic Rain at Three Locations.

Species	Concentration μeq-1		
	Sjöängen, S. Sweden[a]	Hubbard Brook, New Hampshire[b]	Pasadena, Calif.[c]
SO_4^{2-}	69	110	39
NO_3^-	31	50	31
Cl^-	18	12	28
NH_4^+	31	22	21
Na^+	15	6	24
K^+	3	2	2
Ca^{2+}	13	10	7
Mg^{2+}	7	32	7
H^+	52	114	39
pH	4.30	3.94	4.41

a,1973-75 (7); b,1973-74 (10); c, 1978-79 (12).

Observations on major ions of rain at many locations for the past several decades suggest a universal set of input components which account for the net acidity, pH and resulting chemical species in most rain. Recent observations on rainfall chemistry at different locations in the Los Angeles basin of southern California (Figure 1) provide a convenient illustration of variations in components. The ratio of $[SO_4^{2-}]$ to $[NO_3^-]$ on an equivalent basis ranges from 1.5 at Westwood (6 km from the Pacific coast) to 1.1 at Pasadena (40 km inland) to 0.9 at Riverside (70 km inland). The majority of fossil-fuel burning stations are sited near the coast. Qualitatively similar variations in composition are seen over far greater distances in Northern Europe and the Eastern United States.

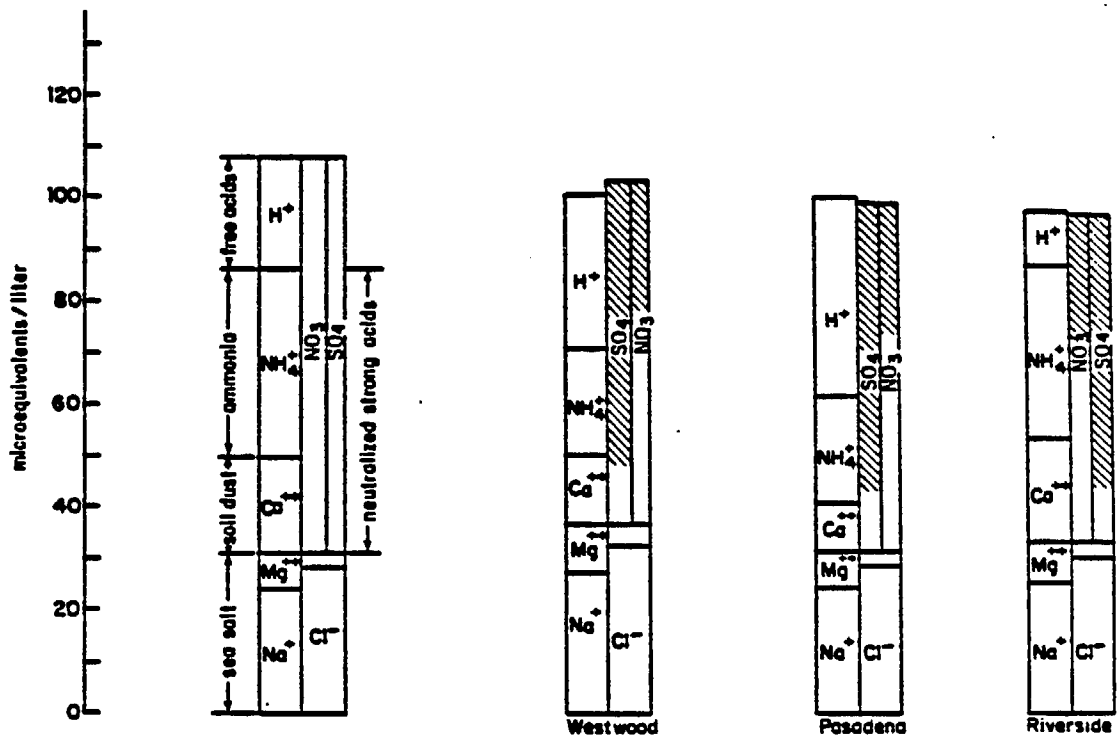

Fig. 1 - Composition of rain in southern California, 1978-79, interpreted in terms of input components and source type. (Coast → inland, left → right; widths of SO_4^{2-} and NO_3^- bars indicate relative amounts; crosshatchings indicate stationary sources, non-hatched, mobile) (12).

A set of components that accounts for observed net acidity or alkalinity of rainfall at European stations was proposed by Granat (6). Figure 1 illustrates application of the concept in term of the "components" strong acids, sea salt, soil dust and ammonia. The corresponding chemical components could then be (consistent with Table 2 and Figure 1): NaCl, KCl, $MgSO_4$, $CaCO_3$, NH_3, H_2SO_4 and HNO_3. This choice of acid-base-salt components accounts for commonly-reported chemical analyses. Other components can be chosen to describe ultimate sources of acidity or alkalinity in rain and to relate sources to gas phase, aerosol, or aqueous phase species involved in transport and transformation processes leading to acidification. In the absence of significant anthropogenic emissions, organic sulfur compounds and H_2S are major precursors for H_2SO_4 formation in the atmosphere. For nitrogen the principal natural and anthropogenic precursor of atmospheric and rainfall acidity is nitric oxide, NO (when grouped together with NO_2, referred to as NO_x). The dominant man-made precursor emission of sulfur is sulfur dioxide, SO_2. Interplay of acid-base (proton transfer) and oxidant-reductant (electron transfer) reactions in air and water is better accounted for by the emission components: NaCl, KCl, $MgCl_2$, $MgSO_4$, $NaHCO_3$, $CaCO_3$, NH_3, HCl, H_2S, RSR', SO_2, H_2SO_4, and NO. In the oxidizing atmosphere H_2S, RSR' and SO_2 are transformed to H_2SO_4 (with characteristic times ranging from less than a day to weeks, depending on chemical and physical conditions in the atmosphere). Both homogeneous photochemical oxidations and heterogeneous aqueous-phase, (and possibly particulate solid phase) oxidation processes take part. Emitted NO is oxidized to nitrous acid, HNO_2, and nitric acid, HNO_3, over homogeneous photochemical and chemical pathways in the gas phase.

The general picture for acid and basic components entering rain is summarized schematically in Figure 2.

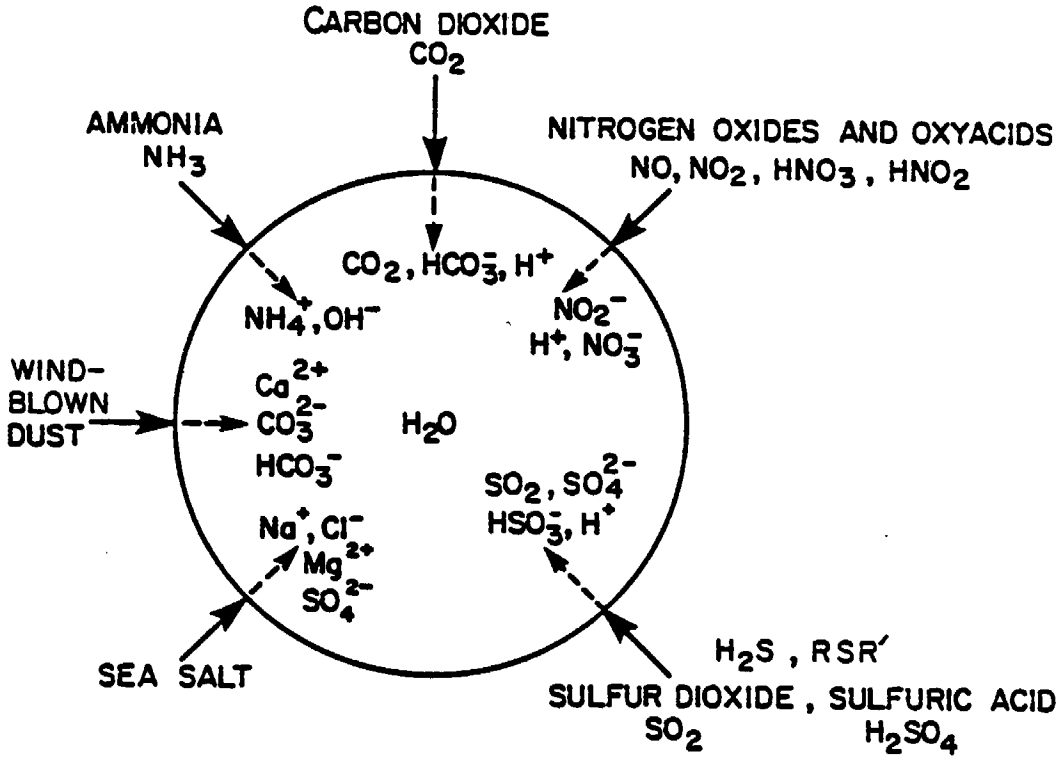

Fig. 2 - Source and chemical components known to take part in rain acid-base chemistry.

Acidity and Base Neutralizing Capacity

The commonly-used definitions of acidity and alkalinity in water chemistry are based on the choice for a reference level of CO_2 aqueous solutions resulting from equilibrium between water and CO_2 at its partial pressure (fugacity) in the atmosphere. A temperature of interest is specified, thus fixing the pH, which depends on two acidity constants for CO_2(aq) and Henry's law constant for CO_2. At an atmospheric CO_2 concentration of 335 ppmv (molecules of CO_2 per million molecules of air), the reference pH is 5.65. Solutions of pH > 5.65 and at equilibrium with the atmosphere have acid neutralizing capacity. This capacity factor is defined as the alkalinity. Solutions at pH < 5.65 at equilibrium with the atmosphere have base neutralizing capacity. This capacity factor is referred to as "mineral acidity;" it results from the presence of acids stronger than CO_2 in water.

The "strong acids" (HCl, HNO_3, H_2SO_4) are, of course, all stronger than CO_2. Chemical compositions in Table 2 and Figure 1 show that base neutralizing capacity of rain with respect to the CO_2 reference level, $[BNC]_{CO_2}$, is attributable entirely to the strong acids H_2SO_4 and HNO_3. The precipitation-weighted mean Pasadena rain (Table 2) was formed (per liter of rain) from 18 μmol H_2SO_4 (deducting the SO_4^{2-} contributed by seawater), 31 μmol HNO_3, 21 μmol NH_3 and 3.3 μmol $CaCO_3$. The value of $[BNC]_{CO_2}$ for rain with only these components is $[BNC]_{CO_2} = 2[H_2SO_4]_o + [HNO_3]_o - 2[CaCO_3]_o - [NH_3]_o$ or 39 $\mu eq\ell^{-1}$. At Pasadena, the potential acidity or input acidity was 67 $\mu eq\ell^{-1}$. Component bases NH_3 and $CaCO_3$ neutralized 42% of the potential acidity. At Hubbard Brook, approximately 30% of potential acidity was neutralized, and at Sjöängen, approximately 45%.

The charge balance for rain with HNO_3, H_2SO_4 and HCl as the net acid components and with $CaCO_3$ and NH_4 as the only net basic components is $[H^+] + 2[Ca^{2+}] + [NH_4^+] = 2[SO_4^{2-}] + [NO_3^-] + [Cl^-] + [HCO_3^-] + 2[CO_3^{2-}] + [OH^-]$. The base neturalizing capacity in terms of actual solution species is $[BNC]_{CO_2} = [H^+] - [HCO_3^-] - 2[CO_3^{2-}] - [NH_3] - [OH^-]$. For rain at equilibrium with atmospheric CO_2 knowledge of $[BNC]_{CO_2}$, and the equilibrium constants for CO_2 solubility, CO_2 and HCO_3^- acidity and water ionization, plus constants for NH_3 solubility and NH_4^+ acidity, is sufficient to find $[H^+]$ or $\{H^+\}$and all other species activities. (If other acid-base bases, e.g., SO_2, HNO_2, NO_2, etc. are involved, their equilibria enter into the calculation via the charge balance.) $[BNC]_{CO_2}$ can be obtained experimentally by titration to the CO_2 reference pH, or calculated for known or assumed input components.

Alkaline rain existed earlier at locations now acidic and exists today in regions with strong sources of alkaline windblown dust and ammonia in excess of sources of SO_2, H_2S, organic sulfur and NO_x. The United States NADP network shows

extensive regions of Western North America with rain of pH > 5.7, unlike the Eastern U.S. and Canada, and unlike Northern Europe. Using 1955-56 rain analyses for the Western U.S. it is possible to estimate pH values by application of charge-balance, CO_2-equilibrium relationships. The pH values obtained are considerably higher than those observed today in the Northeast United States or calculated for 1955-56 (11) from charge balances. Geographical relation to sources of acid and basic emissions and the transport-transformation times from source locations are recognized generally to be among the factors governing pH of rain.

Alternative Proton Reference Levels

It should be kept in mind that the reference level chosen for defining a neutralizing capacity is an arbitrary datum taken for convenience (analytical or computational), and may not necessarily have direct environmental significance without further interpretation. Chemical speciation, i.e., pH, metal ion, ligand and complexes in rain and in aquatic systems depends on absolute input concentrations or acid-base components and redox components. A reference level has no intrinsic significance for describing changes in H^+ availability and acidity. The concept of a proper background level for neutralizing capacity or proton activity should be distinguished from that of a reference level. For example, if rain at a location has been characterized at an earlier time by, say pH 7.5 and ALK = 100 $\mu eq\ell^{-1}$, and at a later time by pH 4.3 and $[BNC]_{CO_2} = 50$, it is clear that the overall change in the acidity-alkalinity balance is $\Delta[BNC]_{CO_2} = +150\ \mu eq\ell^{-1}$. Total acid (proton) input is $\sum\Delta[BNC]$ and can be compared with changes in emissions or changes in resultant $[BNC]_{CO_2}$ of aquatic systems (waters, sediments, soils) (14).

ACIDITY AND OXIDATION (pH AND pε)

Proton transfer and electron transfer are analogous notions. The pH corresponds to activity of aqueous protons. A solution of low pH has relatively strong proton donating tendency; one

of high pH has relatively strong proton accepting tendencies. Electron transfers formally describe an oxidation-reduction process. For example, the half-reactions for peroxide reduction

$$H_2O_2(aq) + 2H^+ + 2e = 2H_2O$$

and SO_2 oxidation

$$SO_2(aq) + 2H_2O = SO_4^{2-} + 4H^+ + 2e$$

combine to yield the overall reaction of $SO_2(aq)$ with H_2O_2:

$$H_2O_2 + SO_2 = SO_4^{2-} + 2H^+$$

generating increased H^+ and $[BNC]_{CO_2}$. Figure 3 summarizes the energetics of proton transfer reactions (part (a)) and electron transfer reactions (part (b)) in terms of the standard equilibrium constant for proton donation, K_a, and the standard equilibrium constant for unit electron acceptance, K_e which is simply a measure of the free energy per

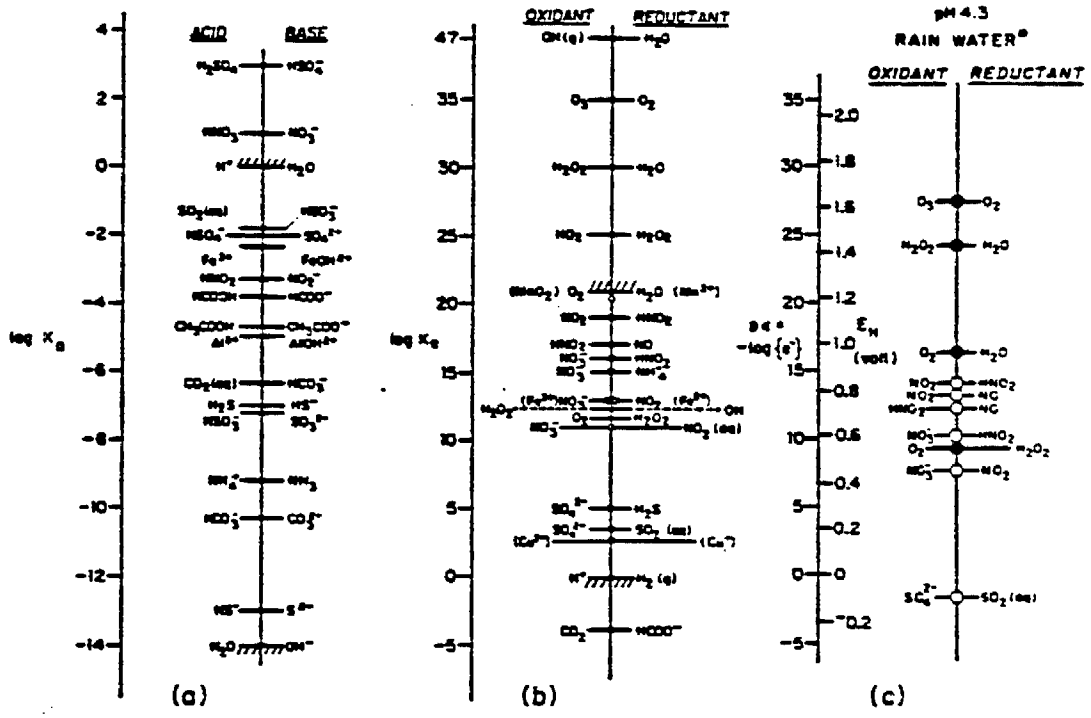

Fig. 3 - Energetic levels for (a) proton-transfer ($HA=A^- + H^+$, K_a) and (b) electron-transfer ($OX + e = Red$, K_e) reactions (19). Part (c) shows non-equilibrium pε values estimated for rain at Pasadena (13).

electron transferred. For H_2O_2 reduction to H_2O, log K_e is 30; for SO_2 oxidation to H_2SO_4, log K_e^{-1} is -3; for SO_2 oxidation by H_2O_2, (two electrons) log K = 54, which corresponds to the standard potential difference of 1.6 volts. The pε and E_H scales are linearly related by $p\varepsilon = E_H/2.3\ RTF^{-1}$ (19). Figures 3(a) and 3(b) emphasize a useful analogy between acid-base and oxidant-reductant reactions. The analog of $pH = -\log\{H^+\}$ is $p\varepsilon = -\log\{e^-\}$. Systems of low pε are strong electron donating (reducing) systems. As $pH = pK_a + \log$ (base/acid), so $p\varepsilon = p\varepsilon^o + \log$ (oxidant/reductant) for each half-reaction system. At complete equilibrium, the pH and pε values reflect the respective acid/base and oxidant/reductant compositions for all pairs.

In Figure 3(a), acids higher on the scale can transfer protons to the bases lower on the scale. In Figure 3(b), higher oxidants and lower reductants have a similar relationship. For acids, the "energy ladder" leads to the concepts of $[BNC]_{CO_2}$ and TOTH.

Any acidity capacity implies a defined redox reference level as well. Thus NH_3 oxidation to HNO_3, H_2SO_4 reduction to H_2S, CH_3COOH oxidation to CO_2, etc. change acidity capacity by creating or destroying acidity. This simply says that the complete equilibrium state requires specification of both pH and pε, i.e., the acid-base and oxidant-reductant states.

An oxidation capacity for rain can be readily identified in terms of Figure 3(b). Any electron reference level can be selected, say $K_{e,ref}$. Then, the oxidation capacity, [OX], is $\sum$[equivalent oxidants, $K_e > K_{e,ref}$] - [equivalent reductnats, $K_e < K_{e,ref}$]. If the SO_4^{2-}/SO_2(aq) electron level is chosen, only Cu^+, H_2, $HCOO^-$, and SO_2 among the reductants would enter into the oxidation capacity. Not all half-reactions included are compatible in an equilibrium solution. In practice, as for BNC, only a limited number of species, e.g., SO_2, HSO_3^-, SO_3^{2-} are related by proton equilibria.

Figure 3(c) is an example of calculated apparent (non-equilibrium) pε values for rain at Pasadena (13), based on measured aqueous concentrations or gas-phase concentrations of O_3, H_2O_2, O_2, SO_2, HNO_2, NO_3^-, NO and NO_2. (Ozone and hydrogen peroxide would be unstable in the rain, being much stronger oxidants than O_2. NO_2, NO, and NO_3^- are out of equilibrium, because of slow two-phase kinetics.) From the concentrations of the oxidants and reductants an apparent oxidation capacity, [OX] can be calculated with respect to the SO_4^{2-}/SO_2 reference level. For $[O_2] = 3\times10^{-4}$M, $[NO_3^-] = 8\times10^{-5}$M, and $[SO_2] + [HSO_3^-] = 3\times10^{-6}$M, $[OX] = 1.38\times10^{-3}$ eqℓ^{-1}. O_2 and NO_3^- dominate. The median levels of the known powerful and kinetically active oxidants, O_3 and H_2O_2, 3×10^{-10}M and 2×10^{-8}M, respectively, are less than equivalent to the median S(IV) reductant level, 3×10^{-6}M, at air-rain equilibrium for pH 4.3. However, true levels of H_2O_2 are not well known. The equilibrium scavenging level could be as high as 10^{-5}M, or 2×10^{-5} eqℓ^{-1} of aqueous H_2O_2 for an initial air concentration of 1 ppbv, based on Henry's law constant for H_2O_2 at 25°C.

TOTAL ATMOSPHERIC ACIDITY

Acid base and redox processes may take place in the gas phase, in aerosol phases and in cloud and fog. The acidity of rain is a reflection of the components and species entering into the various atmospheric phases, e.g., HNO_3, H_2SO_4, H_2S, SO_2, NH_3, $(CH_3)S$, SO_2, etc. It can be useful to define the total acidity (over several phases) of a volume of atmosphere, by stoichiometrically relating actual components and species to acid and base species that would donate or accept protons. For example, H_2SO_4 releases two protons; upon oxidation, NO_2 releases one proton, etc. (An extension to total oxidation capacity is evident.) As for acidity of rain, alternative pH levels and redox states can be chosen, e.g. $[BNC]_{CO_2}$ and most-oxidized or TOTH and partially-oxidized, etc. Assuming some set of levels,

$$\left\{\begin{matrix}\text{Total}\\ \text{Acidity}\end{matrix}\right\} = \left\{\begin{matrix}\text{Aerosol}\\ \text{Acidity}\end{matrix}\right\} + \left\{\begin{matrix}\text{Gas Phase}\\ \text{Acidity}\end{matrix}\right\} + \left\{\begin{matrix}\text{Cloud}\\ \text{Acidity}\end{matrix}\right\} + \cdots$$

In terms of known gas partial pressure, p_i, concentrations in water, $[X_i]$, aerosol-phase concentrations, (X_i), and a corresponding set of stoichiometric acid (>0), or base (<0) coefficients b_i, g_i and a_i, which depend on H^+ and e^- reference levels chosen,

$$\left\{\begin{matrix}\text{Total}\\ \text{Acidity}\end{matrix}\right\} = \frac{1}{RT}\sum b_i p_i + L\, g_i[X_i] + \sum a_i (X_i)$$

where the acidity is referred to unit volume of air and L is liquid water volume per volume of air. Total acidity represents a way of defining potential acidification by rain, fallout, etc., and a basis for constructing an acidity balance in terms of a conserved property, subject to precise definition of H^+ and redox reference levels. Different levels are appropriate, for different environmental situations, e.g., short-term vs long-term or oxidizing vs reducing conditions.

PRODUCTION OF RAIN ACIDITY

Availability of H^+ and the base neutralizing capacity of rain are determined by: (i) transfer or scavenging of pre-existing acidic and basic aerosol and gaseous species, and (ii) generation of acids in cloud and rain. Mechanisms and rates of the scavenging processes determine the initial composition of cloud and rain and thus set the aqueous chemical conditions (pH, metals, buffers, ligands, aqueous SO_2 and NO_x, and oxidants such as O_3 and H_2O_2 for heterogeneous SO_2 oxidation) which in turn affect the H^+ and acidity of rain. Gaseous and aerosol species scavenged by atmospheric water are formed by homogeneous photochemical reactions and multiphase gas-to-particle conversion processes. Emitted reduced sulfur compounds: H_2S, RSR' and SO_2 are partially oxidized in the troposphere to H_2SO_4 via photochemical, free-radical pathways involving O_3, OH, H_2O_2, HO_2, RO_2, and $O(^3P)$. Emitted NO and NO_2 are partially oxidized to HNO_2 and HNO_3 by similar photochemical pathways (in which NO and NO_2 themselves play key

roles in O_3 formation) with OH, O_3, RO, and H_2O_2 as reactants and products.

Unoxidized SO_2 in the air dissolves in clouds or aerosol water where O_2, O_3, or H_2O_2 oxidation produces H_2SO_4. Unoxidized SO_2 also is removed from the trophosphere by dry deposition. Reaction of H_2SO_4 with NH_3 leads to ammonium sulfate aerosols, e.g., NH_4HSO_4 or $(NH_4)_2SO_4$. The aerosols may be scavenged during cloud formation (nucleation scavenging) and by aerosol-droplet collisions in the clouds (diffusion). Both SO_2(gas) and sulfate aerosol are scavenged by raindrops. Efficiency of rain drop aerosol scavenging depends strongly upon the aerosol size distribution (smaller particles are poorly captured). SO_2 scavenging by cloud and rain can be treated as a reversible gas-aqueous distribution since mass transfer is generally rapid. Dry deposition is a slow process for the submicron aerosol fraction, which dominates for H_2SO_4.

Nitric acid reacts rapidly with ammonia to produce NH_4NO_3 aerosol, which is scavenged by clouds and rain or removed by dry deposition. NH_4NO_3 has a relatively high vapor pressure for $NH_4NO_3 \longrightarrow NH_3 + HNO_3$, and the variation with temperature is great. This may have implications for scavenging efficiency. Gas phase HNO_3 can be scavenged by cloud and rain (as can HNO_2) or be absorbed at the earth's surface. At higher relative humidity HNO_3 will tend to condense on aerosol particles.

A potential liquid water sink for NO and NO_2 is reaction via the two-phase equilibria

$$2NO_2(g) + H_2O(\ell) \rightleftharpoons 2H^+ + NO_3^- + NO_2^-$$

$$NO(g) + NO_2(g) + H_2O(\ell) \rightleftharpoons 2H^+ + 2NO_2^-$$

However, the overall two-phase rates are not rapid, showing characteristic times much longer than typical cloud life or rainfall time (9). Possibilities of other, more rapid two-

phase mechanisms involving NO and NO_2 need exploration (e.g., catalysis in aerosols or in cloud water). Other products of photochemical oxidations of NO and NO_2 (N_2O_5, organic nitrates, peroxynitric acid) are either dry-deposited or taken up in aerosols or precipitation. N_2O_5 yields nitric acid directly in an aqueous phase.

Factors which should govern rain acidity from SO_2 and H_2SO_4 components include: (a) concentrations of SO_2 and sulfuric acid aerosol in the air and their vertical distributions; (b) aerosol particle size distributions and associated chemical distributions of H_2SO_4 and $(NH_4)_xH_y(SO_4)_{(x+y)/2}$ species; (c) vertical distributions of O_3 and H_2O_2 concentrations in the air, with their possible roles in aqueous phase H_2SO_4 formation from SO_2; (d) initial air concentration of neutralizing bases, e.g., NH_3 and $CaCO_3$, which set initial pH values together with CO_2, SO_2, H_2SO_4 and HNO_3; (e) microphysical characteristics (sizes and numbers of cloud droplets as well as other characteristics, e.g., evaporation); (f) rain drop size distributions; (g) rate of precipitation ("dilution effect").

For acidification by the NO- and NO_2-derived acids, HNO_3, HNO_2 (and N_2O_5 intermediate) governing factors are roughly similar. The tropospheric concentrations of gas-phase HNO_3, N_2O_5, and HNO_2 and of species associated with the aerosol HNO_3 component are of central importance. Size distributions (submicron vs above) and temperature effects on NH_4NO_3 volatility are of particular interest.

It is clear that the acidic species in the air available to be scavenged by clouds and rain at a particular location depend on source magnitudes of S and N compounds, geography of sources, air trajectories, regional photochemical setting (and thus upon <u>all</u> relevant emissions, e.g., hydrocarbons, SO_2, NO, CO, etc., and upon season of the year) in addition

to scavenging factors. Theoretical considerations suggest that cloud nucleation scavenging, interception and impaction of coarse aerosol particles and SO_2 cloud scavenging followed by oxidation (O_3, H_2O_2) in that order are dominant acidification mechanisms leading to H_2SO_4 in rain (3). For a given distribution of HNO_3(g) and nitrate particle concentrations it appears that nucleation scavenging in clouds can play an important role, depending on the size distributions, particle properties, and temperature. If gaseous HNO_3 concentrations in air are comparable to those for aerosol NO_3^-, gas scavenging in cloud and by rain will be important. HNO_3 scavenging can be close to 100% because of the large (10^6M atm^{-1}) Henry's constant for HNO_3/H_2O. If larger aerosol particle sizes are important for HNO_3, impaction and interception by raindrops can contribute significantly to acidification as well. Particle size distribution data are not abundant for nitrates. It is difficult to draw conclusions about scavenging of HNO_3 in comparison to that of sulfur acids.

Concentrations From Scavenging

For aerosol scavenging of component X the resulting cloud or rain concentrations can be related by $[X] = (X)\varepsilon f/L$ (8) in which [X] is aqueous concentration, (X) is aerosol concentration (e.g., mole per volume of space), ε is efficiency, f accounts for net cumulative evaporation or dilution, and L is the liquid water content per volume of air. For equilibrium gas scavenging aqueous concentration is given by (scavenged component being conserved per unit volume of space): $[X_i] = (P_{i,o}K_H\alpha_o^{-1})/(1 + LRTK_H\alpha_o^{-1})$ in which $P_{i,o}$ is initial gas partial pressure, K_H is Henry's law constant (M atm^{-1}) and α_o is the fraction of undissociated dissolved gas in solution, a function of pH and acidity constants, hence temperature. For a "completely" scavenged and undissociated gas, the concentration is just $[X_i] = P_{i,o}/LRT$. At the pH of acidic rain HNO_3 is completely scavenged, NH_3 is scavenged well in excess of 90%, and SO_2 is scavenged to just a few percent. H_2O_2 is completely scavenged, independent of pH. O_3 is scavenged to

a very small extent.

Rain chemistry data at Pasadena (Table 2, Figure 1) and the sulfate and nitrate aerosol data at times of precipitations suggest that scavenging of aerosols may contribute substantially to observed rain concentrations, perhaps greater than 50% for each. However, there is considerable uncertainty as to scavenging efficiencies and washout ratios. At least 12% of excess sulfate at Pasadena can be accounted for by SO_2 scavenging and subsequent oxidation; the corresponding value at Riverside is in excess of 24% (12). With respect to annual emissions, for which the equivalent potential acid ratio of NO_x to SO_2 (1975-76) was $\sim$ 2.3, HNO_3 is less efficiently scavenged by precipitation in the L. A. Basin than is H_2SO_4 ($[HNO_3^-]/2[SO_4^{2-}] \sim 0.8$ for mean rain). This may also reflect the fact that dry deposition and advection are by far the major output terms, as well as the kinetic differences in S and N removal processes.

Importance of Heterogeneous Oxidations

The residence time of sulfur in the troposphere is believed to be on the order of one week or so. Photochemical reactions yield characteristic $SO_2 \longrightarrow H_2SO_4$ conversion times on the order of a week, but not under winter conditions. Known homogeneous photochemical mechanisms for sulfur seem unable to account for observed year-round levels of SO_4^{2-} in rainfall. Oxidations of absorbed SO_2 by H_2O_2 and O_3 in cloud and fog appear to account for very high rates where photochemical paths cannot (15). Figure 3(b) shows that MnO_2 and Fe^{3+} can oxidize SO_2 in acid solutions, suggesting that a catalytic process involving Mn or Fe can be initiated. In Los Angeles high sulfuric acid formation rates are correlated with high relative humidity, giving added support for an important aqueous phase pathway for SO_2 conversion. A kinetically-attractive alternative path to photochemical oxidation of NO_x has not been delineated; catalyzed oxidations in aqueous aerosol phases or cloud have been mentioned as possibilities.

Interactions and Feedback in the Sulfur-Nitrogen System

The key role of the OH radical (and also H_2O_2) in the photochemical oxidation mechanisms of both NO_2 and SO_2 together with a faster rate for NO_2 by a factor of ~10 has suggested the possibility that the rate of homogeneous atmospheric oxidation of SO_2 might be slowed by high emissions of NO_2. Rodhe, Crutzen and Vanderpol (16) have advanced a simple photochemical and transport model which indicates that long-range transport of HNO_3 can be less-pronounced than for H_2SO_4. In the model NO_2 emissions delay and decrease the oxidation of SO_2 to H_2SO_4 because of competition for OH. The tentative conclusion was advanced that a linear dependence of atmospheric concentrations on emission rates may not be assumed because of non-linear photochemical mechanism interactions.

In heterogeneous aqueous phase conversion of scavenged SO_2 ($SO_2(aq)$ and HSO_3^- species) certain rate laws, e.g., those with O_2 or O_3 as oxidant, predict slower conversions upon acidification, in part because total dissolved $[SO_2 + HSO_3^-]$ decreases with lowering pH. Rapid HNO_3 scavenging might thus lead to inhibition of the aqueous SO_2 oxidation rate. Interestingly, the laboratory rate law for oxidation of $[SO_2+HSO_3^-]$ by $H_2O_2(aq)$ does not exhibit this negative feedback at lower pH. Interactions between the gas-phase and aqueous-phase oxidations of SO_2 and NO_2 deserve greater attention under chemical conditions actually encountered in the atmosphere.

Background Acidities and pH

The global background emissions of H_2S, RSR', SO_2 and NO_x might provide a rough estimate of background inputs of $[BNC]_{CO_2}$ and resulting pH of rain (although the idea of a "global" background is probably untenable, with S residence times as short as a week or less). If we take the following estimated input fluxes for sulfur and odd nitrogen based on the SCOPE report (20), F_S = 30 Tg S y^{-1} and F_{NO_x} = 15 Tg N y^{-1}, the equivalent acid flux is 3 T eq y^{-1}. Perhaps two-thirds enters the rain. Dividing by the global annual rainfall,

4.5×10^{17} ℓ y^{-1}, gives a $[BNC]_{CO_2}$ of 4 μeq ℓ$^{-1}$ and pH of 5.3 (by solving the proton balance equation for 25°C). If a background ammonia flux is estimated, say 30 Tg N y^{-1} (20), then, since NH_3 is extensively scavenged by rain, $[NH_4^+] \sim 5$ μeq ℓ$^{-1}$, $[BNC]_{CO_2} \sim -1$ μeq ℓ$^{-1}$ and pH ∿ 5.8. More base, e.g., sea salt or alkaline dust would further elevate the pH; more acidic aerosol particles or gas would lower it. The buffer intensity, $d[BNC]_{CO_2}/d$ pH is <u>small</u> in this pH region. A background pH is difficult to characterize. Small variations in fluxes of acids and bases could easily cause pH variations between, say 5.0 and 6.0.

Another approach is to examine the pH of cloud water for certain assumed aerosol, gas phase and water content conditions. If, for a remote location, (HNO_3) is 0.5 μg/m^3, (H_2SO_4) is 1.1 μg/m^3, p_{SO_2} is 10^{-10} atm and p_{NH_3} is 10^{-10} atm, the pH of cloud can be computed for any degree of scavenging by solving the charge balance equation with p_{CO_2}, $p_{NH_3,0}$ (the initial value) and $p_{SO_2,0}$ as constants and assuming a cloud liquid water content, say $L = 10^{-6}$ (vol water/vol air). Alternatively, a titration curve can be constructed showing added net <u>non-volatile</u> acids and bases (H_2SO_4, HNO_3, $CaCO_3$), or $[BNC]^*_{CO_2}$, vs pH. Response to variations of total input BNC can then be examined directly. Figure 4 shows the result for assumed constraints (25°C). A value of $f\varepsilon \sim 1$ has been taken for aerosol scavenging. The resulting scavenged acid concentrations are $[HNO_3]_0 = 8$ μM and $[H_2SO_4]_0 = 11$ μM, yielding $[BNC]^*_{CO_2}$ of 30 μeq ℓ$^{-1}$. This gives pH = 4.6 (curve A). In the absence of NH_3 and SO_2 (curve B) the pH would be ∿ 0.1 unit lower. The pH of rain would depend on the actual values of $f\varepsilon$ locally. At smaller net acid, dissolved NH_3 provides greater buffering. Lower temperatures would raise curve A and lower curve B in the pH range ∿ 4.5-6. Around $[BNC]^*_{CO_2} \sim 0$, NH_3, alkaline dust, and small acid inputs can alter background pH significantly. (The alkalinity contribution from sea salt is ∿ 0.2 μeq ℓ$^{-1}$ per mg/ℓ of Na^+.) Similar considerations have recently been put forward in an

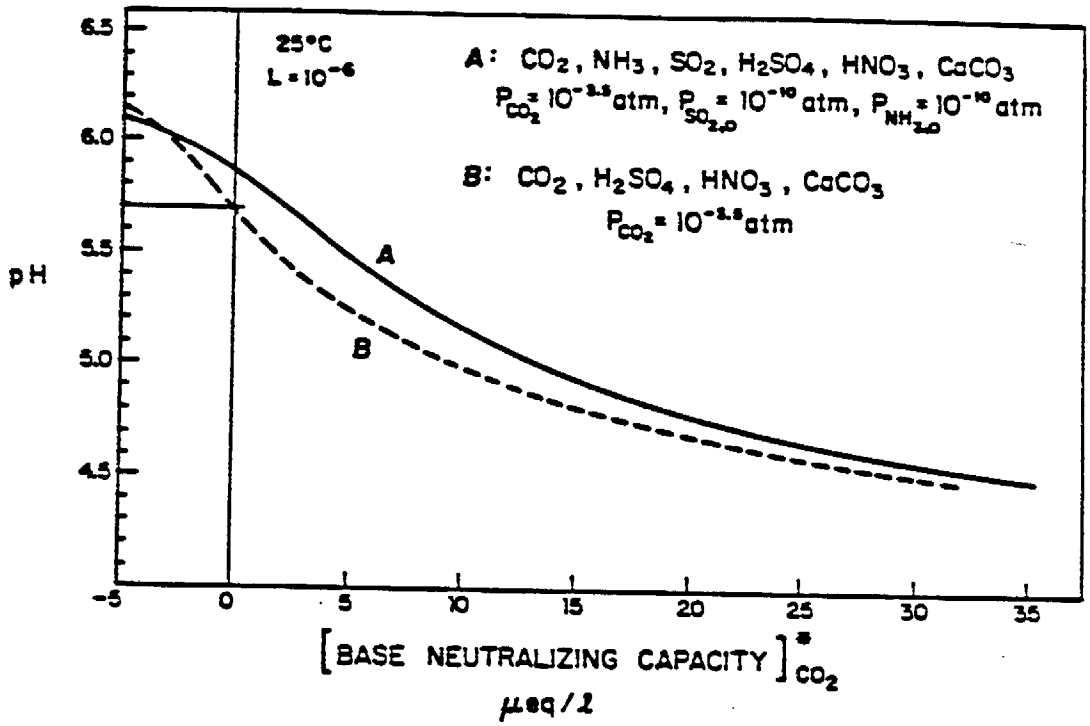

Fig. 4 - Titration curve for two-phase aqueous-gas systems with indicated components. $[BNC]^*_{CO_2}$ is the total added equivalent concentration of non-volatile acids of bases. (The titrations combine mass-conservation in two phases with open-phase equilibria.)

elegant analysis by Charlson and Rodhe (2).

Present Day Global Acid Fluxes

The SCOPE (20) estimates place recent (1970) man-made NO_x emissions at around 20 Tg N y^{-1}, and man-made SO_2 emissions at around 70 Tg S y^{-1}. This corresponds to an equivalent flux of $\sim$ 6 T eq y^{-1}. A rough estimate of increased acidity $\Delta[BNC]^*_{CO_2}$, in rain would be about 9 $\mu eq\ell^{-1}$ on a "global" basis. If the inputs were spread uniformly, then ΔpH of rain would be about 0.3 to 0.6 "globally," depending on the background pH. Local and regional scales have been most affected. It is not unexpected to find pH values in the range 5 to 4 and even lower in rain downwind from local and regional NO_x and SO_2 emissions which together yield equivalent acid wet

deposition fluxes in excess of regional alkaline inputs by $\sim 2x10^2$ to $\sim 2x10^3$ eq H^+ ha^{-1} y^{-1}. "Global" potential H^+ loadings ($\sim 10^2$ eq ha^{-1} y^{-1}) and Eastern N. American loadings ($\sim 10^3$) are in this range. The physical and chemical details of regional acid-base and redox "titrations" are highly complex in time and space and depend, in addition to the matrix of emissions, on the different climatologic, meteorologic, photochemical, and geologic features of regions. Present-day global and regional emission loadings predict acidic rain; experience confirms this in many regions of the world.

SOME QUESTIONS AND PROBLEMS

It seems important to ask whether photochemical mechanisms can predict HNO_3 inputs to rain spatially and temporally. If not, what processes can account for observed NO_3^- levels in rain? The suggested non-linear character of emissions vs. atmospheric concentrations of HNO_3 and H_2SO_4 invites further examination. Control strategy questions may hinge on this aspect of atmospheric acidity. Better understanding of local scavenging of H_2SO_4- and HNO_3-bearing species by cloud and rain requires detailed information on particle size distributions of HNO_3 and H_2SO_4 aerosol acidities and on the $HNO_3(g)/NO_3^-$ (particle) distribution. Key questions related to heterogeneous SO_2 oxidations (cloud, aerosol) concern chemical speciation factors in the solution for reductant, oxidants, and catalysts.

REFERENCES

(1) Bates, R. B. 1959. Concept and determination of pH. In Acids-Bases in Analytical Chemistry, eds. I. M. Kolthoff and S. Bruckenstein, pp. 362-404. New York: Interscience.

(2) Charlson, R. J., and Rodhe, H. 1982. Factors controlling the acidity of natural rainwater. Nature 295:683-685.

(3) Garland, J. A. 1978. Dry and wet removal of sulphur from the atmosphere. Atmos. Environ. 12: 349-362.

(4) Gorham, E. 1955. On the acidity and salinity of rain. Geochim. Cosmochim. Acta 7: 231-239.

(5) Gorham, E. 1981. Scientific understanding of atmosphere-biosphere interactions: a historical overview. In Atmosphere-Biosphere Interactions. Washington, National Academy Press.

(6) Granat, L. 1972. On the relation between pH and the chemical composition in atmospheric precipitation. Tellus 24: 551-560.

(7) Granat, L. 1978. Sulfate in precipitation as observed by the European atmospheric network. Atmos. Environ. 12: 413-424.

(8) Junge, C. E. 1963. Air Chemistry and Radioactivity. New York: Academic Press.

(9) Lee, Y.-N., and Schwartz, S. E. 1981. Evaluation of the rate of uptake of nitrogen dioxide by atmospheric and surface liquid water. J. Geophys. Res. 86: 11, 971-11, 983.

(10) Likens, G. E.; Wright, R. F.; Galloway, J. N.; Butler, T. J. 1979. Acid Rain. Sci. American 241: 43-51.

(11) Liljestrand, H. M., and Morgan, J. J. 1979. Error analysis applied to indirect methods for precipitation acidity. Tellus 31: 421-431.

(12) Liljestrand, H. M., and Morgan, J. J. 1980. Spatial variations of acid precipitation in Southern California. Environ. Sci. Technol. 15: 333-339.

(13) Liljestrand, H. M., and Morgan, J. J. 1982. Chemical source, equilibrium and kinetic models of acid precipitation. In Energy and Environmental Chemistry, v. 2, Acid Rain, ed. L. H. Keith. Ann Arbor: Ann Arbor Science.

(14) Odén, S. 1976. The acidity problem -- an outline of concepts. Water, Air, Soil Poll. 6: 137-166.

(15) Penkett, S. A.; Jones, B. M. R.; Brice, K. A.; Eggleton, A. E. J. 1979. The importance of atmospheric ozone and hydrogen peroxide in oxidizing sulfur dioxide in cloud and rainwater. Atmos. Environ. 13: 123-137.

(16) Rodhe, H.; Crutzen, P.; Vanderpol, A. 1981. Formation of sulfuric acid and nitric acid during long-range transport. Tellus 33: 132-141.

(17) Sillén, L. G. 1965. Oxidation state of earth's ocean and atmosphere. Ark. Kemi 25: 159-175.

(18) Smith, R. A. 1872, Air and Rain. London: Longmans, Green.

(19) Stumm, W., and Morgan, J. J. 1981. Aquatic Chemistry. New York: Wiley-Interscience.

(20) Svenssen, B. H., and Söderlund, R., Eds. 1976. Nitrogen Phosphorus and Sulphur - Global Cycles. SCOPE Report 7. Ecol. Bull. (Stockholm) 22: 89-134.

Acknowledgements.
I thank Dr. H. N. Liljestrand of the University of Texas for his help and advice. I also thank Drs. J. N. Galloway and G. E. Likens for interesting me in acid rain. The support of the Air Resources Board of California is acknowledged.